# The role of N-truncated Aβ peptides in Alzheimer's Disease

Dissertation

for the award of the degree

"Doctor rerum naturalium" (Dr.rer.nat.)

of the Georg-August-Universität Göttingen

within the doctoral program *Molecular Physiology of the Brain*

of the Georg-August University School of Science (GAUSS)

submitted by

José Sócrates López Noguerola

from Pachuca de Soto, Mexico

Göttingen, 2018

**Thesis Committee**

Prof. Dr. Thomas A. Bayer
Division of Molecular Psychiatry, University Medical Center Göttingen
Prof. Dr. Dr. Hannelore Ehrenreich
Department of Clinical Neurosciences, Max Planck Institute of Experimental Medicine, Göttingen
Prof. Dr. Silvio O. Rizzoli
Department of Neuro- and Sensory Physiology, University Medical Center Göttingen

Members of the Examination Board

Reviewer: Prof. Dr. Thomas A. Bayer
Division of Molecular Psychiatry, University Medical Center Göttingen
Second Reviewer: Prof. Dr. Dr. Hannelore Ehrenreich
Department of Clinical Neurosciences, Max Planck Institute of Experimental Medicine, Göttingen

Further members of the Examination Board

Prof. Dr. Silvio O. Rizzoli
Department of Neuro- and Sensory Physiology, University Medical Center Göttingen
Prof. Dr. Thomas Dresbach
Department of Anatomy and Embryology, University Medical Center Göttingen
Prof. Dr. Hubertus Jarry
Department of Endocrinology, University Medical Center Göttingen
Prof. Dr. Tiago Outeiro
Department of Neurodegeneration and Restaurative Research, University Medical Center Göttingen

Date of oral examination: June 26th, 2018.

## Affidavit

I hereby declare that my doctoral thesis entitled "The role of N-truncated Aβ peptides in Alzheimer's disease" has been written independently with no other sources and aids than quoted.

José Sócrates López Noguerola

Göttingen, March 2018

# List of publications

Publications included in this thesis:

**Lopez-Noguerola JS**, Giessen NME, Ueberück M, Meißner JN, Pelgrim CE, Adams J, Wirths O, Bouter Y, Bayer TA. (2018). Synergistic Effect on Neurodegeneration by N Truncated Aβ4-42 and Pyroglutamate Aβ3-42 in a Mouse Model of Alzheimer's Disease. *Front Aging Neurosci*. 2018 Mar 8;10:64. DOI: 10.3389/fnagi.2018.00064.

Publications not included in this thesis:

Bouter Y, **Lopez-Noguerola JS**, Tucholla P, Crespi GA, Parker MW, Wiltfang J, Miles LA, Bayer TA. (2015). Abeta targets of the biosimilar antibodies of Bapineuzumab, Crenezumab, Solanezumab in comparison to an antibody against N-truncated Abeta in sporadic Alzheimer disease cases and mouse models. Acta Neuropathol. 2015 Nov;130(5):713-29. DOI: 10.1007/s00401-015-1489-x

# Abstract

The N-terminally truncated pyroglutamate Aβ3–42 (AβpE3–42) and Aβ4–42 peptides are known to be highly abundant in the brain of Alzheimer's disease (AD) patients. Both peptides show enhanced aggregation and neurotoxicity in comparison to full-length Aβ, suggesting that these Aβ isoforms play an important role in the pathogenesis of AD. Hence, in the current work, the *in vivo* effect of the combination of AβpE3–42 and Aβ4–42 on ongoing AD-related neuron loss, pathology, and neurological deficits was investigated using the newly generated TBA42/Tg4-42 mouse model.

The TBA42/Tg4-42 mouse model was generated by crossing the established TBA42 and Tg4-42 models expressing AβpE3–42 and Aβ4–42, respectively. TBA42/Tg4-42 mice exhibited an accelerated loss of CA1 pyramidal neurons in comparison to homozygous single transgenic TBA42 and Tg4-42 mice, which nicely correlated with prominent intraneuronal Aβ accumulation in the CA1 region. Additionally, reduced anxiety levels and enhanced motor deficits were determined in TBA42/Tg4-42 mice in an age-dependent manner. The sensory-motor deficits strongly correlated with the robust intracellular Aβ accumulation within motor neurons and extracellular Aβ deposition in the spinal cord. Despite the massive neuron loss in the CA1 region, no deficits in working and spatial refence memory could be detected in TBA42/Tg4-42 mice at any ages studied. Furthermore, aggregation kinetics analysis indicates that under physiological conditions, when AβpE3-42 and Aβ4-42 peptides are combined, aggregation propensity is enhanced. These observations confirm the importance of AβpE3-42 and Aβ4-42 in the progression of AD and suggest a possible *in vivo* interaction between these two N-truncated Aβ peptides.

One of the key pathological hallmarks of AD is the extracellular aggregation and deposition of Aβ in the form of plaques. However, the presence of Aβ plaques has also been found in cognitively normal subjects. Additionally, accumulated evidence from AD brains suggests that the levels of soluble Aβ oligomers correlate better with the risk and severity of the disease than insoluble amyloid plaques. In order to study the association between soluble Aβ oligomers and insoluble fibrillar plaques *in vivo*, the 5XFAD and the

Tg4-42 mouse models were crossed to produce the novel FAD4-42 model. The 5XFAD model exhibits early and aggressive amyloid pathology, while the Tg4-42 develops age-dependent CA1 neuron loss and does not develop amyloid plaques. FAD4-42 mice showed an increased amyloid burden compared to 5XFAD mice at 3 months of age.

However, at 12 months of age, no differences could be detected between 5XFAD and FAD4-42 mice. Furthermore, no neuron loss in the CA1 region of the hippocampus was observed in the FAD4-42 model at 3 or 12 months of age. These results indicate that soluble $A\beta_{4-42}$ binds to amyloid plaques resulting in a reduction of $A\beta_{4-42}$ toxicity, suggesting a potential protective effect of amyloid plaques against soluble toxic $A\beta$ oligomers.

# CONTENTS

# 1. INTRODUCTION

## 1.1 ALZHEIMER'S DISEASE

It was more than 100 years ago when the German psychiatrist and pathologist Alois Alzheimer gave his seminal presentation to the 37th Meeting of South-west German Psychiatrists held in Tübingen, Germany. Alois Alzheimer described the case of a 51-year-old female patient named Auguste Deter, who had developed severe loss of memory, disorientation, aphasia, agnosia and delusions. Post-mortem histopathological examination showed general cortical atrophy accompanied by striking neurofibrillary pathology (Alzheimer 1907). Further analysis also revealed "miliary foci" (senile plaques), which together with the neurofibrillary tangles are recognized nowadays as one of the typical features of Alzheimer 's disease (AD).

## 1.2 EPIDEMIOLOGY

According to the World Health Organization (WHO), it is estimated that around 50 million people worldwide are living with dementia. AD is the most common type of dementia and contributes approximately to 60-70 % of the cases. The total number of people with dementia is projected to increase to 82 million in 2030 and 152 million in 2050 (WHO, 2018). It is suggested that much of the increase will take place in low and middle-income countries. In 2015, deaths due to dementia were of 1.54 million worldwide, making it the 7th leading cause of global deaths. For 2018, the total estimated cost of dementia is around a trillion dollar, rising to approximately US$ 2 trillion by 2030 (Alzheimer's Association 2015).

## 1.3 RISK FACTORS FOR ALZHEIMER'S DISEASE

### 1.3.1 Nongenetic risk factors

The strongest known risk factor for AD is aging. Most patients with the disease are 65 years or older. After the age of 65, the probability of developing AD doubles about every five years. The risk reaches nearly 50% beyond the age of 85 (Alzheimer's Association, 2018). On the other hand, further epidemiological studies have linked AD with general health status. Raised systolic blood pressure and high cholesterol levels in midlife increase the risk of developing AD in later life (Kivipelto *et al.* 2001; Kennelly *et al.* 2009). Additionally, underweight, overweight and obesity at midlife are associated with an increased risk of AD at older age (Kivipelto *et al.* 2005; Anstey *et al.* 2011). Furthermore, longitudinal population-based studies have shown that the risk of AD is higher among people with diabetes mellitus than in the general population (Leibson *et al.* 1997; Zhang *et al.* 2017). Other modifiable risk factors such as smoking, alcohol consumption, depression and traumatic brain injuries have also been reported (Barnes *et al.* 2012; Giunta *et al.* 2012; Weiner *et al.* 2014; Stirland *et al.* 2017; Topiwala & Ebmeier 2017). Interestingly, accumulated evidence has demonstrated that high education, consumption of certain food, an active and socially integrated lifestyle might delay the onset of AD and have a positive impact on cognitive function (Fratiglioni *et al.* 2004; Fratiglioni & Wang 2007; Gu *et al.* 2010; Wang *et al.* 2012).

### 1.3.2 Genetic risk factors

After age, family history is the second strongest risk factor for AD (Bertram *et al.* 2010). AD can be divided into two forms based on its age of onset: (1) early-onset AD (EOAD, onset < 65 years), which accounts only for a small fraction of all AD cases (≤5%) and (2) late onset AD (LOAD, onset > 65 years), accounting for > 95% of AD cases (Reitz & Mayeux 2014). The EOAD form, also called familial AD (FAD), is caused by dominantly

inherited mutations in the β-amyloid precursor protein (APP) located at chromosome 21q21 (Goate *et al.* 1991), presenilin 1 (PSEN1) located at chromosome 14q24.3 (Sherrington *et al.* 1995) and its homolog presenilin 2 (PSEN2) located at chromosome 1q31-q42 (Levy-Lahad *et al.* 1995; Rogaev *et al.* 1995). To date, more than 50 dominant mutations have been identified in APP, 215 mutations in PSEN1 and 31 mutations in PSEN2 (Cruts *et al.* 2012). The majority of these mutations exhibit a high penetrance (>85%) and have been suggested to increase the production of total Aβ, the Aβ42 to Aβ40 ratio and Aβ aggregation, leading to EOAD (Holtzman *et al.* 2011; Reitz & Mayeux 2014).

Mutations in the APP, PSEN1 and PSEN1 genes account for all the cases in FAD, whereas the Apolipoprotein E (APOE) is the strongest genetic factor for LOAD or so-called sporadic AD (SAD). The APOE gene is located at chromosome 19q13.2 and encodes three common alleles (ε2, ε3 and ε4) that differ on two amino acid residues at either position 112 or 158 (Siest *et al.* 1995). Several studies have shown an association of APOEε4 in FAD and SAD. The presence of one copy of the APOEε4 allele increases the risk to develop AD by 3-fold, while having two copies is associated with a 15-fold increase (Corder *et al.* 1993; Pastor *et al.* 2003). Moreover, APOEε4 is associated with a dose-dependent decrease in age of onset. Interestingly, APOEε2 has been associated with a protective effect by decreasing the risk for LOAD and delaying age of onset (Corder *et al.* 1994). Unlike the mutations in the APP and PSEN1/2, the APOEε4 was considered neither sufficient nor necessary to cause AD (Myers *et al.* 1996). However, a recent study has demonstrated that APOEε4 is a risk factor not only for LOAD but also for EOAD, suggesting that APOE should be reconsidered as a "major genetic risk factor" (Genin *et al.* 2011). Regardless of the well-known genetic association of APOE in AD, its role in the pathogenesis of AD has to be clarified. *In vitro* and *in vivo* evidence suggests that APOE binds to Aβ and influences the clearance of soluble Aβ, leading to Aβ aggregation (Kim *et al.* 2009; Castellano *et al.* 2011). Indirectly, APOE also regulates Aβ metabolism by interacting with low-density lipoprotein receptor-related protein 1 receptors (Verghese *et al.* 2013). In addition, it has been shown that APOE influences the structure, level and amount of intraparenchymal Aβ deposits in an isoform-specific manner (Holtzman *et al.* 2000; Fagan *et al.* 2002).

In the last few years, the advancement of technologies able to evaluate simultaneously millions of single nucleotide polymorphisms (SNPs) have contributed to the quest for new LOAD genetic risk factors. Several genome wide associated studies (GWAS) have identified more than 20 genes with common variants associated to LOAD risk (Naj *et al.* 2017). These novel potential risk genes include *ABCA7*, *BIN1*, *CASS4*, *CD33*, *CD2AP*, *CELF1*, *CLU*, *CR1*, *DSG2*, *EPHA1*, *FERMT2*, *HLA-DRB5-DBR1*, *INPP5D*, *MS4A*, *MEF2C*, *NME8*, *PICALM*, *PTK2B*, *SLC24H4 RIN3*, *SORL1*, *ZCWPW1* (Bertram *et al.* 2008; Harold *et al.* 2009; Hollingworth *et al.* 2011; Naj *et al.* 2011; Lambert *et al.* 2013). Many of these common variants identified through GWAS have been implicated in inflammatory response, APP processing, Tau pathology, cell migration, lipid metabolism and endocytosis, reinforcing the relevance of these pathways in LOAD etiology (Karch & Goate 2015). Additionally, whole genome and exome sequencing studies have also given evidence of rare coding variants in two genes with moderate to large effects associated with LOAD risk: *TREM2* (triggering receptor expressed on myeloid cells 2) (Guerreiro *et al.* 2013; Jonsson *et al.* 2013) and *PLD3* (phospholipase D3) (Cruchaga *et al.* 2014). TREM2 is expressed on microglia and has been associated with the activation of the immune response and regulation of phagocytosis, suggesting that the role of TREM2 in AD may be trough the clearance of Aβ and/or neuroinflammatory mechanisms (Neumann & Takahashi 2007; Guerreiro *et al.* 2013). On the other hand, little is known about the function of PLD3 and its role in AD. Recent *in vitro* studies have demonstrated that overexpression of PLD3 influences APP metabolism by lowering extracellular Aβ levels, while knockdown of PLD3 has the opposite effect. However, the exact mechanism still needs to be elucidated (Cruchaga *et al.* 2014).

## 1.4 PATHOLOGICAL HALLMARKS OF ALZHEIMER'S DISEASE

### 1.4.1 Amyloid deposits

One of the main pathological hallmarks of AD is the presence of extracellular deposits (also known as senile/amyloid plaques) mainly composed of amyloid-β (Aβ) peptide (Glenner & Wong 1984a; Masters *et al.* 1985), which is a 37 to 43 amino acid peptide derived by proteolytic cleavage from the larger β-amyloid precursor protein (APP). Two different types of amyloid plaques can be distinguished based on morphological criteria, namely diffuse and neuritic or dense-core plaques (Fig. 1). In diffuse plaques, Aβ is aggregated in a non-β sheet conformation (non-fibrillar) and can be detected by anti-Aβ antibodies. The size of these plaques ranges from 50 μm to several hundred μm. On the other hand, neuritic plaques are composed of aggregated Aβ in a β-sheet conformation (fibrillar) and can be visualized with dyes such as Congo red or Thioflavin-S, as well as with immunohistological methods. Neuritic plaques are commonly surrounded by dystrophic neurites (axons and dendrites), activated astrocytes and microglial cells, and are also associated with detrimental effects including synaptic and neuron loss (Itagaki *et al.* 1989; Masliah *et al.* 1994; Knowles *et al.* 1999; Urbanc *et al.* 2002; Vehmas *et al.* 2003). The spatiotemporal progression of Aβ deposition is poorly predictable. However, it has been proposed by Thal et al. that Aβ deposition in the brain follows a descendent progression. According to the authors, Aβ deposition starts in isocortical areas, followed by allocortical and limbic structures, and at later stages, spreads to subcortical areas comprising basal ganglia and some diencephalic and brainstem nuclei (Thal *et al.* 2002). Interestingly, diffuse plaques have been detected in the brains of healthy elderly subjects with intact cognitive functions. Therefore, it has been suggested that diffuse plaques may not be directly pathological but rather neuritic plaque precursors (Delaère *et al.* 1990; Dickson *et al.* 1992). However, although Aβ deposition is a key pathological hallmark of AD, accumulative evidence has shown a poor correlation between amyloid burden and cognitive impairment (Katzman *et al.* 1988; Hulette *et al.* 1998; Price & Morris 1999; Aizenstein *et al.* 2008). In addition to the amyloid deposits found in the brain parenchyma, Aβ

aggregates can also be detected inside the vessel walls in the form of cerebral amyloid angiopathy (CAA) (Vinters 1987). CAA is highly present in AD patients, however, it can also appear in some subjects lacking parenchymal Aβ plaques (Smith & Greenberg 2009; Brenowitz *et al.* 2015)
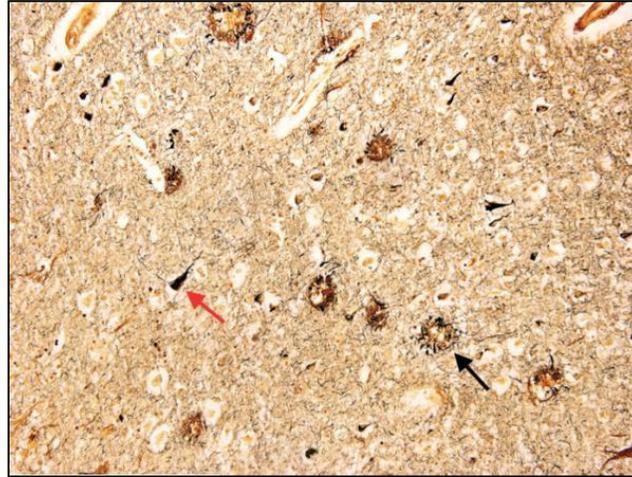


**Fig. 1. Aβ plaques and neurofibrillary tangles (NFTs).** Senile neuritic plaques (black arrow) and NFTs (red arrow) in the cortex of an Alzheimer's disease patient visualized by a Bielschowsky stain. Picture taken from (Perl, 2010)

## 1.4.2 Neurofibrillary tangles

Besides the senile plaques, neurofibrillary tangles (NFTs) are another important pathological hallmark of AD which were first described more than one century ago by Alois Alzheimer as intraneuronal, filamentous inclusions in the perikaryal and processes of pyramidal neurons (Fig. 1) (Alzheimer 1907). However, it was not until the early-sixties when it was discovered that NFTs were mainly made of paired helical filaments (PHFs), namely fibrils of ~10 nm in diameter forming pairs with a helical tridimensional conformation (Kidd 1963). Twenty years later, further studies revealed that PHFs are predominantly composed of aberrantly misfolded and highly phosphorylated forms of the microtubule-associated protein tau (Grundke-Iqbal *et al.* 1986; Kosik *et al.* 1986; Wood *et al.* 1986; Lee *et al.* 1991). Tau is an axonal

phosphoprotein highly abundant and produced in all neuron types. In humans, tau is encoded by a single gene on chromosome 17 and alternatively spliced, resulting in six major isoforms (Goedert *et al.* 1989; Himmler *et al.* 1989). Under normal physiological conditions, tau functions as a microtubule-binding and stabilizing protein (Weingarten). However, in AD, tau undergoes abnormal hyperphosphorylation, which leads to its disassociation from microtubules and following self-aggregation, giving rise to NFTs and to neuropil threads (dystrophic neurites with hyperphosphorylated and aggregated tau) (Iqbal *et al.* 2010). NFTs can be detected with Thioflavin-S fluorescent dye, or by immunostaining with anti-tau antibodies (Braak *et al.* 1994; Augustinack *et al.* 2002). Tau pathology follows a predictable and stereotypical progression, starting in the transentorhinal region, followed by limbic structures (hippocampus and amygdala) and finally progressing to all isocortical areas (Arnold *et al.* 1991; Braak & Braak 1991; Braak *et al.* 2006). Unlike amyloid pathology, clinicopathological evidence has demonstrated that NFT amount and distribution strongly correlates with the severity and duration of AD (Arriagada *et al.* 1992; Gomez-Isla *et al.* 1997; Giannakopoulos *et al.* 2003; Ingelsson *et al.* 2004).

### 1.4.3   Brain atrophy and neuronal loss

At the macroscopic level, brain atrophy is the most notable characteristic of AD. Nonetheless, cerebral atrophy can also be found in other types of dementia and even in normal ageing brains (Fig. 2) (Blennow *et al.* 2006). In AD patients, atrophic changes are first observed in the medial temporal lobe, including the entorhinal cortex, the hippocampus and the amygdala (Duyckaerts *et al.* 2009). Additionally, atrophy concentrates in the inferior temporal and the superior and middle cortices, but not in the inferior frontal and orbitofrontal cortices (Halliday *et al.* 2003). As a consequence of this cortical thinning, the lateral ventricles appear conspicuously enlarged. Using magnetic resonance imaging (MRI), subtle changes in the stereotypical pattern of cortical atrophy can be detected in asymptomatic individuals almost 10 years before

dementia. (Dickerson *et al.* 2011). Therefore, it can be utilized as a potential clinical diagnostic method of AD.

Neuronal loss is considered to be the main pathological alteration that causes the region-specific cortical atrophy observed in AD. Among other structures, neuronal death has been reported in the layer II of the entorhinal cortex, the cornu ammonis area (CA1) pyramidal layer of the hippocampus, the amygdala and some areas of the frontal, parietal, and temporal neocortex of AD patients (Vereecken *et al.* 1994; West *et al.* 1994; Gomez-Isla *et al.* 1996; Grignon *et al.* 1998). However, the cause of the neuron loss is still a matter of debate. Early observations found a direct relationship between the presence of NFTs and the neuron loss (Cras *et al.* 1995), while later studies reached opposite results, showing that neuron loss exceeds NFTs (Gomez-Isla *et al.* 1997; Kril *et al.* 2004). Alternatively, growing evidence from transgenic mice and human patients suggests that intraneuronal Aβ accumulation and/or soluble Aβ oligomers might be the principal driving forces behind the events leading to neuronal death (Haass & Selkoe 2007; LaFerla *et al.* 2007; Bayer & Wirths 2011).

In addition to neuronal death, synaptic pathology also contributes to the atrophic changes in AD brains. Ultrastructural and immunohistochemical methods have been applied to describe the loss of synaptic terminals. Synaptic and neuron loss overlap in their spatiotemporal and laminar pattern. In specific cortical areas, synaptic pathology can exceed neuronal loss (Duyckaerts *et al.* 2009; Serrano-Pozo *et al.* 2011a). Early studies showed that synaptic loss correlates better with cognitive decline than neuronal loss or amyloid plaques (Terry *et al.* 1991). More recently, analysis of the synaptic density in the stratum radiatum of the hippocampal CA1 subfield showed that individuals with mild AD had 55% less synapses compared to MCI and healthy patients. Hence, synaptic loss represents a major correlate of cognitive impairment and may be one of the first pathological events in AD (Scheff *et al.* 2007).
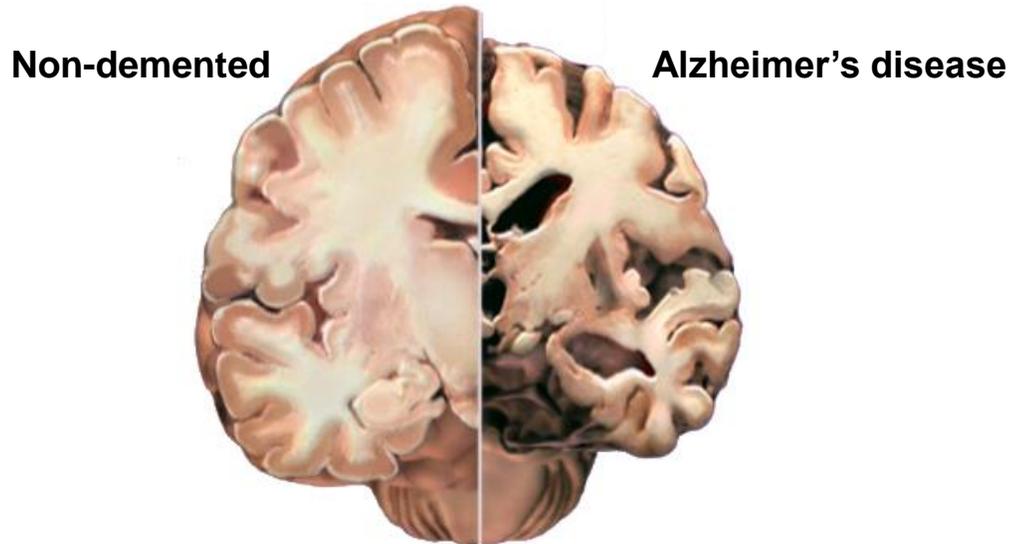
**Fig. 2. Brain atrophy.** While the non-demented control (left) shows a normal brain volume, an AD brain (right) is characterized by enlarged ventricles, shrinkage of gyri and widening of sulci. Modified from http://www.alz.org/braintour.asp.

### 1.4.4  Inflammation

Next to the previously mentioned neuropathological hallmarks, neuroinflammatory processes such as micro- and astrogliosis are prominently found in AD brains (Fig. 3). Activated microglia and reactive astrocytes are usually associated to neuritic plaques, suggesting a major role of Aβ as an activator of glial response (Itagaki *et al.* 1989; Pike *et al.* 1995a; Vehmas *et al.* 2003). However, more recent observations have also found a significant positive correlation between reactive glia and NFT burden (Ingelsson *et al.* 2004; Serrano-Pozo *et al.* 2011b). Some studies revealed that plaque-associated microglia and astrocytes can exert a neuroprotective role via endocytosis and degradation of Aβ (Nagele *et al.* 2003; Wyss-Coray *et al.* 2003; Koistinaho *et al.* 2004; Nicoll *et al.* 2006). Conversely, glial activation may also trigger a cascade of neuropathological events trough the expression of several inflammation-related factors (Wyss-Coray & Rogers 2012). Therefore, it is still unclear whether inflammation causes, contributes or protects against AD pathology.
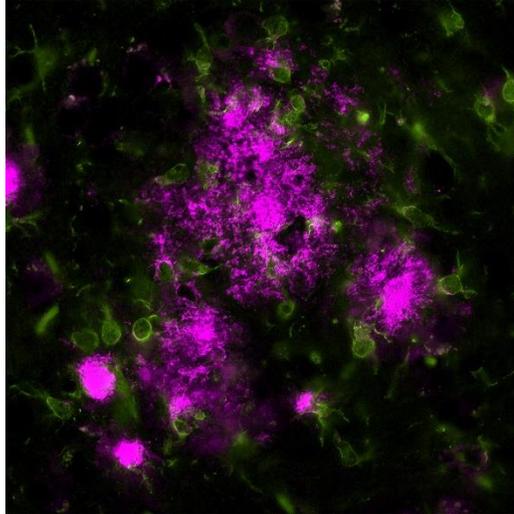
**Fig. 3. Neuroinflammatory response in AD.** Confocal image of activated Iba1-positive microglia cells (green) in the cortex of 12-month-old 5XFAD mice. Amyloid plaques (pink) are surrounded by the activated immune cells.

## 1.5 THE AMYLOID PRECURSOR PROTEIN

The isolation and characterization of Aβ from the amyloid plaque cores of AD and Down syndrome (DS) brains led to the assumption that the gene encoding Aβ was located on chromosome 21(Glenner & Wong 1984b; Masters *et al.* 1985). A few years later, cloning of the gene encoding Aβ demonstrated that it was indeed located on chromosome 21 and that Aβ was synthesized from a much larger precursor protein named the amyloid precursor protein (APP) (Goldgaber *et al.* 1987; Kang *et al.* 1987; Robakis *et al.* 1987; Tanzi *et al.* 1987). APP is a member of a family of highly conserved type I single-pass transmembrane proteins that also includes the two APP-like proteins (APLP) 1 and 2 in mammals (Wasco *et al.* 1992, 1993; Slunt *et al.* 1994). APP and APLP1/2 proteins share a significant homology in their ectodomains and cytoplasmic carboxy-terminal portions. Importantly, the Aβ containing domain is not conserved and is unique to APP (Bayer *et al.* 1999). The human APP gene is ubiquitously expressed and contains 18 exons that, by alternative splicing, generate several APP isoforms ranging from 365 to 770 amino acids residues. Among these, the major isoforms are APP695, APP751 and APP770, named after the number of amino acids residues. (Kang *et al.* 1987; Yoshikai

*et al.* 1991; Lamb *et al.* 1993). APP751 and APP770 contain a protease inhibitor domain in the extracellular sequence and are preferentially expressed in non-neuronal tissues. The shorter APP695 isoform lacks the protease inhibitor domain and is mainly expressed in neurons accounting for the majority of APP in the brain (Kitaguchi *et al.* 1988; Tanzi *et al.* 1988; Tanaka *et al.* 1989; Sola *et al.* 1993). Upon expression, APP can undergo post-translational modifications like palmitoylation, phosphorylation, sulphation and glycosylation before it reaches the plasma membrane (Selkoe 2001; Bhattacharya *et al.* 2013). The majority of APP is retained in the trans-Golgi network under basal conditions, whereas just a small fraction is transported to the plasma membrane (Koo *et al.* 1996). Once there, if proteolytic cleavage does not occur, APP is quickly internalized and subsequently trafficked into endosomes where it can be recycled (Lai *et al.* 1995; Marquez-Sterling *et al.* 1997). Also, a small portion can undergo degradation in lysosomes (Haass *et al.* 1992).

Despite the large amount of evidence accumulated since the molecular cloning of APP, its physiological functions are not yet completely understood. Nevertheless, a number of *in vitro* and *in vivo* studies have shown that APP is a multimodal protein that participates in a diversity of different processes like cell proliferation and differentiation, neurite outgrowth and synapse development (Dawkins & Small 2014; Müller *et al.* 2017). APP has also been implicated in synaptic plasticity and neuroprotection (Ludewig & Korte 2016). Furthermore, some APP isoforms (APP751/770) are believed to play a role in the blood coagulation cascade (Van Nostrand *et al.* 1989; Smith *et al.* 1990).

## 1.5.1   APP processing

### 1.5.1.1   Amyloidogenic and non-amyloidogenic pathways

Physiologically, APP can undergo complex proteolytic processing by at least three different secretases called alpha- (α), beta- (β) and gamma- (γ) secretase. This results in the formation of distinct biologically active fragments. APP processing occurs mainly

via two alternative and competing pathways commonly referred to as the "amyloidogenic" and the "non-amyloidogenic" pathways, respectively (Fig. 4) (Müller *et al.* 2017).

In the non-amyloidogenic pathway, APP is cleaved within the Aβ region (between residues Lys16 and Leu17) by the α-secretase, thus precluding the formation of Aβ (Esch *et al.* 1990; Sisodia *et al.* 1990). Various zinc metalloproteases members of the "a disintegrin and metalloprotease" (ADAM) family, including ADAM9, ADAM10 and ADAM17, can function as α-secretases (Allinson *et al.* 2003). However, in the brain, the main constitutive α-secretase activity is mediated by ADAM10 (Kuhn *et al.* 2010; Prox *et al.* 2013). The α-secretase cleavage of APP liberates a large soluble α-APP fragment (sAPPα) into the extracellular/lumen and generates the membrane-associated 83-residue α-carboxyl-terminal fragment (αCTF or C83), which lacks the N-terminal portion of the Aβ domain. The αCTF is subsequently cleaved by γ-secretase producing a 3-kDa truncated Aβ peptide named p3, which is readily degraded and apparently has no important function (Haass *et al.* 1993). Simultaneously, γ-secretase generates the APP intracellular domain (AICD) (Gu *et al.* 2001; Sastre *et al.* 2001), which is released into the cytoplasmic space and which may have a function in regulation of gene expression (Cao & Sudhof 2001; von Rotz *et al.* 2004).

Alternatively, in the amyloidogenic pathway, APP is processed by the consecutive cleavage of β- and γ-secretase (Haass 2004). First, cleavage is initiated by β-secretase generating a soluble large part of the ectodomain of APP (sAPPβ) and a membrane-tethered 99-residue β-carboxyl-terminal fragment (βCTF or C99) (Vassar *et al.* 1999). Thereafter, βCTF is cleaved by γ-secretase in multiple sequential steps within the transmembrane domain, resulting in the production of Aβ and AICD (Haass *et al.* 2012).

The β-secretase that mediates the initial steps during Aβ production is the β-site APP cleaving enzyme-1 (BACE1), which was originally named memapsin 2 or aspartyl protease 2 (Sinha *et al.* 1999; Vassar *et al.* 1999; Yan *et al.* 1999; Hong *et al.* 2000). BACE1 is a type 1 transmembrane aspartyl protease with its active site facing the lumen/extracellular space and is structurally similar to that of the pepsin family (Hong *et al.* 2000). BACE1 can cleave APP at the Asp1 and Glu11 of the Aβ domain (Liu *et al.*

2002a). BACE2 was identified as a homolog of BACE1 (Solans *et al.* 2000), however, it has been demonstrated in both human and mouse brains to be considerably lower expressed than BACE1 (Bennet). Also, as BACE2 cleaves APP more efficiently near the α-secretase site, its activity might not be directly involved in Aβ production (Yan *et al.* 2001). Studies using BACE1 knockout mice confirmed the relevance of BACE1 in amyloidogenesis. BACE1 KO mice showed no major phenotypical deficits and no detectable levels of Aβ (Luo *et al.* 2001). However, further studies found some subtle phenotypic abnormalities in BACE1 null mice, such as hyperactive behavior, memory impairment, changes in spontaneous activity and hypomyelination (Harrison *et al.* 2003; Dominguez *et al.* 2005; Hu *et al.* 2006). Besides APP, other BACE1 substrate have been identified including neuroligin-1, voltage-gated sodium channels, APP-like proteins and interleukin-like receptor II (Vassar *et al.* 2009).

γ-Secretase is a high molecular transmembrane complex that consists of four protein subunits: presenilin (PS) 1 or PS2, nicastrin (NCT), anterior pharynx defective (APH)-1a or APH-1b and the presenilin enhancer 2 (PEN2)(Wolfe *et al.* 1999; Yu *et al.* 2000; Francis *et al.* 2002; Kimberly *et al.* 2003). PSs possess the catalytic region for APP cleavage consisting of two highly conserved aspartyl residues within the transmembrane domains 6 and 7, while the biological functions of NCT, APH-1a/b and PEN2 are not well known. Yet, the four components are indispensable for the proper γ-secretase activity (Steiner *et al.* 2008; De Strooper *et al.* 2012). The APP intramembrane cleavage by γ-secretase is a type of regulated intramembrane proteolysis (RIP) and can occur at distinct sites. These cleavage sites are known as the ε-, ζ- and γ- sites, which are approximately three amino acids separated from each other (Lichtenthaler *et al.* 2011). Therefore, the final γ-secretase cleavage can occur at different sites within the Aβ domain, yielding a variety of Aβ peptides ranging from 37 to 43 amino acids in length. Under non-pathologic physiological conditions, the most common isoform produced is $A\beta_{1-40}$ and to a minor extend $A\beta_{1-42}$, the more amyloidogenic isoform (Thinakaran & Koo 2008).
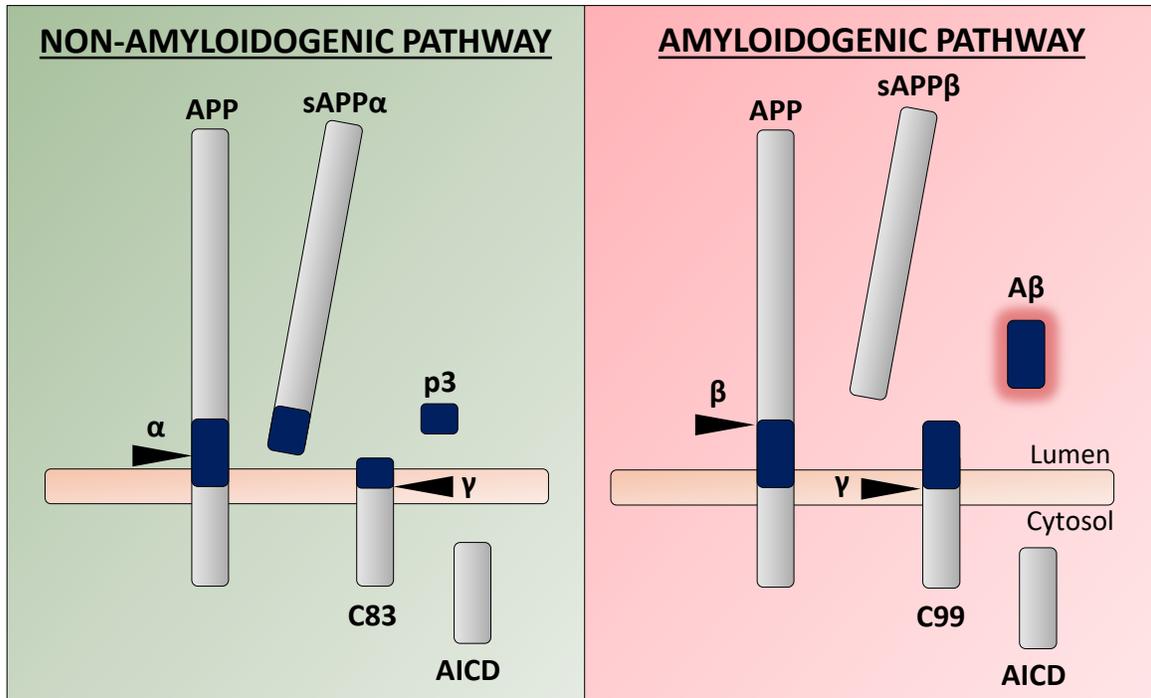
**Fig. 4. APP processing.** In the non-amyloidogenic pathway (left), APP is cleaved by the α- and γ-secretases which results in the release of p3 and AICD. During the amyloidogenic pathway (right), APP initially is cleaved by the β-secretase BACE1 followed by subsequent cleavage by γ-secretase. The second cleavage event leads to the release of the Aβ peptide and AICD. Adapted from (Haass *et al.* 2012)

## 1.5.2 The amyloid cascade hypothesis

Almost 30 years ago it was first proposed that accumulation of Aβ, the main constituent of plaques, is the causative factor in AD pathogenesis. This assumption was termed as "the amyloid cascade hypothesis", also commonly known as "the amyloid hypothesis" (Fig. 5). According to the amyloid cascade hypothesis, amyloid-β deposition and aggregation renders the downstream pathological events associated with AD such as the neurofibrillary tangles, neuron death, brain atrophy, vascular damage, cognitive impairments and other associated clinical symptoms (Beyreuther & Masters 1991; Hardy & Allsop 1991; Selkoe 1991; Hardy & Higgins 1992). Several lines of evidence support this theory. For instance, DS patients, who exhibit a triplication of the gene encoding for APP, develop the amyloid and tau pathology typically found in AD brains (Wisniewski *et al.* 1985). Genetic studies of FAD cases strongly support the amyloid

cascade hypothesis by demonstrating that mutations or duplications in APP, PS1 and PS2 genes enhance production and aggregation of Aβ causing EOAD (Rovelet-Lecrux *et al.* 2006; Reitz & Mayeux 2014). Furthermore, the most relevant genetic risk factor in LOAD, APOE ε4, is related with an increase in Aβ aggregation and reduction in Aβ clearance (Kim *et al.* 2009; Castellano *et al.* 2011). In addition, transgenic mice overexpressing FAD mutations develop some of the pathological key features of AD including amyloid plaques, neuroinflammation and memory impairment in an age-dependent manner (Duyckaerts *et al.* 2008; Radde *et al.* 2008). Interestingly, in a more recent study, researchers found a coding mutation in the *APP* gene (Ala to Thr; A673T) that protects against AD. *In vitro,* the mutation caused a ~40% reduction in Aβ generation. Also, they found that elderly heterozygous individuals carrying the mutation performed better in cognitive tests than control subjects. This protective effect provides additional support for the amyloid hypothesis by showing that reducing Aβ production may be protective against AD (Jonsson *et al.* 2013). On the other hand, tau mutations cause frontotemporal dementia with parkinsonism, which is characterized by severe tau pathology in the brain with no amyloid deposition (Hutton *et al.* 1998; Poorkaj *et al.* 1998; Goedert & Spillantini 2000). Analysis of transgenic mice overexpressing mutant tau and APP revealed an enhanced neurofibrillary tangle pathology in comparison with mice overexpressing mutant tau only, while amyloid pathology remained unaltered (Lewis *et al.* 2001). Taken together, this suggests that the NFTs observe in AD brains are likely to be a consequence of either APP or Aβ and not the cause of the AD pathological events.

Nonetheless, the amyloid cascade hypothesis remains controversial. One of the main arguments undercutting this hypothesis is that, in contrast to the amount of NFTs, amyloid burden correlates poorly with the cognitive status in AD. Likewise, *post mortem* analysis of brains from non-demented individuals revealed abundant amyloid deposits (Katzman *et al.* 1988; Hulette *et al.* 1998; Price & Morris 1999; Aizenstein *et al.* 2008). Furthermore, transgenic AD mouse models overexpressing APP and/or PSs, exhibit no correlation between Aβ plaques and cognitive deficits or neurodegenerative alterations (Benilova *et al.* 2012).

Due to the development of better qualitative and quantitative methods for analyzing Aβ, in addition to more recent evidence from transgenic AD mouse models, cell culture and human genetic data, modifications to the early versions of the amyloid cascade hypothesis have been proposed in the last years.

### 1.5.3 The soluble amyloid hypothesis

As mentioned above, the "original" amyloid cascade hypothesis attributed AD onset to the toxic effect caused by the large insoluble amyloid fibrils. However, a number of studies have demonstrated that either synthetic or natural soluble oligomeric forms of Aβ (e.g., dimers, trimers, dodecamers and higher oligomers larger than 100kDa) are neurotoxic and might have direct neurodegenerative effects, whilst fibrillar or monomeric Aβ appeared to be less detrimental *in vitro* (Lambert *et al.* 1998; Dahlgren *et al.* 2002; Wang *et al.* 2002), as well as *in vivo* using animal models (Walsh *et al.* 2002; Cleary *et al.* 2005; Lesne *et al.* 2006; Shankar *et al.* 2008)*.* Additionally, a series of studies utilizing brain tissue extracts from AD patients collected *post mortem* have revealed the presence of soluble oligomeric Aβ species (Kuo *et al.* 1996; Roher *et al.* 1996; Shankar *et al.* 2008; Tomic *et al.* 2009). Also, it has been shown that the existence of such soluble Aβ species is a better correlate of the presence and the degree of cognitive decline than amyloid plaques in AD (McLean *et al.* 1999; Mc Donald *et al.* 2010; Esparza *et al.* 2013). This gave rise to the concept that soluble bioactive Aβ oligomers might be the key players in AD pathogenesis and not the inactive insoluble amyloid plaques. This concept has also been supported by several laboratories demonstrating that nearly all Aβ oligomer species can impair synaptic function through changes in dendritic spine morphology, altered long-term potentiation (LTP) and long-term depression (LTD) in hippocampal slice cultures (Walsh *et al.* 2002; Wang *et al.* 2002; Li *et al.* 2009; Wu *et al.* 2010). Moreover, electrophysiological and behavioral alterations have been observed in APP transgenic mice in the absence of amyloid plaques (Holcomb *et al.* 1998; Hsia *et al.* 1999; Mucke *et al.* 2000; Tomiyama *et al.* 2010).

**1.5.4 Intraneuronal amyloid hypothesis**

Soon after the discovery of Aβ as the main component of extracellular amyloid plaques three decades ago, the first reports describing that Aβ is first deposited intracellularly and later in the extracellular space started to appear (Masters *et al.* 1985; Grundke-Iqbal *et al.* 1989). Subsequent studies demonstrated that intracellular Aβ highly accumulates in neurons from regions susceptible of developing early AD pathology. These regions include the hippocampus and the entorhinal cortex. Curiously, intracellular Aβ accumulation occurred prior to the appearance of NFTs and extracellular Aβ deposition (Gouras *et al.* 2000; Fernandez-Vizarra *et al.* 2004). Likewise, it has been shown that intraneuronal Aβ strongly accumulates in young DS patients, but it declines as extracellular amyloid plaques accumulate. The subsequent maturation of the amyloid plaques induce inflammatory responses prior the formation of NFTs (Mori *et al.* 2002).

More recently, studies combining laser capture microdissection and sensitive Aβ ELISA showed elevated levels of Aβ$_{1-42}$ and an increase in the ratio Aβ$_{1-42}$/Aβ$_{1-40}$ in CA1 pyramidal and Purkinje neurons of both sporadic and familial AD compared to control subjects. Yet, the levels of Aβ$_{1-40}$ remain unchanged between AD cases and controls, suggesting that high intraneuronal concentration of Aβ$_{1-42}$ correlates with increase susceptibility to AD pathology (Aoki *et al.* 2008; Hashimoto *et al.* 2010). Using immuno-electron microscopy, the subcellular site of intraneuronal Aβ accumulation was determined. Neurons of normal mouse, rat, and human brains exhibited localization of Aβ$_{1-42}$ predominantly on endosomal multivesicular bodies (MVBs). In transgenic APP mice and AD brains, intraneuronal Aβ$_{1-42}$ increased in an age-dependent manner and localized in MVBs within pre- and post-synaptic compartments (Takahashi *et al.* 2002). Furthermore, evidence from neuron cultures (Runz *et al.* 2002; Takahashi *et al.* 2004; Almeida *et al.* 2006) and AD brains (Cataldo *et al.* 2004; Van Broeck *et al.* 2008) have also revealed intraneuronal Aβ$_{1-42}$ accumulation within endosomes and lysosomes. It has also been demonstrated that Aβ accumulation in the aforementioned sites might lead to neuronal death probably via disruption of the endosomal/lysosomal system

functions (Nixon 2005; Liu *et al.* 2010) or inhibition of the ubiquitin-proteasome system (Oh *et al.* 2005; Almeida *et al.* 2006; Tseng *et al.* 2008).

Besides intracellular Aβ production, an alternative source that might contribute to intraneuronal Aβ accumulation is the re-uptake of Aβ from the extracellular space. Several potential internalization mechanisms have been proposed to mediate this process. One possible mechanism implicates the binding of Aβ to α7nicotinic acetylcholine receptors which are then internalized resulting in intracellular Aβ accumulation (Nagele *et al.* 2002; Oddo *et al.* 2005). It has been suggested that in addition to Aβ production, APOE receptors, members of the low-density lipoprotein receptor (LDLR) family, may also modulate Aβ cellular uptake(Bu *et al.* 2006). Additional other mechanisms involving integrins, N-methyl-D-aspartate (NMDA) (Bi *et al.* 2002) and advanced glycation end products (RAGE) receptors (Takuma *et al.* 2009) as well as passive diffusion of extracellular Aβ (Nagele *et al.* 2002) have been suggested. The role of intraneuronal Aβ in AD pathology has also been supported by evidence collected from transgenic mouse models (LaFerla *et al.* 2007; Bayer & Wirths 2010). For instance, early intraneuronal Aβ accumulation has been reported in transgenic mice carrying FAD mutations such as the APP/PS1 (Schmitz *et al.* 2004), the APP/PS1KI (Casas *et al.* 2004; Christensen *et al.* 2008; Breyhan *et al.* 2009) and the 5XFAD model (Oakley *et al.* 2006; Jawhar *et al.* 2012), which nicely correlates with neuron loss, synaptic and behavioral alterations. Additionally, intraneuronal Aβ accumulation has been observed in more recently generated transgenic mouse models expressing only N-truncated Aβ$_{pE3-42}$ (Wirths *et al.* 2009; Wittnam *et al.* 2012) or Aβ$_{4-42}$ (Bouter *et al.* 2013). In these models, severe hippocampal neuron loss and associated neurological deficits were detected as well (Wittnam *et al.* 2012; Bouter *et al.* 2013; Meissner *et al.* 2015). Interestingly, extracellular amyloid deposits were scarcely detected in these animals. Overall, accumulating evidence suggests that intraneuronal Aβ accumulation is likely to be an early step in AD pathogenesis, preceding the formation of extracellular amyloid plaques and tau pathology (Wirths *et al.* 2004).

| THE CLASSICAL AMYLOID CASCADE | THE MODIFIED AMYLOID CASCADE |
|---|---|
| Risk factors: Age, Down Syndrome, APP or PSEN1/2 mutations | Risk factors: Age, Down Syndrome, APP or PSEN1/2 mutations |
| ↓ | ↓ |
| Increased levels of extracellular Aβ40/42 | Increased levels of intracellular Aβ40/42 |
| ↓ | |
| Extracellular Aβ40/42 deposition in form of plaques | Intraneuronal Aβ40/42 accumulation / Soluble extra-cellular Aβ40/42 |
| ↓ | |
| Synaptic and neuronal dysfunction | Dysfunction of neurons And synapses / Formation of amyloid plaques |
| ↓ | |
| Loss of synapses and neurons | Brain atrophy |
| ↓ | |
| Atrophy of distinct brain areas | Dementia and other AD symptoms |
| ↓ | |
| Dementia and other symptoms of AD | |

**Fig. 5. Classic and modified amyloid cascade hypothesis.** While the classical amyloid hypothesis (left) states that the extracellular deposition of Aβ plaques is the causative event of AD pathology, the modified amyloid cascade (right) rather considers intracellular accumulation of Aβ as the key event during AD pathology. Adapted from (Wirths *et al.* 2004).

## 1.5.5 Amyloid peptide heterogeneity

The Aβ peptide can be found in a plethora of different isoforms, being $A\beta_{1-42}$ and $A\beta_{1-40}$ the two major variants. It was reported that $A\beta_{1-42}$ is the main component of amyloid plaques, while $A\beta_{1-40}$ is abundantly present in CAA (Iwatsubo *et al.* 1994; Suzuki *et al.* 1994; Saido *et al.* 1995). Hence, particular interest has been focused on $A\beta_{1-42}$ and its association with AD pathology. *In vitro* and *in vivo* studies have demonstrated that PS AD-associated mutations enhance $A\beta_{1-42}$ production at the expense of $A\beta_{1-40}$, thus, altering the $A\beta_{1-42}$ /$A\beta_{1-40}$ ratio, which is a critical factor by which PS mutations cause FAD (Borchelt *et al.* 1996). Moreover, it has been shown that $A\beta_{1-42}$ is more neurotoxic and prone to aggregate than the shorter $A\beta_{1-40}$ variant (Jarrett *et al.* 1993; Jan *et al.* 2008). In addition to the so called full length $A\beta_{1-40/42}$ peptides, other isoforms differing in their C-terminal domain ranging from $A\beta_{1-39}$ down to $A\beta_{1-17}$ have been found (Wiltfang *et al.* 2002; Portelius *et al.* 2011; Reinert *et al.* 2016). Moreover, longer Aβ peptides including $A\beta_{1-43/45/46/48}$ have been described in cell lines (Qi-Takahara *et al.*

2005; Yagishita *et al.* 2006). Longer forms of Aβ have also been detected in transgenic mice (Esh *et al.* 2005; Shimojo *et al.* 2008; Van Vickle *et al.* 2008). Furthermore, in sporadic and familial AD brains, the Aβ$_{x-43}$ variant was more frequently found in amyloid plaque cores than Aβ$_{x-40}$ (Welander *et al.* 2009).

### 1.5.6  Amino-terminally truncated amyloid beta peptides

Besides various C-terminal Aβ isoforms, several N-terminally truncated Aβ variants have been reported (Bayer & Wirths 2014). In fact, different studies have shown that these N-terminal Aβ isoforms constitute the majority of Aβ species in AD brains (Masters *et al.* 1985; Mori *et al.* 1992; Sergeant *et al.* 2003; Portelius *et al.* 2010). This has been further supported by a very recent study using high-resolution mass spectrometry where Wildburger and colleagues analyzed the brains of severely demented AD patients. They found that approximately 70% of the total Aβ species detected corresponded to N-terminal Aβ proteoforms including Aβ$_{2/3/4/5/8/11-x}$. (Wildburger *et al.* 2017). So far, little is known about the specific enzymes involved in the N-truncation of Aβ; nevertheless, some potential candidate enzymes have been suggested (Bayer & Wirths 2014). The Aβ$_{2-x}$ variants have been found to be elevated in AD brains (Arai *et al.* 1999; Wiltfang *et al.* 2001). Treatment with aminopeptidase A (APA) inhibitor in cells over- expressing the Swedish APP mutations increased full length Aβ levels, thereby, suggesting APA as the enzyme responsible for the cleavage of Asp-1 (Sevalle *et al.* 2009). Furthermore, more recent studies demonstrated that the metalloprotease meprin-β was capable to cleave APP in a BACE1-independent manner, generating Aβ isoforms with N-terminals starting at Asp-1 or Arg-2. Therefore, it was proposed that besides APA, meprin-β might also participate in Aβ$_{2-x}$ production (Bien *et al.* 2012; Schonherr *et al.* 2016). Moreover, it has been demonstrated that one of the major Aβ-degrading enzymes, the zinc-metalloprotease neutral endopeptidase or neprilysin (NEP), cleaves Aβ species at several sites. Among other cleavage sites, NEP is supposed to cleave Aβ peptides between Arg-2 and Glu-3, Glu-3 and Phe-4 or Arg-5 and His-6, generating Aβ$_{3-x}$, Aβ$_{4-x}$ and Aβ$_{6-x}$, respectively. In contrast, NEP had no effect

on full-length APP metabolism (Howell *et al.* 1995; Leissring *et al.* 2003). Another enzyme, the myelin basic protein (MBP), has been suggested in the N-terminal truncation of Aβ. Mass spectrometry analysis showed that *in vitro*, MBP is able to cleave between Phe-4 and Arg-5 of the Aβ sequence (Liao, 2009). Hu et al. demonstrated that the angiotensin converting enzyme (ACE) degrades Aβ by cleaving Aβ$_{1-40}$ at the site between Asp7 and Ser8, leading to the production of Aβ$_{8-40}$. Interestingly, they also found that ACE inhibited Aβ aggregation and cytotoxicity *in vitro* (Hu *et al.* 2001). Besides the generation of Aβ$_{1-x}$, BACE1 also mediates Aβ$_{11-x}$ liberation by the cleavage of Aβ between Tyr-10 and Glu-11 (Vassar *et al.* 1999).

Pike and collaborators reported that N-terminally truncated Aβ peptides exhibit enhanced aggregation and neurotoxicity in relation to full-length Aβ *in vitro* (Pike *et al.* 1995b). The authors compared the biophysical and bioactive properties of Aβ peptides with progressively shortened N-termini (starting at positions Asp-1, Phe-4, Ser-8, Val-12, and Lys-17) and C-termini extending to residue 40 or 42. Altogether, peptides with N-terminal truncations and ending at residue 42 showed enhanced peptide aggregation relative to full-length species. Moreover, N-truncated Aβ peptides exhibited fibrillar morphology as seen by transmission electron microscopy, and significant toxicity in cultures of rat hippocampal neurons (Pike *et al.* 1995b).

Besides N- and C- terminal truncations, post-translational modifications of Aβ such as oxidation, glycosylation, phosphorylation, isomerization, racemization, nitration and pyroglutamation have been identified (Kummer & Heneka 2014). These modifications generate Aβ peptides with different biophysical and bioactive properties that might be relevant for AD progression as well.

### 1.5.7  Pyroglutamate-modified amyloid beta 3-42

Mori and colleagues were the first who described the presence of Aβ peptides bearing a pyroglutamate at their N-terminus in AD brains  (Mori *et al.* 1992). Using a pyroglutamyl peptide hydrolase they were able to unravel the glutamate blocked by conversion to pyroglutamate. Further amino acid sequencing and mass spectrometric

analysis of the Aβ peptides extracted and purified from cortices of AD brains, revealed that ~15 to 20 % of the total N-terminally truncated Aβ fragments corresponded to species starting at Glu-3. The presence of pyroglutamate modified Aβ$_{3-x}$ (Aβ$_{pE3-x}$) was further sustained by Saido et al. trough immunohistochemical and biochemical methods. They showed that Aβ$_{pE3-x}$ is present in equivalent or even greater quantities than full length Aβ$_{1-x}$ in senile plaques. Additionally, the authors suggested that Aβ$_{pE3-x}$ deposition may precede that of Aβ$_{1-x}$ based on their observations in DS brains (Saido *et al.* 1995). In line with this, analysis of frontal cortex extracts from AD and DS patients using specific sandwich ELISAs revealed that Aβ$_{pE3-42/43}$ represented ~25% of total Aβ$_{x-42/43}$. Additionally, Aβ$_{pE3-40}$ was closely related with the extent of Aβ deposition in blood vessels, which was not the case for Aβ$_{pE3-42/43}$ (Harigaya *et al.* 2000). Ever since, further studies employing different technical and methodological approaches have supported the presence of Aβ$_{p3-x}$ as an important pathological component in AD brains (Sergeant *et al.* 2003; Guntert *et al.* 2006; Portelius *et al.* 2010; Moore *et al.* 2012; Rijal Upadhaya *et al.* 2014).

### 1.5.8  Pyroglutamate amyloid beta formation

Prior AβpE formation, the removal of the first two amino acids of the Aβ sequence is required in order to expose the glutamate at position 3. As mentioned earlier, it is thought that this process might involve the proteolytic activity of neprilysin (Bayer & Wirths, 2014). Additionally, it was proposed that truncated Aβ$_{3-40/42}$ might be generated by Cu$^{2+}$-mediated amide hydrolysis (Drew *et al.* 2009). The enzyme glutaminyl cyclase (QC) was identified as the enzyme responsible to catalyze Aβ$_{3-40/42}$ conversion to form Aβ$_{pE3-40/42}$ *in vitro* and *in vivo*. In addition to glutamate, QC can also catalyze N-glutamine cyclization (Schilling *et al.* 2004, 2008; Cynis *et al.* 2006). Furthermore, QC expression was found to be upregulated in the cortices of AD patients which correlated with the occurrence of pyroglutamate modified Aβ (Schilling *et al.* 2008).

It has been shown that $A\beta_{pE3}$ modification leads to alterations in the biophysical and biochemical properties. Saido and coworkers suggested that the formation of the lactam ring in combination with the loss of two negative charges and one positive charge substantially increases hydrophobicity resulting in more stability and aggregation tendency of $A\beta_{pE3}$ (Saido *et al.* 1996). On the other hand, it has also been proposed that the loss of N-terminal charges may decrease charge repulsion between strands, facilitating β-sheet formation (He & Barrow 1999). Additionally, *in vitro* studies of Russo et al. revealed that $A\beta_{pE3-40/42}$ are more cytotoxic than full-length $A\beta_{1-40/42}$. Also, they reported that $A\beta_{pE3-40/42}$ peptides exhibited significant degradation resistance by astrocytes, while full-length $A\beta$ peptides were partially degraded (Russo *et al.* 2002). In a similar manner, other studies showed that treatment of neuroblastoma cells with mixtures of $A\beta_{pE3-42}$ to $A\beta_{1-42}$ at ratios resembling to those detected in AD, resulted in an increased cell membrane permeability and reduced cell viability compared to $A\beta$ mixtures consisting of $A\beta_{pE3-42}/A\beta_{1-42}$ ratios similar to that found in non-demented brains (Piccini *et al.* 2005).

The toxic effect of $A\beta_{pE3-42}$ has also been studied *in vivo* using different approaches. It was demonstrated that pharmacological inhibition of QC in two different transgenic AD mouse models resulted in reduction of $A\beta_{pE3-42}$ and amyloid plaque burden, which was accompanied by improvement in cognitive tests performance. On the other hand, overexpression of QC by crossing mice expressing human QC and transgenic AD mice resulted in increased $A\beta_{pE3-42}$ levels, enhanced amyloid plaque load and more severe behavioral deficits (Jawhar *et al.* 2011). Passive immunization of transgenic AD mice with specific anti-$A\beta_{pE3-x}$ antibodies has been shown to reduce amyloid plaque burden and reverse cognitive impairments (Wirths *et al.* 2010). Moreover, to directly investigate the toxic effect of $A\beta_{pE3-42}$ *in vivo*, transgenic mouse models expressing exclusively truncated mutant human $A\beta_{pE3-42}$ have been created. Such models include the TBA2 and TBA2.1/2.2 lines, which exhibit strong intraneuronal accumulation of $A\beta_{pE3-42}$, progressive motor deficits, neurodegeneration and inflammatory responses (Wirths *et al.* 2009; Alexandru *et al.* 2011). In addition, a more recent TBA42 mouse model also expressing $A\beta_{pE3-42}$ has been well characterized.

### 1.5.9 Amino-truncated amyloid beta 4-42

When Masters and colleagues isolated and sequenced the amyloid plaque cores of patients with SAD and DS back in 1985, they found that the majority of Aβ species started with a phenylalanine at position 4 of amyloid-β (Aβ$_{4-x}$) (Masters *et al.* 1985). Curiously, they reported that 64% of the peptides in amyloid plaques of the SAD cases analyzed begin with a Phe-4 residue. Later studies utilizing Matrix-assisted laser-desorption/ionization-time-of-flight (MALDI-TOF) mass spectrometry of core amyloid extracts from AD brains revealed high heterogeneity of peptides ending with Ala-42, whereas CAA possessed less N- and C-terminal heterogeneity. In the amyloid core preparation, the major component started with Phe-4 followed by Ser-8 and Glu-3. Also, the MALDI-TOF data suggested the presence of pE-3 and pE-11 (Miller *et al.* 1993). Furthermore, Näslund et al. tested SAD and FAD brain tissue by means of electrospray-ionization (ESI) mass spectrometry. They found that Aβ$_{4-42}$ together with Aβ$_{8-42}$ were the most prevalent minor Aβ isoforms (Näslund *et al.* 1994). More recent studies have supported these previous findings. Lewis and colleagues analyzed Aβ peptides extracted from *post mortem* cerebral cortices of patients with AD, vascular dementia and non-demented elderly controls. According to their mass spectrometric data, N-terminally truncated Aβ4-42 species represent the most prominent Aβ variants in all groups tested (Lewis *et al.* 2006). Furthermore, in a detailed study by Portelius et al. using immunoprecipitation in combination with mass spectrometry (IP/MS) analysis, they determined the Aβ variants pattern in three different brain regions of SAD, FAD and non-demented controls (Portelius *et al.* 2010). The authors reported that in all the regions studied, Aβ$_{1-42}$, Aβ$_{pE3-42}$, Aβ$_{4-42}$ and Aβ$_{1-40}$ were the most prominent isoforms, of which Aβ$_{1-42}$ and Aβ$_{4-42}$ were the dominating variants in the hippocampus and cortex of all groups analyzed. In a similar approach, Moore and colleagues profiled the Aβ species present in the prefrontal cortex obtained from brain tissue of (i) patients with AD, (ii) individuals with pathological aging (PA) (AD-like neuropathology without clinical cognitive symptoms), and (iii) elderly subjects with no clinical evidence of dementia. They found that in the SDS soluble fractions Aβ$_{1-42}$, Aβ$_{4-42}$ and Aβ$_{1-40}$ were the most dominant peptides in all groups tested, while in the plaque-associated (insoluble)

fractions, the group with PA revealed higher $A\beta_{4-42}$, $A\beta_{pE3-42}$ and $A\beta_{1-42}$ levels in comparison with the non-demented control group (Moore *et al.* 2012). More recently, these findings were supported and extended by studies showing that besides $A\beta_{1-40/42}$ species, $A\beta_{4-42}$ and $A\beta_{pE3-42}$ are the most abundant peptides present in AD and PA brains. However, in AD subjects, $A\beta_{4-42}$ was found to be ~4 times more elevated than in PA subjects (Portelius *et al.* 2015).

Despite the high amount of evidence showing that $A\beta_{4-42}$ is one of the major components of amyloid plaques, relatively little is known about its properties and role in AD pathology. It has been suggested that $A\beta_{4-x}$ may originate from the cleavage of full-length $A\beta$ between Glu-3 and Phe-4 by NEP (Bayer & Wirths 2014). *In vitro* assays, have shown that similar to the $A\beta_{pE3-42}$ isoform, $A\beta_{4-42}$ is rapidly converted into soluble oligomers and its propensity to aggregation is more pronounced than the one of intact $A\beta_{1-42}$ (Pike *et al.* 1995b; Bouter *et al.* 2013). In addition, cell viability assays have shown that exposure to $A\beta_{4-42}$ has similar toxic effects as $A\beta_{pE3-42}$ and $A\beta_{1-42}$ (Bouter *et al.* 2013). The direct toxic *in vivo* effect has been analyzed in the Tg4-42 transgenic mouse model which expresses solely $A\beta_{4-42}$ (Section 1.6.2) In general, these mice develop strong intraneuronal $A\beta$ accumulation accompanied by massive neuron loss in the hippocampus and spatial reference memory deficits (Bouter *et al.* 2013).

## 1.6  TRANSGENIC ALZHEIMER'S DISEASE MOUSE MODELS

### 1.6.1  The TBA42 mouse model

The TBA42 mouse model was created to exclusively produce and secrete the N-terminally truncated $A\beta_{pE3-42}$ peptide. TBA42 mice (truncated beta amyloid 42) express the murine thyrotropin-releasing-hormone-$A\beta$ (mTRH-$A\beta$3-42) under the control of the murine Thy1.2 regulatory sequence (Fig. 6) (Wittnam *et al.* 2012). In order to facilitate enhanced production of $A\beta_{pE3-42}$, the glutamate at position 3 of the $A\beta$ sequence was mutated into glutamine. Accordingly, the TBA42 mice express

unmodified Aβ$_{3Q-42}$ (as for now called Aβ$_{3-42}$), which can be readily converted to Aβ$_{pE3-42}$ (Cynis *et al.* 2006; Wirths *et al.* 2009; Wittnam *et al.* 2012).
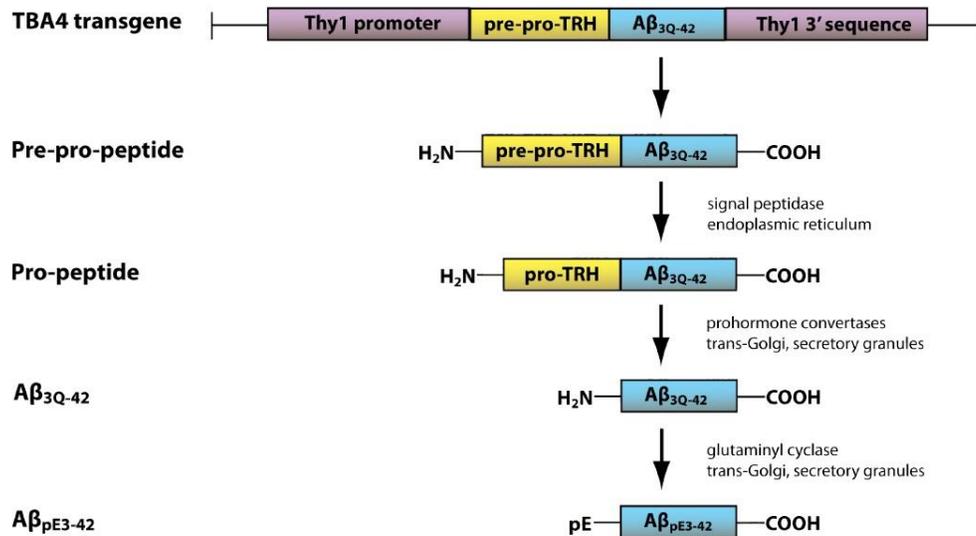


**Fig. 6. The TBA42 transgene.** The Aβ$_{3Q-42}$ sequence is fused to the pre-pro-TRH peptide in order to ensure secretion of the peptide. The neuronal expression is induced by the Thy1 promoter. After the release of Aβ$_{3Q-42}$, its free N-terminus can undergo cyclization by QC which results in the formation of Aβ$_{pE3-42}$. Picture taken from (Wittnam, 2012).

Already at the age of three months, abundant intracellular Aβ accumulation can be detected in the pyramidal neurons of the CA1 area of the hippocampus in the TBA42 mice. Moreover, at 6 months of age, intraneuronal Aβ accumulation can be detected in the cerebellar nuclei. Marked astrogliosis is observed in the hippocampus of 12-month-old mice with additional Aβ accumulation in the spinal cord (Wittnam *et al.* 2012). Extracellular Aβ deposits are barely observed in the TBA42 at all ages studied. Furthermore, unbiased-stereology quantification revealed a significant 35% percent neuron loss in the pyramidal layer of the CA1 area at 12 months of age (Meissner *et al.* 2015).

Age-dependent behavioral and cognitive alterations have been detected in the TBA42 mice. Using the cross maze, working memory deficits were revealed at 12 months of age. Also, learning and spatial working memory impairment is observed at

12 months of age as measured by the Morris water maze test (MWM) (Meissner *et al.* 2015). TBA42 mice also develop reduced anxiety levels in an age-dependent manner. At 6 months of age, motor and sensory deficits are detected, which aggravate as the animals age (Wittnam *et al.* 2012; Meissner *et al.* 2015). Taken together, the TBA42 model reveals that long-term exposure to $A\beta_{pE3-42}$ induces neurodegeneration in the CA1 region of the hippocampus, which is accompanied by cognitive and behavioral deficits. Interestingly, this model does not develop amyloid plaque pathology, thus supporting the concept that soluble Aβ oligomeric forms are likely to play a pivotal role in AD pathogenesis.

### 1.6.2   The Tg4-42 mouse model

The recently created Tg4-42 model is the first, and currently only mouse model uniquely expressing the N-truncated human $A\beta_{4-42}$ peptide, one of the most abundant Aβ variants found in the brain of AD patients (Masters *et al.* 1985; Lewis *et al.* 2006; Portelius *et al.* 2010). In order to produce and secrete the Aβ4-42 peptide, the human $A\beta_{4-42}$ sequence was fused to the TRH signal peptide under the control of the Thy1 promoter, thus ensuring extracellular secretion of $A\beta_{4-42}$ in a neuron-specific fashion (Bouter *et al.* 2013). Unlike the TBA42 model, Tg4-42 mice overexpress $A\beta_{4-42}$ without any mutation.

At two months of age, intraneuronal Aβ can be detected predominantly in the CA1 region of the hippocampus in the hemizygous Tg4-42 mice (Tg4-42[hem]). In addition, Aβ is also found in the occipital cortex, striatum, superior colliculus and piriform cortex (Bouter, 2013). Active astrocytes and reactive microglia accompany hippocampal Aβ expression beginning at two months of age. The Tg-4-42 mice do not develop extracellular amyloid plaques, yet the secreted $A\beta_{4-42}$ forms soluble neurotoxic oligomers that induce severe neuron loss in the CA1 region of the hippocampus in an age- and dose-dependent manner (Bouter *et al.* 2013; Antonios *et al.* 2015). At 8 months of age, Tg4-42[hem] mice show a 38% neuron loss, which is even enhanced in age-matched homozygous Tg4-42 mice (Tg4-42[hom]) with a massive 66% neuron loss when compared

to wild-type (WT) controls (Bouter *et al.* 2013). Moreover, 12-month-old Tg4-42$^{hem}$ mice display a 49% decline in neuron numbers compared to WT controls. The loss of neurons is accompanied by spatial reference learning and memory deficits as measured by the MWM in 6-month-old Tg4-42$^{hom}$ and 12-month-old Tg4-42$^{hem}$ mice (Bouter *et al.* 2013). These latter mice also display impaired contextual learning as demonstrated by the contextual and tone fear conditioning task (Bouter *et al.* 2014). However, in spite of the exacerbated neuron death and cognitive deficits developed in the Tg4-42 model, these mice are able to respond to different therapeutic approaches. For instance, passive immunization of Tg4-42 mice with an antibody against N-terminal Aβ$_{4-x}$ resulted in a diminished CA1 neuron loss and a rescue of spatial reference memory deficits (Antonios *et al.* 2015). Likewise, it was demonstrated that long-term voluntary exercise and cognitive stimulation reduces hippocampal neuron loss and completely rescues spatial memory deficits in Tg4-42 mice (Hüttenrauch *et al.* 2016).

Additionally, unlike the majority of transgenic AD mouse models relying on APP/PS mutations, the Tg4-42 model is devoid of any mutation, thereby, it represents a convenient model to study SAD which accounts for the majority of AD cases.
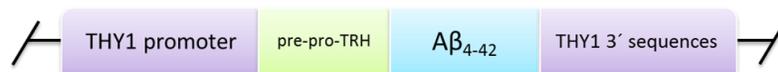


**Fig. 7. The Tg4-42 transgene.** The Aβ$_{4-42}$ sequence is fused to the pre-pro-TRH peptide in order to ensure secretion of the peptide. The neuronal expression is induced by the Thy1 promoter. Figure adapted from (Bouter *et al.* 2013).

### 1.6.3   The 5XFAD mouse model

The extensively-used 5XFAD mouse model first described by Oakley et al. is an APP/PS1 double transgenic mouse line co-expressing a total of five FAD mutations (Oakley *et al.* 2006). Overexpression of both transgenes is driven by the neuron-specific murine Thy1 promoter (Fig. 8). These animals co-overexpress the human APP695 isoform harboring the Swedish K670N/M671L, Florida I716V, and London V717I FAD mutations, and

human PS1 containing the M146L and L286V FAD mutations. 5XFAD mice breed as single transgenics, as shown by the stable genomic cointegration and germline transmission of both transgenes (Oakley *et al.* 2006).
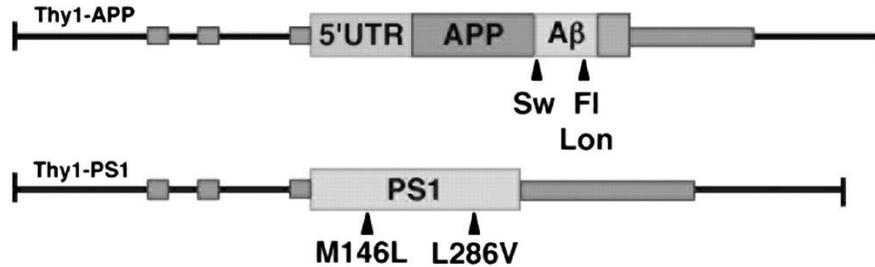


**Fig. 8. The 5XFAD transgenes.** 5XFAD mice are co-expressing the human APP695 and PSEN1 transgenes under the control of the Thy1 promoter. APP695 harbors the Swedish, Florida and London mutation while PSEN1 contains the mutations M146L and L286V. Figure taken from (Bouter *et al.* 2013).

The specific FAD mutations present in the 5XFAD mice increase Aβ levels and accelerate amyloid plaque formation. While the Swedish mutation enhances the production of total Aβ, the APP Florida/London, and PS1 M146/L286V mutations promote the production of $A\beta_{x-42}$. The additive effects of the five FAD mutations can be already observed at 1.5 months of age with the prominent accumulation of intraneuronal $A\beta_{x-42}$ in the pyramidal neurons of the 5th cortical layer and subiculum prior extracellular Aβ deposition. Moreover, significant neuron loss is detected in these regions beginning at 9 months of age. Surprisingly, no neuron loss is observed in the CA1 region of the hippocampus in which intraneuronal Aβ is lacking (Oakley *et al.* 2006; Ohno *et al.* 2007; Jawhar *et al.* 2012; Eimer & Vassar 2013). Also, Aβ accumulation has been detected within the motor neurons of the spinal cord in the 5XFAD mice (Jawhar *et al.* 2012).

As seen by Thioflavin S staining, amyloid deposits start to appear in the 5XFAD brains at the age of two months (Oakley *et al.* 2006). Amyloid pathology increases in an age-dependent manner spreading to different brain regions including the cortex and the hippocampus. Likewise, the 5XFAD strain exhibits astro- and microgliosis which is

proportional to the Aβ$_{x-42}$ levels and Aβ deposition (Oakley *et al.* 2006). Besides the extracellular Aβ deposition observed in the brain, amyloid plaques have been detected in the spinal cord of 5XFAD animals beginning at three months of age (Jawhar *et al.* 2012). Curiously, the Aβ$_{x-42}$ levels are higher in young female 5XFAD compared to age-matched 5XFAD male mice, however this trend seems to decrease as the mice age (Oakley *et al.* 2006).

5XFAD mice exhibit progressive behavioral deficits already at young ages. Between 4 and 5 months of age, these mice display hippocampus-dependent spatial working memory deficits, as analyzed by the Y-maze task (Oakley *et al.* 2006). Additionally, reduced anxiety levels have been detected at 6 months of age (Jawhar *et al.* 2012). Furthermore, learning and memory deficits in the 5XFAD line have also been reported using other behavioral paradigms such as the MWM, the conditioned taste aversion task, the cross maze and the contextual fear conditioning test. (Ohno *et al.* 2007; Devi & Ohno 2010; Jawhar *et al.* 2012; Bouter *et al.* 2014). In addition, sensory-motor deficits start to appear with 9 months of age (Jawhar *et al.* 2012).

In sum, the 5XFAD mouse model recapitulates some of the major neuropathological hallmarks of AD such as neuron loss, amyloid plaque formation and inflammation, along with characteristic behavioral and cognitive deficits. Therefore, this mouse model represents a suitable tool to study the molecular and cellular mechanisms involved in AD pathogenesis as well as potential therapeutic treatments to fight it.

## 1.7 PROJECT OBJECTIVES

### 1.7.1 Project I: Studies of the combined effect of Aβ$_{pE3-42}$ and Aβ$_{4-42}$ on ongoing Alzheimer's disease pathology using the TBA42/Tg4-42 bigenic mouse model

The N-terminally truncated Aβ isoforms Aβ$_{pE-42}$ and Aβ$_{4-42}$ have been shown to represent major species in the brain of AD patients. Moreover, it has been demonstrated that Aβ$_{4-42}$ is as toxic as Aβ$_{pE3-42}$ and that both peptides show high aggregation propensity when compared to full-length Aβ (Bouter *et al.* 2013). In order to study the direct *in vivo* toxicity of these two N-truncated Aβ peptides, the TBA42 and Tg4-42 mouse models expressing Aβ$_{pE3-42}$ and Aβ$_{4-42,}$ respectively, were previously created in our lab (Wittnam *et al.* 2012; Bouter *et al.* 2013). The TBA42 mouse develops intraneuronal Aβ accumulation, massive pyramidal neuron loss in the CA1 region of the hippocampus, motor impairments and behavioral deficits (Wittnam *et al.* 2012; Meissner *et al.* 2015). In good agreement with the observations in the TBA42 model, Tg4-42 mice expressing only intraneuronal Aβ$_{4-42}$ develop severe hippocampal neurons loss accompanied by spatial reference memory deficits (Bouter *et al.* 2013). Based on the observations that Aβ$_{pE3-42}$ and Aβ$_{4-42}$ play an important role in AD pathology, the aim of the first project was to elucidate a possible impact of a simultaneous expression of both Aβ$_{pE3-42}$ and Aβ$_{4-42}$ on pathological and behavioral deficits in transgenic mice.

The objectives of project I are the following:
- Generation of the TBA42/Tg4-42 mouse model by crossing the established TBA42 and Tg4-42 mouse models.
- Investigate the effect of the co-expression of Aβ$_{pE3-42}$ and Aβ$_{4-42}$ on neuropathology in young and aged mice.
- Study the toxic effect of Aβ$_{pE3-42}$ and Aβ$_{4-42}$ on neuron loss in TBA42/Tg4-42 mice.
- Determine if behavioral and cognitive deficits are enhanced in TBA42/Tg4-42 mice.

- Test if the combination of $A\beta_{pE3-42}$ and $A\beta_{4-42}$ has an effect on their aggregation propensity by measuring their aggregation kinetics.

### 1.7.2 Project II: Exploring the *in vivo* association between Aβ plaques and soluble Aβ aggregates using the FAD4-42 mouse model

According to the classic amyloid cascade hypothesis, the insoluble extracellular amyloid plaques are the triggering factors of AD pathogenesis. However, the presence of amyloid plaques has also been found in non-demented elderly subjects(Katzman *et al.* 1988; Hulette *et al.* 1998; Price & Morris 1999; Aizenstein *et al.* 2008). In addition, several studies have shown the presence of soluble Aβ oligomeric forms in extracts of cerebral tissue from AD patients (Kuo *et al.* 1996; Roher *et al.* 1996; Shankar *et al.* 2008; Tomic *et al.* 2009). Furthermore, based on the analysis of the Aβ soluble and insoluble pools in AD brains, it has been demonstrated that the levels of soluble Aβ oligomers correlate better with the risk and degree of AD than levels of insoluble Aβ (McLean *et al.* 1999; Wang *et al.* 1999; Mc Donald *et al.* 2010; Esparza *et al.* 2013). Additionally, studies suggest that amyloid plaques might act as reservoirs of soluble Aβ oligomers, thus preventing their toxicity (Shankar *et al.* 2008; Koffie *et al.* 2009, 2012; Hong *et al.* 2014). These findings gave rise to the question of whether fibrillar Aβ plaques or soluble Aβ oligomers are the key players in the pathogenesis of AD. Hence, the aim of the second project was to study the association between soluble Aβ oligomers and amyloid plaques in a transgenic mouse model of AD.

The objectives of the project II are the following:

- Generation of the FAD4-42 mouse model by crossing the 5XFAD and Tg4-42 mouse models.
- Study the effect of additional $A\beta_{4-42}$ on the extracellular Aβ deposition in the FAD4-42 mice at 3 and 12 months of age.

- Investigate if extracellular Aβ plaques have an impact on Aβ$_{4\text{-}42}$ neurotoxicity in the CA1 region of the hippocampus of 3- and 12-month-old FAD4-42 mice.

# 2 MATERIAL AND METHODS

## 2.1 AGGREGATION ASSAY

### 2.1.1 Preparation of synthetic Aβ peptides

Stock solutions of synthetic $Aβ_{pE3-42}$ and $Aβ_{4-42}$ peptides (Peptide Specialty Laboratory SL, Heidelberg, Germany) were solubilized in 10 mM NaOH at a final concentration of 1 mg/mL and volumes of 20 µL were aliquoted in 0.5 mL low binding microcentrifuge tubes (Eppendorf®, Hamburg, Germany). Shortly after, aliquots were sonicated for 5 min in a water bath (Sonorex RK 100H, Bandelin electronic, Berlin, Germany) and snap frozen in liquid nitrogen, before their storage at -80°C (modified from Wirths et al., 2010).

### 2.1.2 Thioflavin T aggregation assay

Peptide solutions were prepared on the basis of their molecular mass in a physiological buffer (50 mM PBS (PAN-Biotech, Aidenbach, Germany) 50 mM NaCl (Roth, Karlsruhe, Germany) K, 0.01 % NaN3 (Fluka, St. Louis, MO, USA), pH 7.0) and mixed with 20 µM Thioflavin T (ThT) (Sigma, St. Louis, MO, USA) to a final concentration of 50 µM. An equimolar mixture of $Aβ_{pE3-42}$ and $Aβ_{4-42}$ was prepared by adding 25 µM of each peptide in order to reach a final concentration of 50 µM. Then, 100 µL peptide solution per well was applied in triplicates to a 96-well microplate. The microplate was sealed, incubated at 37°C and shaken at 180 rpm between reads. ThT fluorescence was recorded every 10 minutes using a Synergy HTX Multi-Mode microplate reader (BioTeK Instruments Inc., Winooski, VT, USA). The excitation and emission wavelengths were 440/30 and 485/20 nm, respectively.

## 2.2  LABORATORY ANIMALS

### 2.2.1  Animal housing and general considerations

All mouse lines were maintained in the central animal facility of the University Medicine Göttingen under specific-pathogen-free conditions. Animals were kept under a controlled environment on a 12 hour/12 hour inverted light cycle (light from 8:00 pm to 8:00 am) and provided with free access to food and water. All animal experiments were performed in accordance with the German guidelines for animal care and were approved by the local legal authorities. All effort was made to minimize the number and the suffering of animals used in the present study. All animal experimental procedures were performed during the night cycle (8:00 am to 8:00 pm).

### 2.2.2  TBA42 transgenic mice

The generation of TBA42 mice has been described previously (Section 1.6.1). In brief, TBA42 mice express the murine thyrotropin-releasing hormone-A$\beta$ (mTRH-A$\beta_{3-42}$) sequence under the control of the murine Thy1.2 regulatory sequence. The glutamate at position three of the A$\beta$ amino acid sequence has been mutated into glutamine to facilitate enhanced generation of pyroglutamate A$\beta_{3-42}$ (A$\beta_{pE3-42}$)(Wittnam *et al.* 2012). All animals were generated and maintained on a C57BL/6J genetic background. For the present study, hemizygous TBA42 (TBA42$^{hem}$) and homozygous TBA42 (TBA42$^{hom}$) mice we used. Due to strong motor deficits, the TBA42$^{hom}$ mice had to be sacrificed at an age of 2 months.

### 2.2.3  Tg4-42 transgenic mice

Tg4-42 mice express the human A$\beta_{4-42}$ sequence fused to the signal peptide sequence of the thyrotropin-releasing hormone under the control of the Thy1 promoter. All animals were generated and maintained on a C57BL/6J genetic background. For the

first project, both female and male hemizygous Tg4-42 (Tg4-42$^{hem}$) and homozygous Tg4-42 (Tg4-42$^{hom}$) mice were used. In the second project, only female Tg4-42$^{hem}$ were utilized.

### 2.2.4  TBA42/Tg4-42 bigenic mice

For the first project, the Tg4-42/TBA42 bigenic line was generated by breeding transgene positive Tg4-42 mice with transgene positive TB42 mice. Wild type (WT) and transgenic offspring were identified subsequently using PCR and qRT-PCR. All animals were generated and maintained on a C57BL/6J genetic background. Both female and male TBA42/Tg4-42 mice were utilized

### 2.2.5  5XFAD mice

The generation of the 5XFAD mouse model has been described previously (Oakley *et al.* 2006). In brief, this line expresses the human APP (695) transgene with the Swedish, Florida and London mutations. Additionally, the model expresses a PS1 transgene containing the M146L and L286V mutations. Both, the APP and PS1 transgenes are expressed under the control of the murine Thy1.2 regulatory sequence. The 5XFAD line was originally kept on a B6/SJL hybrid background. Thus, in order to facilitate comparison and mating with other AD transgenic mouse models, these mice were backcrossed for several generations to obtain a pure C57BL/6J genetic background (Jawhar *et al.* 2011). Only female 5XFAD mice were used in the present work.

### 2.2.6  FAD4-42 bigenic mice

For the second project, the FAD4-42 bigenic mouse model was generated by crossing the established familiar (5XFAD) and the sporadic (Tg4-42) AD mouse models. WT and transgenic offspring were subsequently identified using PCR. The mice designated as

FAD/4-42 were hemizygous for both, 5XFAD and Tg4-42 transgenes. Only female mice were used.

## 2.3 GENOTYPING OF TRANSGENIC MICE

### 2.3.1 Isolation of genomic DNA

All mice were genotyped before any further use. To this end, genomic DNA isolated from tail biopsies was used. First, a volume of 500 μL lysis buffer (100 mM Tris/HCl (pH 8.5; Roth, Karlsruhe, Germany) 5 mM EDTA (AppliChem, Darmstadt, Germany), 0.2% dodecyl sulfate (SDS; Biolmol, Hamburg, Germany) and 200 mM NaCl (Roth, Karlsruhe, Germany) supplemented with 5 μL proteinase K (20 mg/ml stock; Peqlab, Erlangen, Germany) was added to every tail biopsy and incubated overnight at 55°C under shaking conditions (450 rpm) in a Thermomixer Compact (Eppendorf, Hamburg, Germany). After incubation, samples were centrifuged for 20 min at 17,000 rpm at 4°C. The supernatants were then transferred into a 1.5 mL microtube containing 500 μL ice-cold isopropanol (Roth, Karlsruhe, Germany) and centrifuged at RT for 10 min at 13,000 rpm. Then, supernatants were discarded and the pellet was washed with 500 μL of ice-cold 70% absolute EtOH (Merck, Darmstadt, Germany), followed by a 13,000 rpm centrifugation step for 10 min at RT (Biofuge Pico, Heraeus). The resulting supernatant was drained and the pellet left to dry at 55°C for 2 h. Finally, the pellet was dissolved in 30 μL molecular-grade water (Braun, Melsungen, Germany), incubated ON at 55°C and stored at 4°C until further use.

### 2.3.2 Nucleic acid concentration calculation

Using a Biophotomer (Eppendorf, Hamburg, Germany), the genomic DNA concentration and purity was measured. Before DNA measurements, 80 μL of molecular-grade water was used as a blank for the photometer settings. Subsequently, 2 μL of genomic DNA

was diluted with 78 µL of molecular-grade water. Samples with A260/A230 and A260/A280 values greater than 1.8 were considered accurate for further analyses.

### 2.3.3 Polymerase chain reaction (PCR)

Genomic DNA samples were diluted to a final concentration of 20 ng/µL and utilized for genotyping by standard polymerase chain reaction (PCR). The reaction mixtures and the thermal cycling program for DNA amplification are given in the Tables 1, 2 and 3, respectively. Afterwards, in order to corroborate the presence of the transgenes in the samples, the PCR products were identified by agarose gel-electrophoresis. For this purpose, a 2% agarose gel was prepared by mixing 3.0 grams of agarose (Lonza, Basel, Switzerland) with 150 mL of 1X TBE  and boiled in a microwave before 4 µL of ethidium bromide [10 mg/mL] (Roth, Karlsruhe, Germany) was added to the mixture. Then, the agarose solution was poured into a casting tray with a comb to form the wells. Once the gel was solidified, 10 µL of the PCR product was mixed with 5 µL of 10X loading buffer and added into the wells. For size identification, a volume of 5 µL 100 bp DNA ladder (Bioron, Ludwigshafen, Germany) was loaded into the first well and gel electrophoresis was conducted at 141 mV for 1 hour. The PCR product bands were then visualized in an UV-chamber (Gel-Doc 2000, BioRad, Hercules, CA, USA) and data were analyzed with the Quantity One software program (Biorad, Hercules, CA, USA).

10XTBE buffer: 108 g Tris (Roth, Karlsruhe, Germany) and 55 g boric acid (Sigma, St. Louis, MO, USA) were dissolved in 900 ml ddH2O. Then 40 ml 0,5 M Na2EDTA (pH 8.0; Roth, Karlsruhe, Germany) was added to the solution and the volume was adjusted to 1 liter with ddH2O. Before use the solution was diluted 1:10 in ddH2O to obtain 1XTBE buffer.

**Table 1.** Reaction mixture for 5XFAD and FAD/4-42 genotyping

| Reagent | Volume (µL) |
| --- | --- |
| DNA (20 ng/µL) | 2 |
| Primer hAPP for | 0.5 |
| Primer hAPP rev | 0.5 |
| dNTP's (2 mM) | 2 |
| $MgCl_2$ (25 mM) | 3.2 |
| 10x reaction buffer | 2 |
| Molecular grade water | 9.6 |
| Taq polymerase (5 U/µL) | 0.2 |
| **Total reaction volume per sample** | **20** |

**Table 2.** Reaction mixture for Tg4-42 and TBA42 genotyping

| Reagent | Volume (µL) |
| --- | --- |
| DNA (20 ng/µL) | 2 |
| Primer Aβ3-42 for | 0.5 |
| Primer Aβ3-42 rev | 0.5 |
| dNTP's (2 mM) | 2 |
| $MgCl_2$ (25 mM) | 3.2 |
| 10x reaction buffer | 2 |
| Molecular grade water | 9.6 |
| Taq polymerase (5 U/µL) | 0.2 |
| **Total reaction volume per sample** | **20** |

**Table 3.** Thermal cycling program for Tg4-42, TBA42, 5XFAD and FAD/4-42 genotyping

| Step | Temperature [°C] | Duration [s] |
|:---:|:---:|:---:|
| 1 | 94 | 180 |
| 2 | 94 | 45 |
| 3 | 58 | 60 |
| 4 | 72 | 60 |
| 5 | Repetition of steps 2-4 (40 cycles) | |
| 6 | 72 | 300 |
| 7 | 4 | ∞ |

### 2.3.4  Quantitative Real-Time PCR for Genotyping

Quantitative Real-Time PCR (qRT-PCR) was applied in order to identify bigenic TBA42/Tg4-42 mice. For this purpose, genotyping was performed using the Biotool™ 2x SYBR Green qPCR master mix which contains ROX as an internal reference dye. The reaction mix and the thermal cycling program for amplification are shown in Table 4 and Table 5 respectively. A total reaction mix volume of 20 µL was added in duplicates into 200 µL qRT-PCR tubes (Biozym Scientific) and spun down briefly. To start the qRT-PCR reaction, tubes were then transferred into a Mx3000P Real-Time Cycler (Stratagene, Santa Clara, CA, USA) and data were gathered using the MxPro Mx3000P software (Stratagene, Santa Clara, CA, USA). The $C_T$-values were measured and averaged from the duplicates. For relative quantification, $C_T$-values of the respective human Aβ$_{3-42}$ and Aβ$_{4-42}$ genes (target genes) were normalized to those of murine APP (reference gene) and calibrated to a selected control mouse using the $2^{-\Delta\Delta C_T}$ method (Schmittgen & Livak 2008) as follows:

For both the test mouse (test) and the control mouse (calibrator), the $C_T$ of the target gene was normalized to that of the reference gene:

$$\Delta C_{T(test)} = C_{T(target,\ test)} - C_{T(reference,\ test)}$$

$$\Delta C_{T(calibrator)} = C_{T(target,\ calibrator)} - C_{T(reference,\ calibrator)}$$

Then, the $\Delta C_T$ of the test mouse was normalized to the $\Delta C_T$ of the calibrator:

$$\Delta\Delta C_T = \Delta C_{T(test)} - \Delta C_{T(calibrator)}$$

Finally, the gene amount of the target gene in the test mouse is $2^{-\Delta\Delta C_T}$ times of the control mouse. An example of the identification of mice carrying both transgenes (TBA42 and Tg4-42) is shown in Fig. 9.

**Table 4.** Reaction mixture for TBA42/Tg4-42 genotyping

| Reagent | Amount per reaction (µL) |
|---|---|
| 2x Biotool™SYBR Green Master Mix | 10 |
| DNA template | 2 |
| Forward Aβ3-42 or mAPP primer | 1.5 |
| Reverse Aβ3-42 or mAPP primer | 1.5 |
| ROX reference dye | 0.4 |
| Molecular grade water | 4.6 |
| **Total reaction volume per sample** | **20** |

**Table 5.** Thermal cycling program for TBA42/Tg4-42 genotyping

| Step | Temperature [°C] | Duration [s] |
|---|---|---|
| 1 | 95 | 600 |
| 2 | 95 | 15 |
| 3 | 60 | 60 |
| 4 | Repetition of steps 2 and 3 (40 cycles) | |
| 5 | 95 | 60 |
| 7 | 55 | 30 |
| 8 | 95 | 30 |
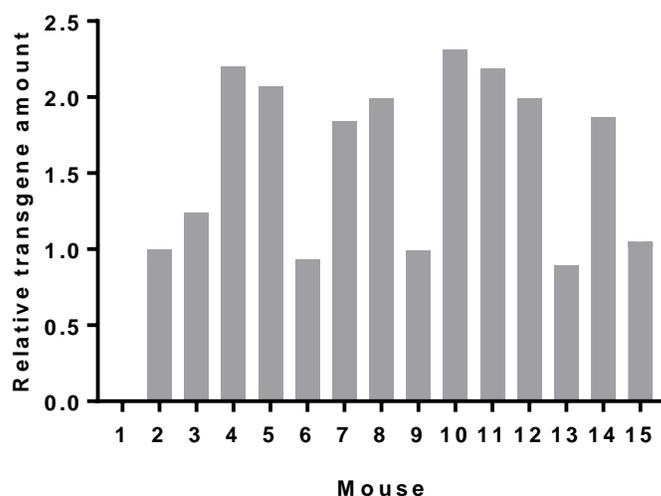
**Fig. 9. Identification of potential TBA42/Tg4-42 bigenic mice.** The presence of $A\beta_{3-42}$ and $A\beta_{4-42}$ was quantified relative to murine APP. All mice were calibrated to control mouse number 1 (negative for both $A\beta_{3-42}$ and $A\beta_{4-42}$). Animals 2 (confirmed TBA42[hem]) and 3 (confirmed Tg4-42[hem]), 4 (confirmed TBA42[hom]) and 5 (confirmed Tg4-42[hom]) were used as positive controls. Then, mice 7, 8, 10, 11, 12 and 14 were identified as bigenic, while the rest of the animals analyzed were considered Tg4-42[hem] as one of the parents was Tg4-42[hom] homozygous.

## 2.3.5  Primers

All primers used for genotyping (Table 6) were used at a final concentration of 10 pmol/µL (100 pmol/µL original stock diluted 1:10 in molecular grade water) and purchased from Eurofins (Ebersberg, Germany).

**Table 6 .** List of primers used for mouse genotyping

| Name | Sequence (5' → 3') | Usage |
|---|---|---|
| Murine APP forward | TCT TGT CTT TCT CGC CAC TGG C | qRT-PCR |
| Murine APP reverse | GCA GTC AGA AGT TCC TAG G | qRT-PCR |
| Human APP forward | GTA GCA GAG GAA GAA GTG | PCR |
| Human APP reverse | CAT GAC CTG GGA CAT TCT C | PCR |

| Aβ3-42 forward | TCC GGC CAG AAC GTC GAT TC | qRT-PCR |
|---|---|---|
| Aβ3-42 reverse | GGA GAA GCA AGA CCT CTG C | qRT-PCR |

## 2.4 TISSUE COLLECTION AND PRESERVATION

### 2.4.1 Perfusion

Mice were anesthetized with an intraperitoneal injection containing a mixture of ketamine (100 mg/kg; Medistar, Ascheberg, Germany) and xylazine (10 mg/kg; Ecuphar, N.V. Oostkamp, Belgium) diluted in molecular-grade water. The pedal withdrawal reflex was used as an indicator of depth anesthesia. Once mice were deeply anesthetized, they were placed on a perfusion tray. A small lateral incision was made through the abdominal wall, the diaphragm was carefully cut and the rib cage was lifted away by cutting it laterally from both sides. After exposing the beating heart, an incision was made in the right atrium to allow for blood to drain from the circulatory system. Then, a sterile needle attached to the tubing system of a peristaltic pump was inserted into the posterior end of the left ventricle. The mice were then perfused with approximately 30 mL ice-cold 0.01 M PBS until the fluid was running clear and the liver was clear of blood. Perfusion continued with and administration of 30 mL ice-cold 4% (weight/volume (w/v)) paraformaldehyde (PFA; Roth, Karlsruhe, Germany) in 0.01 M PBS. Rigidity of the mice's tail indicated a successful perfusion.

Following perfusion, the mice were decapitated. The right brain hemisphere and the cervical/thoracic spinal cord were placed into embedding cassettes and post-fixated with a 4% formalin Histofix solution (Roth, Karlsruhe, Germany) for at least one week before embedding in paraffin. The left brain hemisphere was post-fixated for 24 hours in 4% PFA in 0.01 M PBS. The brain tissue was then placed into a 30% (w/v) sucrose (Roth, Karlsruhe, Germany) solution in 0.01 M PBS for cryoprotection and

incubated until it sank to the bottom of its container. Subsequently, the brain tissue was flash-frozen on dry ice and stored at -80°C until further use.

### 2.4.2 Immunohistochemistry

#### 2.4.2.1 Paraffin embedding of mouse brain and spinal cords

After perfusion, the right brain hemisphere and spinal cord were placed into a TP 1020 Automatic Tissue Processor (Leica). First, the tissue was submerged for 5 min in 4% histofix solution followed by 30 min in deionized water. Then, dehydration was carried out by placing the tissue into aqueous solutions containing different ascending quantities of ethanol (50%(v/v), 60%, 70%, 80%, 90%) for one hour each. Then, the tissue was incubated twice in 100% ethanol for one hour each followed by an incubation in xylol for one hour. Finally, tissue samples were transferred into melted paraffin twice for one hour each, before being embedded in paraffin blocks using an EG1140 H Embedding Station (Leica).

Sagittal brain sections and spinal cord cross sections were cut with a HM 335E microtome (Thermo Fisher Scientific). Sections of 4 µm thickness were transferred into a ddH$_2$O water bath at RT and then mounted onto Superfrost® slides (Thermo Fischer Scientific). The sections were fixed by immerging the slides into a 55°C water bath and followed by 30 min on a 55°C hot plate. Before using them for immunohistochemistry, the sections were incubated at 37°C ON.

#### 2.4.2.2 3,3'-Diaminobenzidine (DAB) immunohistochemistry

DAB immunohistochemistry was performed on 4 µm paraffin sections that were deparaffinized and rehydrated using the following protocol: 2 x 5 min xylol; 10 min 100% EtOH; 5 min in 95% EtOH; 5 min in 70% EtOH and 1 min in ddH$_2$O. Endogenous peroxidases were blocked by treating sections with 0.3% (v/v) H$_2$O$_2$ in 0.01 M PBS for 30 min. Antigen retrieval was achieved by heating sections for 10 min (approx. 2 min

at 800 W (until boiling), approx. 8 min at 80 W) in 0.01 M citrate buffer pH 6.0 and cooling them down for 15 min at RT. Sections were then washed for 1 min in ddH$_2$O, permeabilized for 15 min in 0.01 M PBS supplemented with 0.1% (v/v) Triton X-100 (Roth, Karlsruhe, Germany) and washed for 1 min in 0.01 M PBS. A second antigen retrieval treatment (to reveal intracellular Aβ) was applied by incubating the sections for 3 min in 88% (v/v) formic acid (Roth, Karlsruhe, Germany). Then, two consecutive washing steps of 1 min and then 5 min in 0.01 M PBS were performed to remove any residual content of formic acid. For nonspecific antigen block, sections were circled with a lipid pen and a solution of 10% fetal calf serum (FCS; Thermo Fisher Scientific, Waltham, MA, USA) including 4% (w/v) skimmed milk powder (Roth, Karlsruhe, Germany) in 0.01 M PBS was added. Sections were incubated for 1 hour at RT. Primary antibodies were diluted (Table 7) in 0.01 M PBS containing 10% (v/v) FCS. After removing the blocking solution, diluted primary antibodies were added and sections were incubated ON in a humid chamber at RT.

On the second day, sections were washed for 15 min in 0.01 M PBS supplemented with 0.1% (v/v) Triton X-100 and then rinsed with 0.01 M PBS for 1 min. The corresponding biotinylated secondary antibodies were diluted (Table 8) in 0.01 M PBS containing 10% (v/v) FCS. Then, the sections were incubated with the secondary antibodies for 1 hour at 37°C. During this time, the Avidin-biotin complex (ABC) solution was prepared using the VECTASTAIN Elite ABC Kit (Vector Laboratories). To this end, solution A and B were diluted 1:100 in 0.01 M PBS supplemented with 10% (v/v) FCS and kept at 4°C for at least 30 min prior to use. After the one-hour incubation period with the secondary antibodies, sections were washed for 15 min in 0.01 M PBS and then incubated with the previously prepared ABC solution for 1.5 h at 37°C. The ABC solution was removed by a 15-min wash in 0.01 M PBS. Using DAB as a chromogen, the staining could be visualized. The DAB developing solution was prepared using the DAB Substrate Kit (Vector Laboratories) according to the instructions of the manufacturer. Sections were incubated with DAB solution until the desired staining pattern was observed (incubation time was the same for sections used for plaque load quantification). After development, sections were washed for 15 min in 0.01 M in PBS and then counterstained with a hematoxylin solution for 40 s (except for sections used

for plaque load quantification). Samples were dipped in ddH$_2$O and washed under running tab water for 5 min. Prior to mounting, sections were dehydrated in an ascending series of ethanol baths as follows: 1 min in 70% (v/v) EtOH, 5 min in 95% (v/v) EtOH, 10 min in 100% (v/v) EtOH. Following dehydration, sections were treated twice for 5 min each in xylol. Finally, each section received 2-3 drops of Roti®-Histokit mounting medium before a microscope cover slip was placed onto the slide.

## 2.5 IMAGING AND Aβ QUANTIFICATION ANALYSIS

Extracellular and intracellular Aβ load was evaluated in the cortex (Ctx), subiculum (Sub), dentate gyrus (DG), thalamus (Thal) and spinal cord (SC) of transgenic mice. Serial images of 200X magnification from the Ctx, Sub, DG and Thal were captured on three sections per animal which were at least 30 μm apart from each other. Slides were then imaged using an Olympus BX51 microscope equipped with MoticamPro 282B digital camera. Illumination conditions and exposure settings were maintained stable throughout the analysis. Using the Image J software package (V1.41, NIH, USA), the pictures were binarized to 8-bit black and white images and a fixed intensity threshold was applied defining the DAB signal. The percentage of DAB positive area was calculated as the Aβ deposition load. Respectively, SC sections were analyzed as described but with a 400X magnification objective.

**2.5.1 Quantification of intracellular Aβ accumulation in the motor neurons of the spinal cord**

In order to quantify the number of motor neurons with Aβ accumulation, paraffin sections of the cervical spinal cord were analyzed. The total number of positive Aβ motor neurons in the grey matter of the ventral horn was identified by their large size (nuclear diameter > 9-10 μm; cell body diameter > 20 μm). Aβ accumulation in the motor neurons was based on Aβ staining intensity and were then classified as follows: motor neurons with a) low, b) intermediate or c) high intracellular accumulation. Serial images of 100x magnification were captured on three sections per animal with a minimum of 30 μm distance from each other. For quantification, the Meander Scan option of the StereoInvestigator 7 software package (Microbrightfield, Williston, VT, USA) was used.

**2.6 QUANTIFICATION OF NEURON NUMBERS**

**2.6.1 Sample preparation**

The previously treated left brain hemisphere was cut frontally into 10 series of 30 μm tick sections using a cryostat (Leica CM1850 UV, Germany). Every 10th section was systematically sampled and stored at -80°C until further use. One series was randomly selected and transferred into ice-cold 0.01 M PBS. Sections were then carefully mounted onto Superfrost® slides and allowed to dry overnight at RT prior staining.

**2.6.2 Cresyl violet staining**

Sections were treated as follows: 2 x 10 min in solution A, then for 20 min in solution B and 2 x 10 min in solution A for delipidation. Staining was performed by immerging the section twice for 8 min each with a cresyl violet staining solution (Fluka, St. Louis, MO, USA). Sections were dehydrated by treating them 3 x 1 min with solution A, followed by 3 min in 100% (v/v) EtOH, 10 min in isopropanol and 2 x 5 min in xylol. Finally, 4-5

drops of Roti®-Histokit mounting medium were applied to each slide, then a microscope cover slip was placed onto the slide and left to dry ON before further analysis.

The solutions previously mentioned were prepared as follows:

Working solution A: 40 ml of 1 M sodium acetate was added to 9.6 ml of glacial acetic acid (Merck, Darmstadt, Germany) and completed to 1 L with $ddH_2O$.

Cresyl violet staining solution: 0.1 g cresyl violet was dissolved in 1 L of working solution A, stirred overnight, protected from light and filtered before use.

Working solution B: 20 ml of Triton X-100 was added to 980 mL of $ddH_2O$ and stirred for 1 h. From this solution, 2.5 mL was diluted with 50 mL of $ddH_2O$ and 150 mL of 100% EtOH.

### 2.6.3   Stereological analysis

Cresyl violet stained brain sections were analyzed by design-based stereology to quantify the neuron numbers in the CA1 region of the hippocampus. To this end, a stereology working station BX51 (Olympus, Shinjuku, Japan) with a motorized specimen stage for automatic sampling and the Stereo Investigator 7 software (Microbrightfield Bioscience, Williston, VT, USA) were used. In order to avoid biased counting, quantification was carried out by an observer blinded for the genotype of the mice. The stereological analysis of the project I was carried out together with Nicolai M.E. Giessen.

The CA1 pyramidal cell layer was delineated at a low magnification (4x) from Bregma -1.22 to -3.80 mm (Franklin & G. 2012) and quantified at a high magnification (100x oil objective, NA = 1.35). Neuronal nuclei were sampled in a systematic random manner using optical dissector probes and the total number of neurons was estimated by the optical fractionator method using a 2 µm top guard zone (West *et al.* 1991). The optical dissector height (Z) used on every grid site was 5 µm. The section thickness was measured while counting and the total number of neurons (N) in the area of interest

was estimated according to the principle of stereology (West *et al.* 1991; Schmitz & Hof 2005)(Schmitz and Hof 2005; West 2002; West et l., 1991) by the following formulas:

- $P = asf \cdot ssf \cdot tsf$

- $N = \sum_{i=1}^{n}(P \cdot Q)i$

Where:

$P$ = number of neurons

$asf$ = area sampling fraction ($\delta X \cdot \delta Y \div X \cdot Y$)

$ssf$ = section sampling fraction

$tsf$ = thickness sampling fraction ($T/Z$)

$Q$ = numbers of markers counted

The remaining stereological parameters together with their values are listed in Table 7

**Table 7.** Stereological parameters used for neuron counting analysis in the CA1

| Parameter | Value |
|---|---|
| Sampling grid ($\delta X$) [μm] | 50 |
| Sampling grid ($\delta Y$) [μm] | 150 |
| Sampling grid area ($\delta X \cdot \delta Y$) [μm²] | 5250 |
| Counting frame width ($X$) [μm] | 14 |
| Counting frame height ($Y$) [μm] | 14 |
| Counting frame area ($X \cdot Y$) [μm²] | 196 |
| $asf$ | 26.78 |
| $ssf$ | 10 |
| Mean section thickness ($T$) [μm] | 10.6 |
| Optical dissector height ($Z$) [μM] | 5 |

## 2.7 ANTIBODIES

### 2.7.1 Primary Antibodies

**Table 8.** Primary antibodies for immunohistochemistry

| Antiserum | Host | Isotope | Immunogen | Working dilution | Manufacturer |
|:---:|:---:|:---:|:---:|:---:|:---:|
| 24311 | rabbit | polyclonal | Pan-Aβ | 1:500 | AG Bayer |
| NT4X | mouse | monoclonal | $Aβ_{pE3/4-x}$ | 1:500 | AG Bayer |

### 2.7.2 Secondary Antibodies

**Table 9.** Secondary antibodies used for immunohistochemistry

| Antiserum | Host | Conjugate | Working solution | Manufacturer |
|:---:|:---:|:---:|:---:|:---:|
| anti-rabbit | rabbit | biotinylated | 1:200 | Dako |
| anti-mouse | rabbit | biotinylated | 1:200 | Dako |

## 2.8 BEHAVIORAL TASKS

### 2.8.1 General considerations

Behavioral phenotyping of mice was performed during the dark phase (between 8 a.m. and 8 p.m.) and always at the same time to exclude any effects of circadian rhythms. Young (2-3 months) and aged (5-6 months) WT, TBA42[hem], Tg4-42[hem], Tg4-42[hom] and TBA42/Tg4-42 mice were tested. Both, female and male mice were used. Due to severe motor deficits, the TBA42[hom] mice had to be sacrificed at two months of age. Therefore, these animals were discarded for the behavioral tasks. To minimize stress levels, only

one motor and one cognitive test was carried out per day. Likewise, to reduce the number of animals tested and due to technical limitations, some groups were completed with data previously generated in our lab under the same conditions.

### 2.8.2   String suspension

The string suspension test was performed to evaluate strength and motor coordination and was described in detail previously (Jawhar *et al.* 2012). It consists of a 3-mm tick cotton string (50 cm length) tied between two vertical wooden supports, which is elevated approximately 40 cm above a padded surface. Mice were placed in the middle of the string and permitted to grasp it with their forepaws before they were released. For data evaluation, a scoring system of 0 to 5 was used during a 60 second single trial, where: 0 = unable to stay on the string; 1 = hanging on the string only by fore- or hind paws; 2 = as for 1, but with attempt to climb onto string; 3 = sits on string and holds balance; 4 = four paws and tail around string with lateral movement; and 5 = escape to one of the wooden supports. During a single day of testing, three trials with an interval of at least 10 min between trials were given for every animal and the average score was used for the statistical analysis. Between trials, the string was cleaned with 70% EtOH to avoid odor cues left by previously tested animals.

### 2.8.3   Balance beam

The balance beam task was used to assess balance and fine motor coordination (Wirths & Bayer 2008). The apparatus comprises a 1-cm wide wooden bar (50 cm length) attached between two 44- cm height vertical wooden supports. At both ends of the wooden bar, 9 x 15 cm wooden escape platforms were installed. Each animal was given three 60-second trials during a single day of testing. The time each mouse remained on the beam was recorded and the resulting time of all three trials was averaged. If an animal remained on the beam for 60 seconds or escaped to one of the platforms, the maximum time of 60 seconds was recorded. To diminish olfactory cues, both escape platforms were cleaned with 70% EtOH between trials.

### 2.8.4 Inverted grip task

Neuromuscular abilities, vestibular function and muscle strength, were tested with the inverted grip task (Wirths & Bayer 2008).The testing apparatus consisted of a wire grid (45 cm long and 30 cm wide with a grid spacing of 1 cm). The grid was suspended 40 cm above a padded surface using foam supports. Every animal was positioned onto the center of the grid. The grid was then inverted and the latency to fall was recorded during a single 60 second trial. If the mouse was able to stay on the grid for the entire trial or escaped over the edge of the grid, the maximum time of 60 seconds was recorded. Prior to every trial, the grid was cleaned with 70% EtOH to decrease odor cues.

### 2.8.5 Elevated plus maze

The elevated plus maze test was used to assess anxiety-related behavior (Jawhar *et al.* 2012). The apparatus consisted of four arms arranged in a "+" configuration and raised 75 cm above a padded surface. Two of the arms were open (15 x 5 cm) and situated 180° apart from each other and perpendicular to two closed arms (15 x 5 x 15 cm) with a central region (5 x 5 cm). The 15-cm height walls of the closed arms were made of a transparent plastic material. Before every trial, the apparatus was cleaned with 70% EtOH to reduce olfactory cues. Then, the animal was placed in the 25 cm$^2$ central platform of the maze facing one of the open arms and allowed to freely explore the maze for a single 5 min trial. The distance travelled and the time spent in the open arms was measured using the ANY-Maze automatic video tracking software (Stoelting Co., Wood Dale, IL, USA). The elevated plus maze test is based on the tendency of mice to explore novel environments and the aversion to explore open and elevated spaces (Karl *et al.* 2003; Komada *et al.* 2008; Campos *et al.* 2013). Therefore, the time spent in the open arms was used as an indicator of anxiety-like behavior.

**2.8.6  Cross Maze**

In order to examine the working memory, the spontaneous alternation rate cross maze test was used (Jawhar *et al.* 2012). The entire maze was made of a black plastic material. It consisted of four cross-shaped arms, in which each arm was 30 cm long, 8 cm wide, 15 cm high with a 90° angle extending from a center square platform (8 x 8 cm). Each animal was randomly positioned at the end of one of the arms facing the wall. Then, it was let free to explore for a single trial with a duration of 10 min. The distance travelled and the sequence of the arm entries were recorded using the ANY-Maze automatic video tracking software (Stoelting Co., Wood Dale, IL, USA). Alternation was defined as successive entries into the four arms in overlapping quadruple sets (Arendash *et al.* 2001). The alternation percentage was then calculated as the total of actual alternations made to the potential number of arms entries. Between trials, the apparatus was cleaned of urine and feces with 70% EtOH.

**2.8.7  Morris Water Maze**

The Morris Water Maze (MWM) was used to evaluate spatial reference memory(Morris 1984). The MWM comprised a 110-cm diameter pool filled with opacified water (by adding a non-toxic white paint) which was kept at 20-22°C during the entire experiment. The pool was divided into four virtual symmetrical quadrants that were defined based on their spatial relationship to the escape platform: left (L), right (R), opposite (O) and target (T) quadrant, which contained the goal platform. The MWM comprised a 9-day protocol divided into three stages: cued training, acquisition training and probe trial.

The test began with the three-day cued training. During this stage, a cylindrical platform (15 cm in diameter) marked with a triangular flag was submerged and positioned into one of the quadrants. The mouse was then introduced into the water at the edge of the pool facing the wall. It was given 60 sec to locate the platform. The trial ended once the animal found the platform and remained on it for 1-2 sec. When a mouse was not able to find the platform, it was gently guided to it. Every mouse was allowed

to stay on it for 10 sec and received four training trials per day. Between trials, the platform was moved to a different quadrant and the mouse was introduced from a different location. Animals that showed a significant decrease in the escape latencies were included for the further analyses.

The acquisition training began 24 h after the last day of the cued training. For this phase, the triangular flag was removed from the platform and proximal visual cues (attached to the north, south, east and west edges of the pool) were added. The platform remained hidden in the target quadrant during the 5-day acquisition training. Mice were released into the pool from different entry points and allowed to swim for 60 sec. Trials were automatically stopped once the mice located the hidden platform within the given time. Like in the cued training, animals were given four trials per day.

Twenty-four hours after the last day of the acquisition training stage, the probe trial was carried out to evaluate the spatial reference memory. To this end, the platform was removed from the pool and mice were enabled to swim freely for 60 sec. The percentage of time spent in the target quadrant was recorded and compared to the time spent in the other three quadrants.

The ANY-Maze automatic video tracking software (Stoelting Co., Wood Dale, IL, USA) connected to a digital camera (Computar, Commack, NY, USA) attached to the ceiling was used to record escape latency, swimming speed and quadrant preference.

## 2.9  STATISTICAL ANALYSIS

Differences between groups were tested with one-way analysis of variance (ANOVA) followed by Tukey's multiple comparison test, two-way repeated measures (RM) ANOVA followed by Tukey's multiple comparison test or unpaired t-test. All data were given as means ± standard error of the mean (SEM). Significance levels were given as follows: ***$p<0.001$; **$p<0.01$; *$p<0.05$. All calculations were performed using GraphPad Prism version 7 for Windows (Graph Pad Software, San Diego, USA).

# 3 RESULTS

## 3.1 PROJECT I: STUDIES OF THE COMBINED EFFECT OF ABₚₑ₃-₄₂ AND AB₄-₄₂ ON ONGOING ALZHEIMER'S DISEASE PATHOLOGY USING THE TBA42/TG4-42 BIGENIC MOUSE MODEL

The aim of the present study was to investigate the direct *in vivo* effect of the combination of $A\beta_{pE3-42}$ and $A\beta_{4-42}$ on AD pathology. To this end, the established TBA42 and Tg4-42 mouse models, expressing $A\beta_{pE3-42}$ and $A\beta_{4-42}$, respectively, were crossed. The resulting TBA42/Tg4-42 bigenic mice were then phenotypically characterized in detail. Additionally, WT, TBA42$^{hem}$, TBA42$^{hom}$, Tg4-42$^{hem}$ and Tg4-42$^{hom}$ mice were analyzed for comparison purposes. The animals were divided in groups of young (2-3 months) and aged (5-6 months) mice. The results of sections 3.1.1, 3.1.2.4, 3.1.3, 3.1.4 and 3.1.5 have been already published in Lopez-Noguerola *et al.,* 2018.

### 3.1.1 Abundant intraneuronal Aβ accumulation in the CA1 region of the hippocampus in TBA42/Tg4-42 bigenic mice

Abundant intraneuronal Aβ accumulation in the CA1 region of the hippocampus in the TBA42 and Tg4-42 models has been previously reported by our group (Wittnam *et al.* 2012; Bouter *et al.* 2013). Therefore, in order to evaluate the effect of the co-expression of $A\beta_{pE3-42}$ and $A\beta_{4-42}$ on Aβ accumulation in the CA1 area, brain sections were immunostained using the pan-Aβ antibody 24311. Intraneuronal Aβ accumulation in the CA1 pyramidal layer of the hippocampus was already detected in all the young single transgenic and bigenic mice analyzed (Fig.10 A-E). Particularly, in the young TBA42/Tg4-42 mice prominent intraneuronal Aβ immunoreactivity was observed in the CA1 pyramidal neurons (Fig. 10 E' arrows), which was accompanied by small extracellular granules (Fig. 10E' arrowheads). Conversely, Aβ immunoreactivity in the CA1 region declined with age in all the groups analyzed (Fig. 11 A-D). Besides the hippocampus, Aβ deposition was found in the cortex, inferior colliculus, cerebellum and

brainstem of TBA42/Tg4-42 mice (data not shown). Furthermore, it is worth mentioning that regardless of age and genotype, no neuritic amyloid plaques were found in any of the groups analyzed.
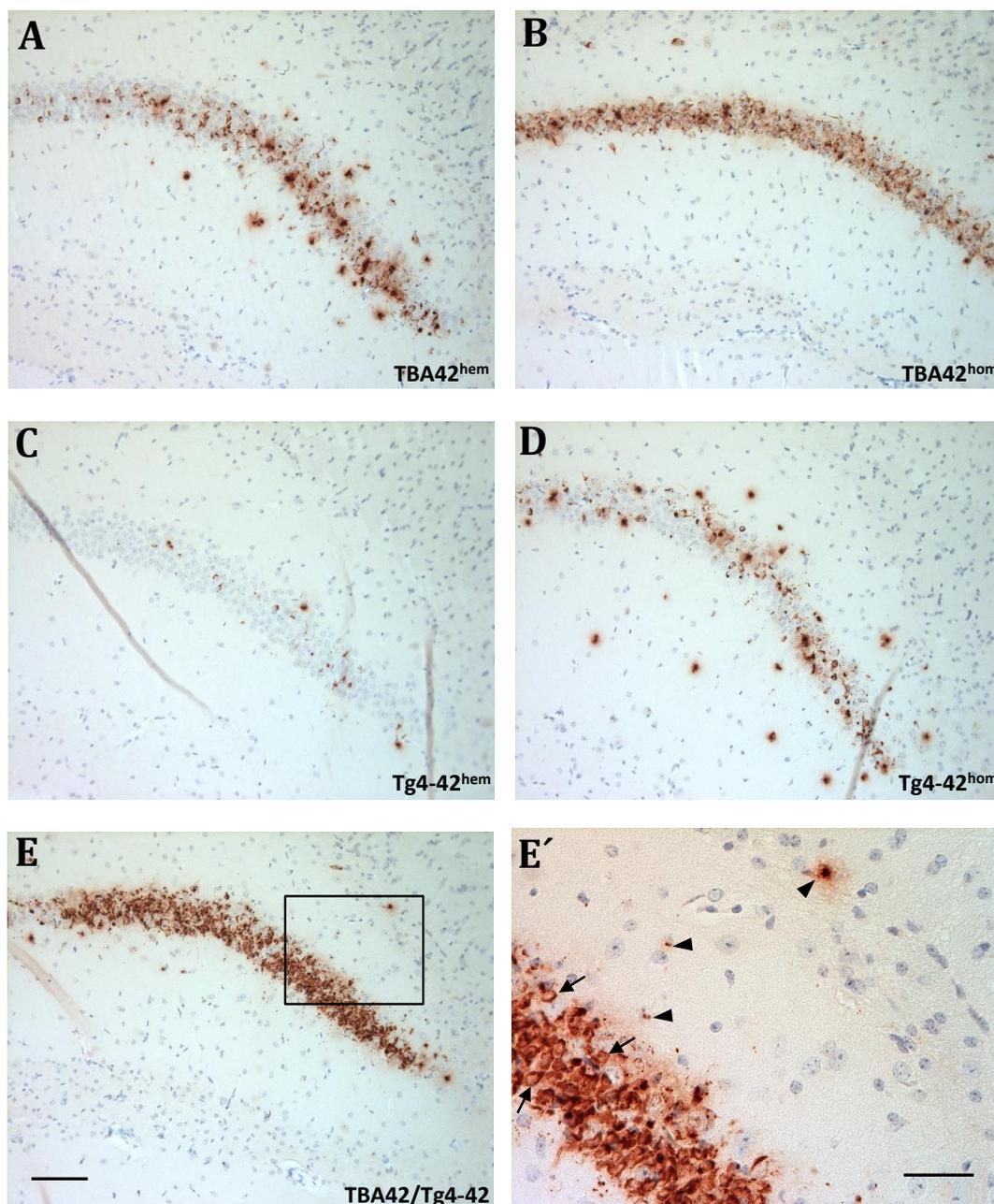


**Fig 10. Strong intraneuronal Aβ accumulation in the CA1 pyramidal cell layer of the hippocampus in TBA42/Tg4-42 mice.** Immunohistochemistry using a pan-Aβ antibody (24311) showed Aβ accumulation already in young (3-month-old) mice of all genotypes tested (A-E). Particularly, prominent intraneuronal Aβ accumulation was observed in young TBA42[hom] mice (B), which was even more pronounced in TBA42/Tg4-42 mice (E). (E') Represents a magnification of (E) demonstrating intraneuronal Aβ (arrows) and small extracellular Aβ aggregates (arrowheads). Scale bars, A-E = 100 µm and E' = 50 µm (Taken from Lopez-Noguerola *et al.,* 2018).
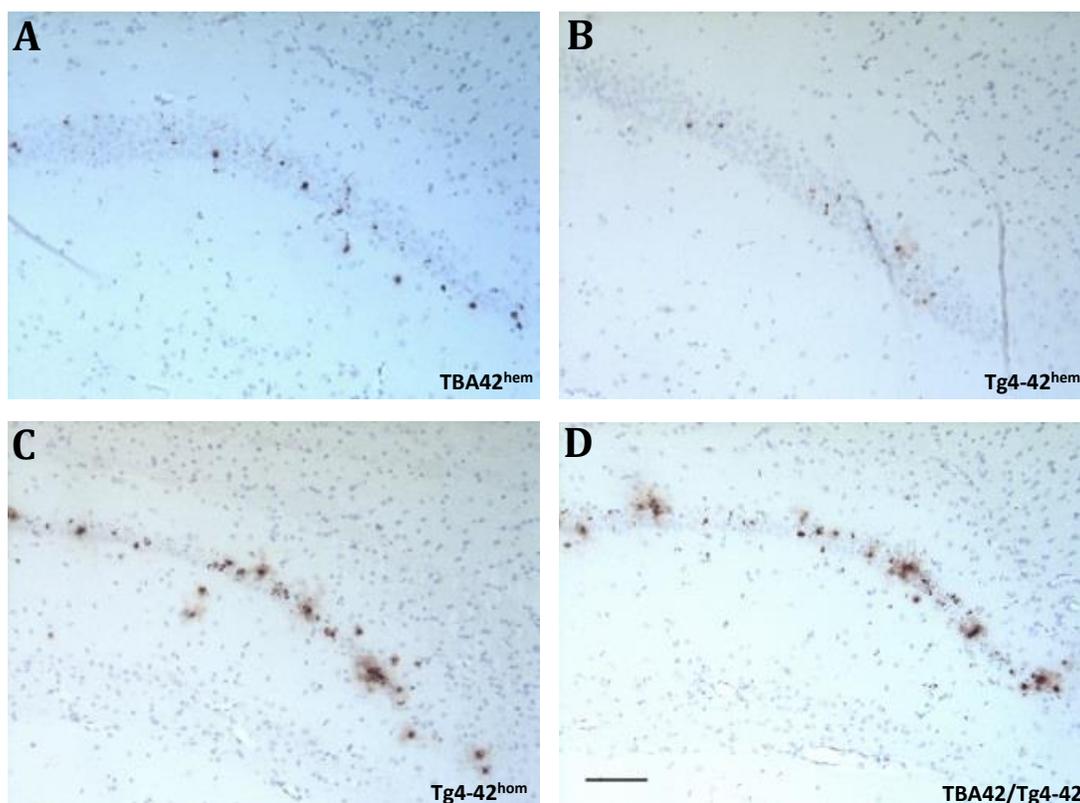
**Fig 11. Aβ immunoreactivity in aged TBA42[hem], Tg4-42[hem], Tg4-42[hom] and TBA42/Tg4-42 mice.**
Reduced immunoreactivity in the CA1 region using a pan-Aβ antibody (24311) was observed in all the aged (5-6 months) mice examined (A-D). Scale bar = 100µm.

## 3.1.2 Behavioral characterization of TBA42/Tg4-42 mice

### 3.1.2.1 Reduced anxiety levels in TBA42/Tg4-42 mice

In order to study if the anxiety behavior of mice is altered when $Aβ_{pE-42}$ and $Aβ_{4-42}$ are combined, the elevated plus maze test was employed. Young TBA42/Tg4-42 mice (mean = 26.44, SEM ± 1.28 %) revealed reduced anxiety levels compared to age-matched WT (One-way ANOVA, mean = 12.22, SEM ± 1.58 %, p = 0.0017) and Tg4-42[hem] (One-way ANOVA, mean =p = 0.0157) mice, as seen by a higher percentage of time spent in the open arms (Fig. 12A). No change in the anxiety-like behavior was found in young TBA42[hem] (mean = 17.08, SEM ± 2.27 %), Tg4-42[hem] (mean = 14.32, SEM ± 1.94 %) and Tg4-42[hom] mice (mean = 20.15, SEM ± 2.02 %). The anxiety levels were even further

decreased in aged bigenic mice (mean = 53.13, SEM ± 16.82 %) when compared to age-matched WT (One-way ANOVA, mean = 5.76, SEM ± 1.06 %, p < 0.0001), TBA42[hem] (One-way ANOVA, mean = 22.98, SEM ± 4.95 %, p = 0.0122), Tg4-42[hem] (One-way ANOVA, mean = 9.41, SEM ± 1.86 %, p = 0.0005) and Tg4-42[hom] animals (One-way ANOVA, mean = 15.38, SEM ± 5.26 %, p = 0.0029) (Fig. 12A). In addition to the time spent in the open arms, the distance travelled during the entire test was used as an index of general activity during the testing period. No significant differences in the distance travelled could be detected in all the young (One-way ANOVA, p = 0.4401) and aged (One-way ANOVA, p = 0.2310) mice tested (Fig. 12B).
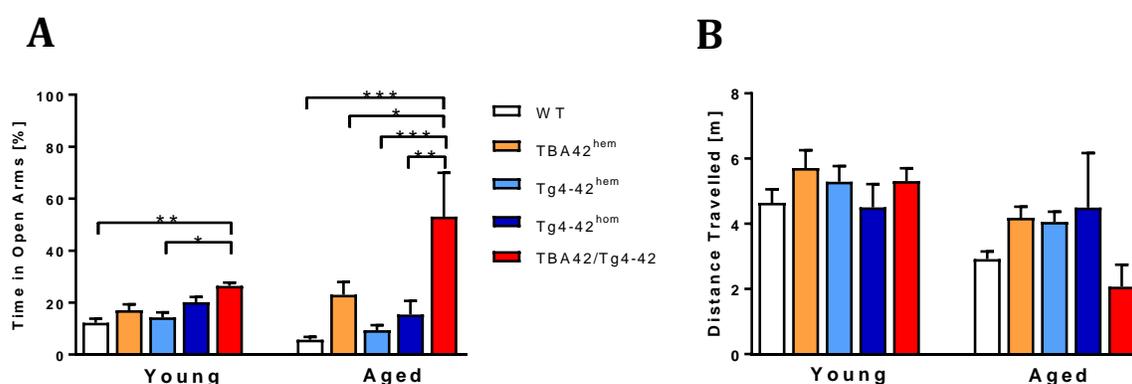


**Fig 12. Reduced anxiety levels in TBA42/Tg4-42 mice.** Reduced anxiety-like behavior could be observed already in young TBA42/Tg4-42 mice as reflected by a significantly greater amount of time spent in the open arms when compared to WT and Tg4-42[hem] mice. Anxiety levels were further decreased in an age-dependent manner in TBA42/Tg4-42 mice compared to age-matched WT, TBA42[hem], Tg4-42[hem] and Tg4-42[hom] mice (A). No difference in the distance travelled between analyzed groups in the young or aged mice could be detected (B). One-way ANOVA followed by Tukey's multiple comparison test. All data were given as means ± SEM *p<0.05; **p<0.01; ***p<0.001; n = 4-12 (Taken from Lopez-Noguerola *et al.*, 2018)

### 3.1.2.2 Intact working memory in TBA42/Tg4-42 mice

In order to evaluate the spatial working memory of TBA42/Tg4-42 bigenic mice, the cross maze alternation task was used. Young and aged WT, TBA42[hem], Tg4-42[hem], Tg4-42[hom] and TBA42/Tg4-42 mice were analyzed. Independent of age and genotype, the results revealed no differences in the alternation rate nor the distance travelled in all animals tested (Fig. 13A, B).

**A**



**B**
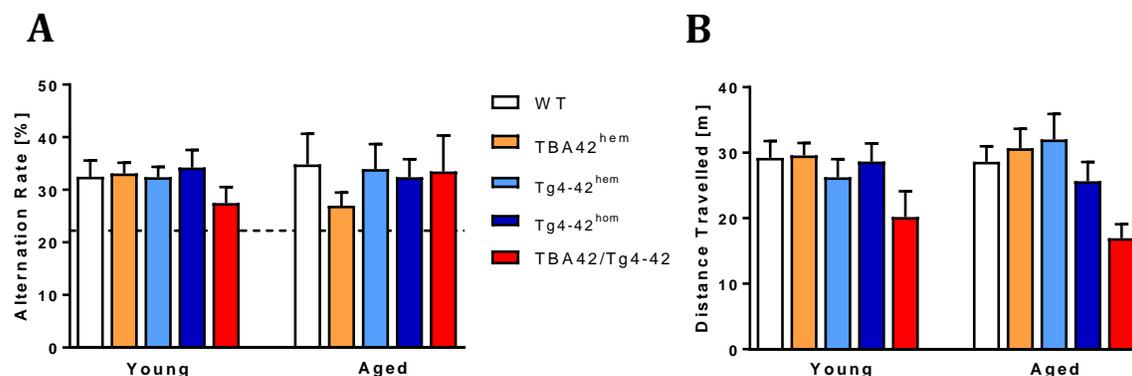


**Fig 13. No working memory deficits in TBA42/Tg4-42 mice.** No differences in alternation rate (A) in young and aged TBA42/Tg4-42 bigenic mice were detected. Likewise, no differences in distance travelled could be detected (B). One-way ANOVA followed by Tukey's multiple comparison test. The dotted line represents the chance level. All data were given as means ± SEM. n = 4-12 per group.

### 3.1.2.3  No spatial reference memory deficits in TBA42/Tg4-42 mice

The Morris water maze test was used to examine spatial reference memory performance in TBA42/Tg4-42, TBA42, Tg4-42[hem], Tg4-42[hom] and wild-type mice. Each animal was subjected to a nine-day protocol, starting with a three-day cued training followed by a five-day acquisition training and a final one-day probe trial.

The three days of the cued training phase serve to familiarize the animals with the pool and to avoid misinterpretation of results due to potential sensory and/or motor deficits. All young mice showed progressively decreased escape latencies in the cued training (Fig. 14 A; two-way repeated measures (RM) ANOVA; main effect of days: p < 0.0001). The swimming speed did not differ between the groups analyzed (Fig. 14B; Two-way RM ANOVA; main effect of genotype: p = 0.64). Nevertheless, due to severe motor deficits observed in the aged TBA42/Tg4-42 mice, these animals failed to reach the criteria to continue the task. Therefore, they were discarded and only young mice were used for the subsequent acquisition training and probe trial.

**A**



**B**
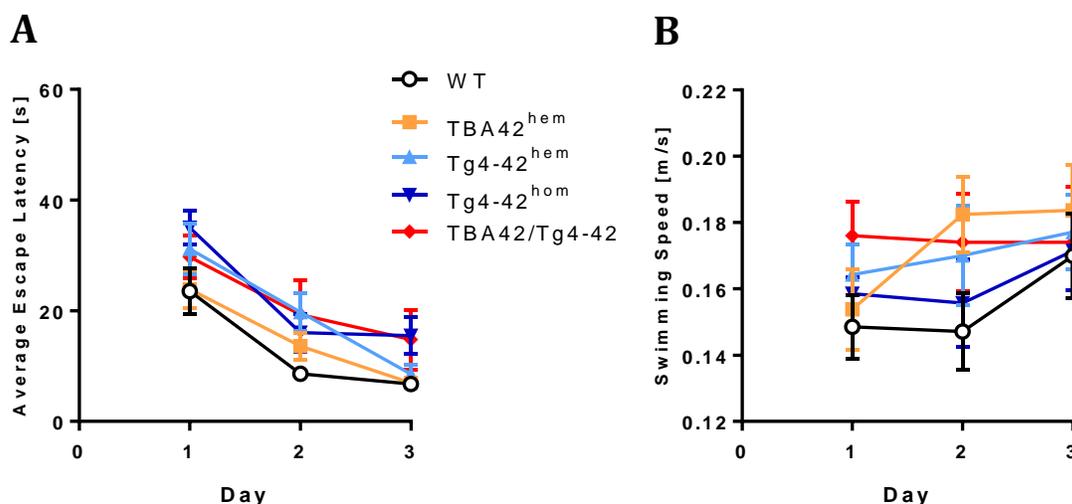


**Fig 14. No deficiencies in eyesight and motor abilities were detected in young TBA42/Tg4-42 mice.** Cued training was conducted to familiarize the mice with the pool and to exclude effects due to sensory and/or motor deficits. Young wild-type, TBA42[hem], Tg4-42[hem], Tg4-42[hom] and TB42/Tg4-42 mice were evaluated. (A) All groups tested showed progressively shorter escape latencies in response to training. (B) Swimming speed did not differ between the groups. (A, B) Two-way repeated measures ANOVA. All data were given as means ± SEM. n = 5-8 per group.

In the five-day acquisition training phase, spatial learning of mice was evaluated by testing their ability to find the location of a hidden platform using proximal and distal cues. All groups tested displayed a significant decrease in escape latencies over the entire duration of the acquisition training (Fig. 15A, two-way RM ANOVA; main effect of days: $p < 0.0001$). No significant differences in the swimming speed could be found between the animals tested (Fig. 15B; two-way RM ANOVA; main effect of genotype: $p = 0.13$).

Finally, a probe trial was performed one day after the last acquisition training trail in order to evaluate spatial reference memory. To this end, the platform was removed and mice were allowed to swim in the pool for 60 seconds. Wild-type, single- and double-transgenic mice exhibited a clear preference for the target quadrant, as shown by the percentage time spent in the different quadrants of the pool (Fig.16 A). Swimming speeds were comparable among the groups analyzed in the probe trial (Fig. 16B).

**A**



**B**
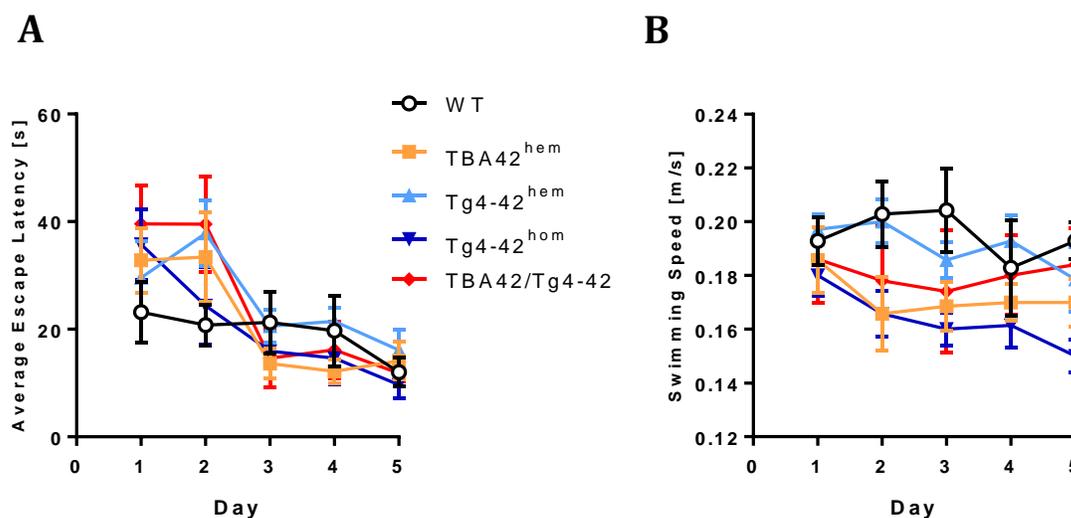


**Fig 15. No spatial learning impairment in young TBA42/Tg4-42 mice.** Acquisition training was performed to evaluate spatial learning. (A) Animals tested revealed progressively decreased escape latencies over the five-day training. (B) Comparable swimming speeds were observed between the groups analyzed. (A, B) Two-way repeated measures ANOVA. All data were given as means ± SEM. n = 5-8 per group.

**A**



**B**
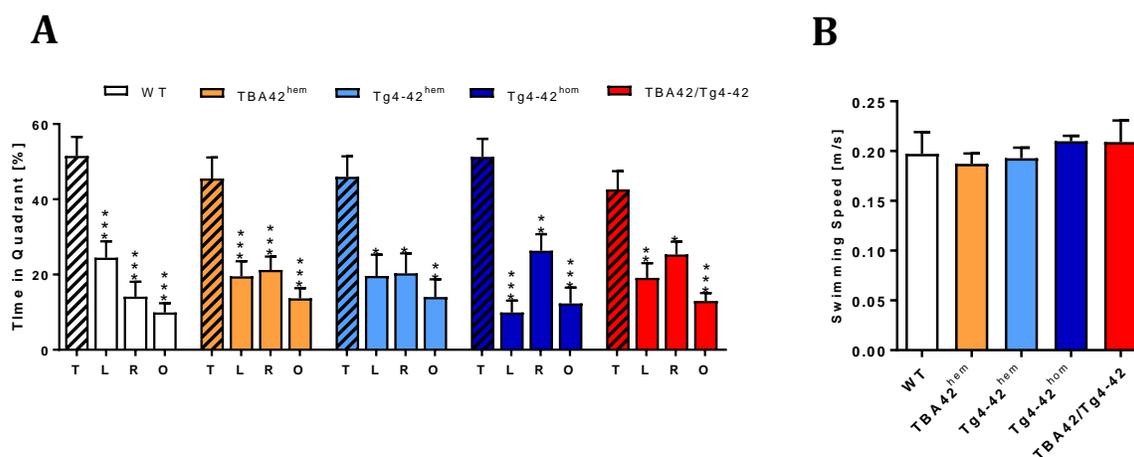


**Fig 16. No spatial reference memory deficits in young TBA42/Tg4-42 mice.** The probe trial was used to evaluate spatial reference memory. (A) Young wild-type, TBA42, Tg4-42[hem], Tg4-42[hom] and TBA42/Tg4-42 mice were examined. All groups tested spent a significantly greater percentage of time in the target quadrant. (B) No significant differences were observed in the swimming speed during the probe trial. (A, B): One-way ANOVA followed by Tukey's multiple comparisons test. All data were given as means ± SEM. *p < 0.05; **p < 0.01; ***p < 0.001; n = 5-8 per group. T = target, L = left, R = right and O = opposite.

### 3.1.2.4  Co-expression of Aβ$_{pE3-42}$ and Aβ$_{4-42}$ aggravates motor function in an age-dependent manner

In order to evaluate whether the co-expression of Aβ$_{pE3-42}$ and Aβ$_{4-42}$ has an impact on the sensory-motor abilities of TBA42/Tg4-42 mice, the string suspension, balance beam and inverted grip tasks were performed.

The string suspension task evaluates motor strength and coordination by measuring the ability of mice to remain on a string (Moran *et al.* 1995). In this task, no significant differences in the scores could be detected in the young TBA42/Tg4-42 mice, as these animals performed similarly to age-matched WT, TBA42[hem], Tg4-42[hem] and Tg4-42[hom] mice (Fig. 17A). Yet, in the aged groups, TBA42/Tg4-42 (mean = 0.33, SEM ± 0.19) mice exhibited a poorer performance compared to same-aged WT (One-way ANOVA, mean = 4.66, SEM ± 0.22, p < 0.0001), Tg4-42[hem] (One-way ANOVA, mean = 4.09, SEM ± 0.42, p < 0.0001) and Tg4-42[hom] mice (One-way ANOVA, mean = 3.52, SEM ± 0.66, p = 0.0003).  Aged TBA42[hem] (mean = 1.33, SEM ± 0.44) also performed poorly compared to age-matched WT (One-way ANOVA, p < 0.0001), Tg4-42[hem] (One-way ANOVA, p = 0.0004) and Tg4-42[hom] mice (One-way ANOVA, p = 0.0061). No significant difference could be observed between aged TBA42[hem] and aged TBA42/Tg4-42 mice in this task.

The balance beam task was used to assess balance and fine motor coordination (Arendash *et al.* 2001). No motor impairment in this task was detected in any of the young mice analyzed, including the TBA42/Tg4-42 mice (Fig. 17B). In contrast, aged TBA42/Tg4-42 (mean = 1, SEM ± 0.14 s) mice performed worse than age-matched WT (One-way, mean =52.5, SEM ± 3.10 s, p < 0.0001), TBA42[hem] (One-way ANOVA, mean = 27.5, SEM ± 5.35 s, p < 0.0039), Tg4-42[hem] (One-way ANOVA, mean = 60, SEM ± 0.0016, p < 0.0001) and Tg4-42[hom] mice (One-way ANOVA, mean = 35.33, SEM ± 8.57 s, p = 0.0007). Motor deficits were also observed in aged TBA42[hem] mice when compared to age-matched WT (One-way ANOVA, p = 0.0023) and Tg4-42[hem] animals (One-way ANOVA, p = 0.0006). In addition, aged Tg4-42[hom] performed poorer than aged Tg4-42[hem] (One-way ANOVA, p = 0.0311).

Finally, motor abilities, vestibular function and muscle strength, were tested with the inverted grip task by analyzing the latency to fall (Erbel-Sieler *et al.* 2004) (Fig. 17C). As observed in the other tasks, regardless of genotype, no motor deficits could be detected in the young groups analyzed. Nevertheless, aged TBA42/Tg4-42 mice (mean = 9.14) demonstrated strong motor deficits shown by shorter latencies to fall compared to same-aged WT (One-way ANOVA, mean = 60, SEM ± 0 s, p<0.0001), TBA42[hem] (One-way ANOVA, mean = 34.75, SEM ± 7.98 s, p = 0.0083), Tg4-42[hem] (One-way ANOVA, mean = 58.29, SEM ± 1.71 s, p < 0.0001) and Tg4-42[hom] mice (One-way ANOVA, mean = 60, SEM ± 0 s, p < 0.0001). Likewise, aged TBA42[hem] performed worse than WT (One-way ANOVA, p = 0.0032) and Tg4-42[hem] animals (One-way ANOVA, p = 0.0179).
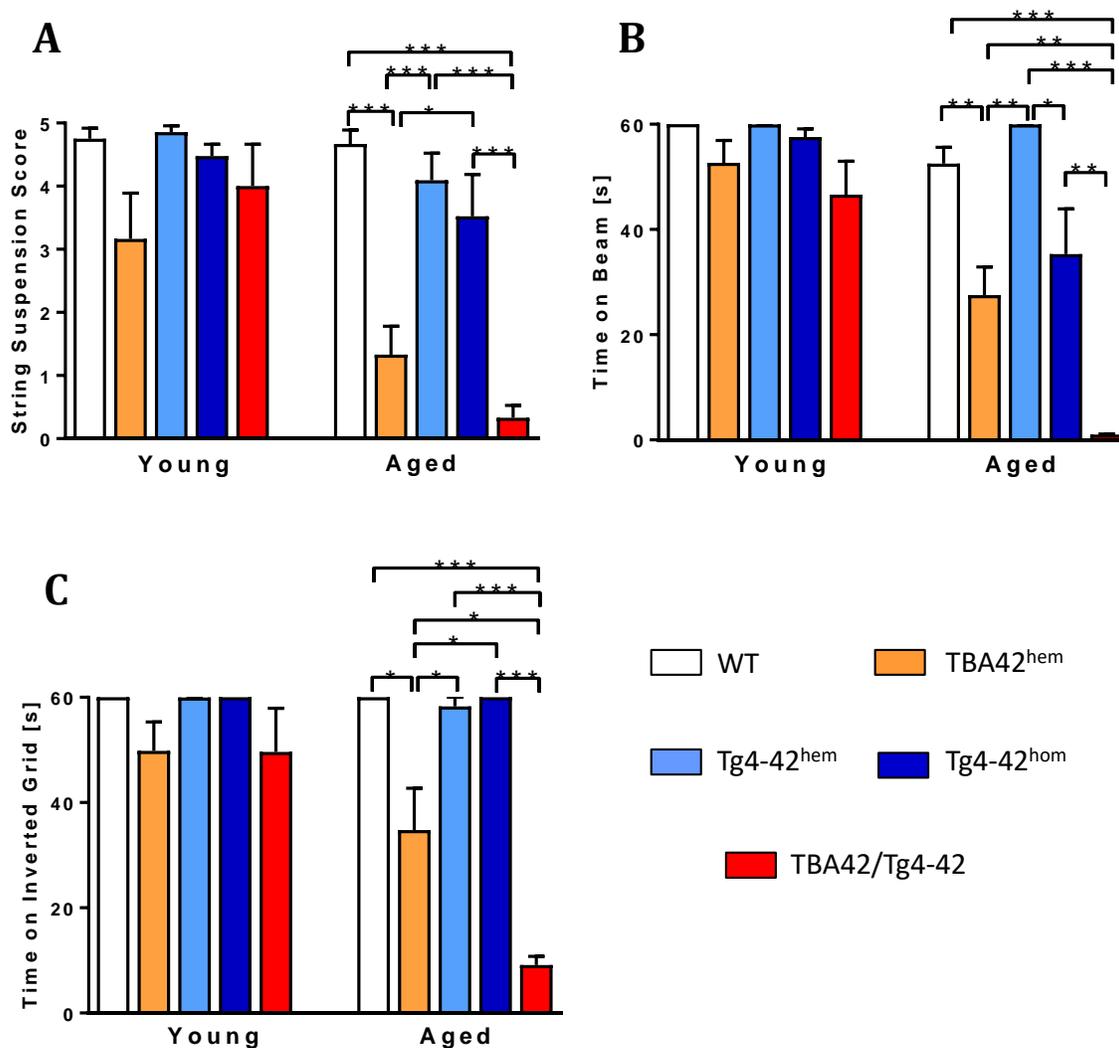
**Fig. 17. Severe motor deficits in TBA42/Tg4-42 mice.** The string suspension (A), the balance beam (B) and the inverted grid task (C) revealed severe motor deficits in aged TBA42/Tg4-42 mice. No significant difference could be observed between aged TBA42[hem] and TBA42/Tg4-42 mice in the string suspension task. One-way ANOVA followed by Tukey's multiple comparison test. All data were given as means ± SEM *p<0.05; **p<0.01; ***p<0.001; n = 5-12 per group (Taken from Lopez-Noguerola *et al.*, 2018)

### 3.1.3  Co-expression of Aβ$_{pE3-42}$ and Aβ$_{4-42}$ accelerates neuron loss in the hippocampus of transgenic mice

In order to analyze the impact of the co-expression of Aβ$_{pE3-42}$ and Aβ$_{4-42}$ on the neuron numbers of the CA1 pyramidal layer of the hippocampus, unbiased designed-based stereological studies were conducted as previously described.
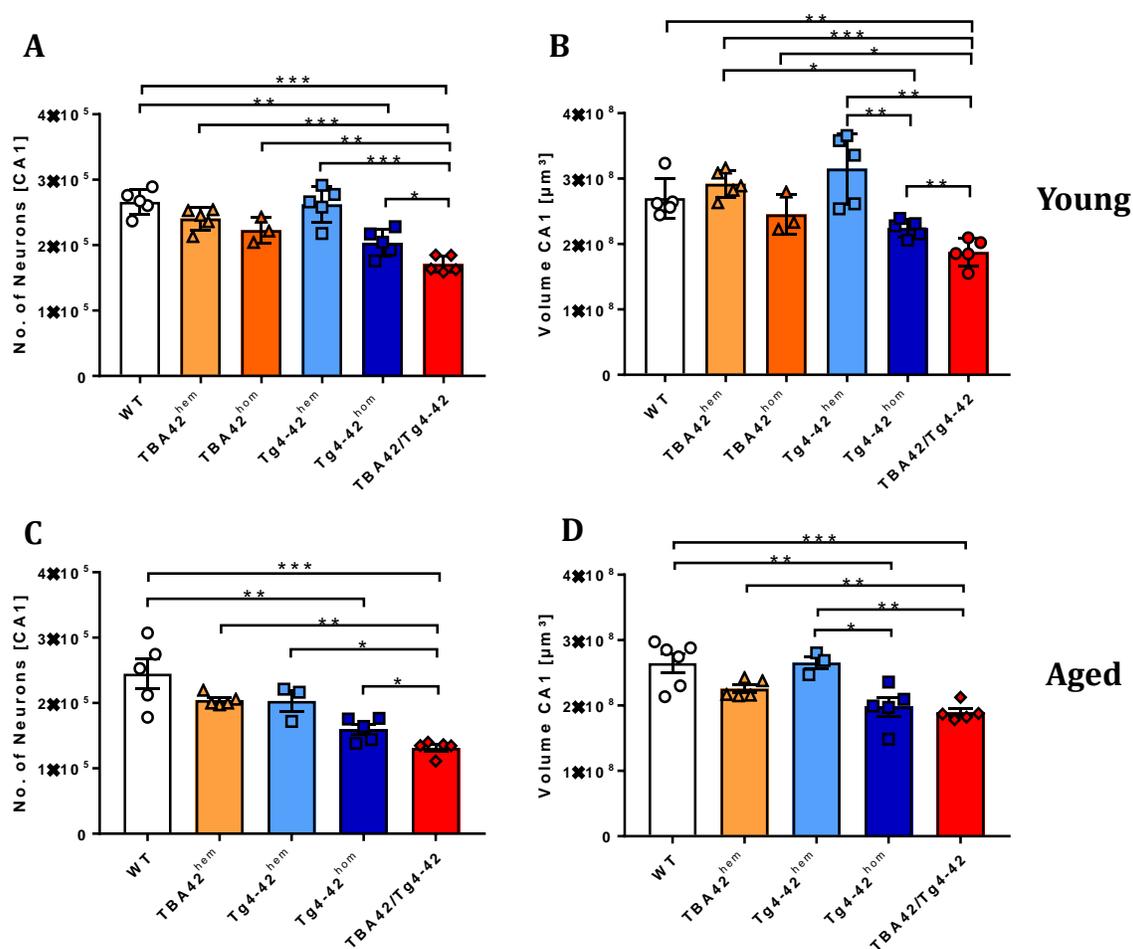


**Figure 18. Accelerated neuron loss in the hippocampal CA1 pyramidal cell layer of TBA42/Tg4-42 bigenic mice.** Design-based stereological analysis revealed a significant reduction in the CA1 neuron numbers of young TBA42/Tg4-42 mice when compared to the rest of the age-matched groups (A). Like for the CA1 neuron numbers, significant reduction in the CA1 volume of young TBA42/Tg4-42 mice was found when compared to same-aged WT, TBA42hem, TBA42hom, Tg4-42hem and Tg4-42hom mice (B). Aged TBA42/Tg4-42 mice showed higher neuron loss when compared to the rest of the age-matched groups (C). Significantly lower CA1 volume could be observed in aged TBA42/Tg4-42 mice compared to the rest of the age-matched groups with exception of the Tg4-42hom mice (D). One-way ANOVA followed by Tukey's multiple comparison test. TBA42/Tg4-42 vs Tg4-42hom: One-way ANOVA followed by un-paired t-test (In A, B and C). All data were given as means ± SEM *p<0.05; **p<0.01; ***p<0.001; n = 3-6 per group (Taken from Lopez-Noguerola *et al.*, 2018)

The neurons of the CA1 pyramidal layer were quantified in young (2-3 months of age) and aged (5-6 months of age) mice. Stereological analysis revealed a highly significant neuron loss (36%) in young TBA42/Tg4-42 mice (Fig. 18A, One-way ANOVA, mean = 170,845, SEM ± 5,744, p<0.001) compared to age-matched WT mice (mean = 266,076, SEM ± 8,723). In young TBA42[hem] (mean = 240,353, SEM ± 7,517), TBA42[hom] (mean = 222,841, SEM ± 11,182) and Tg4-42[hem] (mean = 262,277, SEM ± 12,423) mice, no significant neuron loss could be detected when compared to young WT mice, while Tg4-42[hom] (mean = 203,664, SEM ± 9,155) mice showed a significant neuron loss when compared to Tg4-42[hem] (One-way ANOVA, p = 0.0016) and WT animals (One-way ANOVA, p = 0.0008). Furthermore, young TBA42/Tg4-42 mice exhibited reduced CA1 neuron numbers compared to TBA42[hem] (One-way ANOVA, p = 0.0002), TBA42[hom] (One-way ANOVA, p = 0.0192), Tg4-42[hem] (One-way ANOVA, p < 0.0001) and Tg4-42[hom] mice (t-test, p = 0.0161).

No significant difference in the neuron numbers could be found between aged WT (mean = 253,803, SEM ± 20,581), TBA42[hem] (mean = 204,432, SEM ± 4,023) and aged Tg4-42[hem] mice (mean = 203,092, SEM ± 15,743) (Fig. 18C). However, aged TBA42/Tg4-42 mice (mean = 131,339, SEM ± 5,131) revealed reduced neuron numbers compared to aged WT (One-way ANOVA, p < 0.0001), TBA42[hem] (One-way ANOVA, p = 0.0047) and aged Tg4-42[hem] mice (One-way ANOVA, p = 0.0177). Significant reduction in CA1 neuron numbers between aged TBA42/Tg4-42 and aged Tg4-42[hom] (mean = 159,779, SEM ± 7,882) could be detected after a student's t-test (p = 0.0165).

A quantitative analysis of the CA1 volume was additionally performed in the young and aged mice. Significant CA1 volume reduction was found in the young TBA42/Tg4-42 (mean = $1.87 \times 10^8$, SEM ± $9.33 \times 10^6$ μm$^3$) mice in comparison to age-matched WT controls (One-way ANOVA, mean = $2.701 \times 10^8$, SEM ± $1.37 \times 10^7$ μm$^3$, p = 0.0044) (Fig. 18B). Moreover, young TBA42/Tg4-42 mice revealed a reduced CA1 volume compared to young TBA42[hem] (One-way ANOVA, mean = $2.91 \times 10^8$, SEM ± $9.4 \times 10^6$, p = 0.0003) and young Tg4-42[hem] animals (One-way ANOVA, mean = $3.15 \times 10^8$, SEM ± $2.40 \times 10^7$, p < 0.0001). Additionally, young Tg4-42[hom] showed a significantly lower CA1 volume compared to age-matched TBA42[hem] (One-way ANOVA, p = 0.0003) and Tg4-42[hem] mice (One-way ANOVA, p = 0.0016). Only after an unpaired t-test,

significant differences in the CA1 volume between the young TBA42/Tg4-42 and young TBA42$^{hom}$ (t-test, p = 0.0178) and between young TBA42/Tg4-42 and young Tg4-42$^{hom}$ (t-test, p = 0.0109) animals could be detected. At 6 months of age, a higher decrease in CA1 volume (~48%) in TBA42/Tg4-42 mice (mean = 1.89 x 10$^8$, SEM ± 5.98 x 10$^6$ µm$^3$) was observed compared to age-matched WT (One-way ANOVA, mean = 2.64 x 10$^8$, SEM ± 1.49 x 10$^7$ µm$^3$, p = 0.0008) and Tg4-42$^{hem}$ mice (One-way ANOVA, mean = 2.65 x 10$^8$, SEM ± 9.77 x 10$^6$ µm$^3$) (Fig. 18D). At this age, Tg4-42$^{hom}$ (mean = 1.98 x 10$^8$, SEM ± 1.47 x 10$^7$ µm$^3$) mice also showed significant reduction in CA1 volume compared to age-matched WT (One-way ANOVA, p = 0.0026) and Tg4-42$^{hem}$ (One-way ANOVA, p = 0.0123) mice, while no differences could be detected when compared to aged TBA42/Tg4-42 mice.

### 3.1.4  Amyloid pathology in the spinal cord of TBA42/Tg4-42 mice

Aβ$_{pE3-42}$ and Aβ$_{4-42}$ are expressed under the control of the neuron-specific murine Thy-1 promoter, which is active in both hippocampus and spinal cord. Thus, in order to study the Aβ staining profile in the spinal cord of TBA42/Tg4-42 mice, immunohistochemical staining of spinal cord sections using a pan-Aβ antibody were performed. The immunostainings revealed intraneuronal and small extracellular Aβ aggregates already in the young mice without regard for the genotype (Fig. 19 A-E). However, the extracellular Aβ aggregates and intraneuronal Aβ accumulation looked more prominent in young TBA42$^{hom}$ and TBA42/Tg4-42 mice (Fig.19 B, E). Moreover, with ageing (Fig. 19 F-I), the amyloid spinal cord pathology was specifically increased in the TBA42/Tg4-42 mice (Fig. 19 I).

A further quantitative analysis of the spinal cord area covered by Aβ staining revealed a significant greater abundance in young TBA42$^{hom}$ (mean = 2.49, SEM ± 0.37 %) when compared to age-matched TBA42$^{hem}$ (One-way ANOVA, mean = 0.14, SEM ± 0.03 %, p < 0.0001), Tg4-42$^{hem}$ (One-way ANOVA, mean = 0.11, SEM ± 0.04 %, p < 0.0001), Tg4-42$^{hom}$ (One-way ANOVA, mean = 0.18, SEM ± 0.03 %, p < 0.0001) and TBA42/Tg4-42 (One-way ANOVA, mean = 1.02, SEM ± 0.19 %, p < 0.0001) mice (Fig. 19

J). Additionally, young TBA42/Tg4-42 mice exhibited an increased amyloid pathology when compared to young TBA42[hem] (One-way ANOVA, p = 0.0019), Tg4-42[hem] (One-way ANOVA, p = 0.0014) and Tg4-42[hom] (One-way ANOVA, p = 0.0029) mice. The same held true for aged TBA42/Tg4-42 mice (mean = 1.53, SEM ± 0.39 %), where amyloid pathology was increased in comparison to age-matched TBA42[hem] (One-way ANOVA, mean = 0.25, SEM ± 0.05 %, p 0.0019), Tg4-42[hem] (One-way ANOVA, mean = 0.03, SEM ± 0.01 %, p = 0.0004) and Tg4-42[hom] (One-way ANOVA, mean = 0.32, SEM ± 0.04 %, p = 0.003) mice. Weak Aβ immunoreactivity was detected in the spinal cord of TBA42[hem], Tg4-42[hem] and Tg4-42[hom] at all time points analyzed.
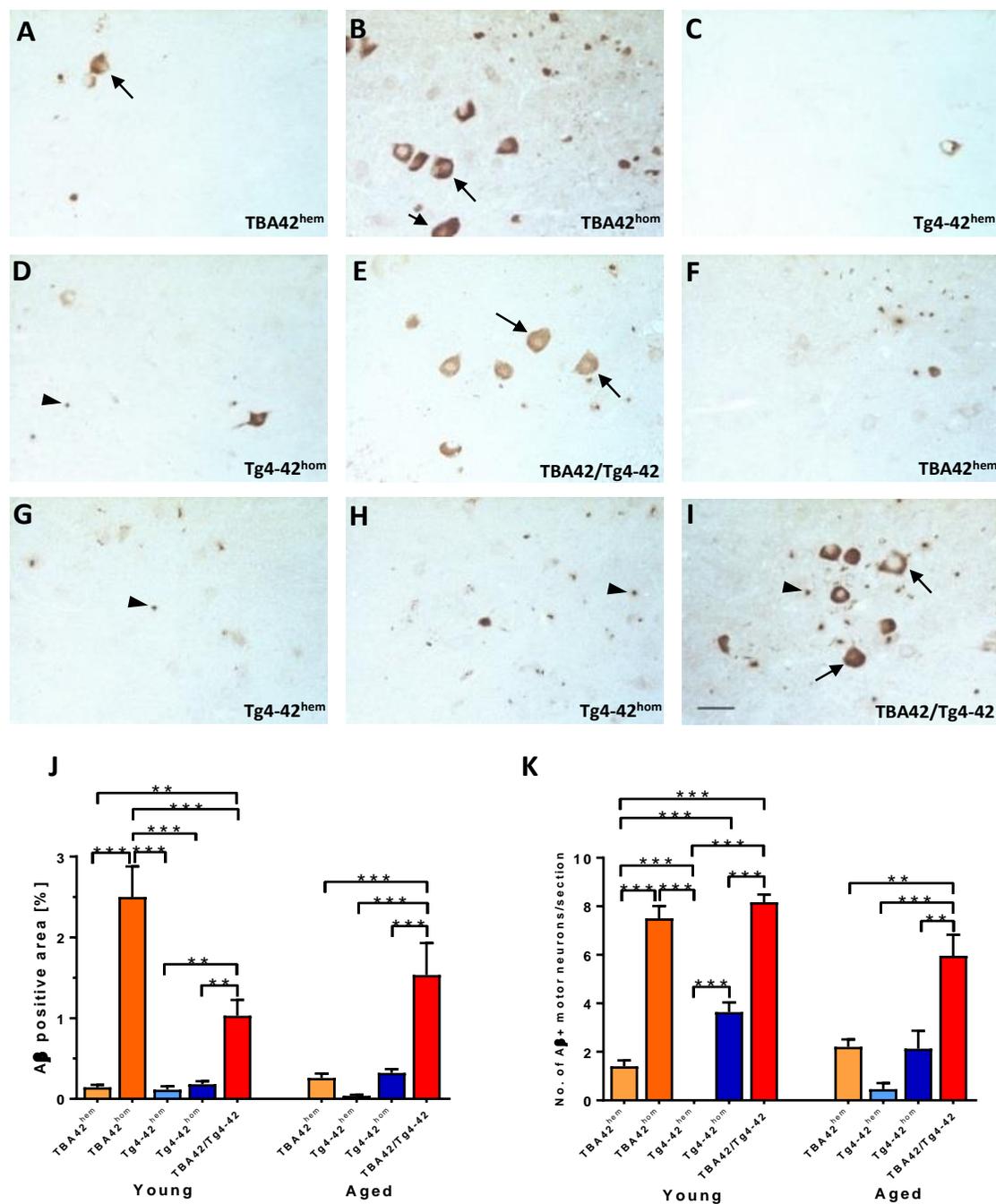
**Fig. 19. Extra- and intraneuronal Aβ deposition in the spinal cord of transgenic mice.** Immunohistochemical staining using the pan-Aβ 24311 antibody revealed extracellular Aβ aggregates and intraneuronal Aβ accumulation in the motor neurons (arrows) of the spinal cord starting already at 2-3 months of age (young mice) (A-E), which increased in aged mice (5-6 months) (F-I). Quantification of the percentage of Aβ positive area showed a high Aβ positive area already in young TBA42[hom] and TBA42/Tg4-42 bigenic mice, which increased in aged TBA42/Tg4-42 mice (J). Similarly, the total number of Aβ-positive motor neurons was significantly higher in young TBA42[hom] and TBA42/Tg4-42 mice when compared to the rest of the analyzed groups. A higher number of Aβ-positive motor neurons was also observed in aged bigenic animals (K). One-way ANOVA followed by Bonferroni's post hoc test. All data were given as means ± SEM *$p<0.05$ **$p<0.01$; ***$p<0.001$; n = 3-5 per group; scale bar = 50µm (Taken from Lopez-Noguerola *et al.*, 2018).

### 3.1.5   High Aβ accumulation in the motor neurons of TBA42/Tg4-42 mice

In order to investigate whether the motor deficits seen in the TBA42/Tg4-42 mice correlated with the spinal cord pathology observed in these animals, a quantification of Aβ positive motor neurons was conducted (Fig. 19 K). The results revealed higher numbers in young TBA42/Tg4-42 mice (mean = 8.16, SEM ± 0.31) when compared to age-matched TBA42[hem] (One-way ANOVA, mean = 1.4, SEM ± 0.24, p < 0.0001), Tg4-42[hem] (One-way ANOVA, mean = 0, SEM ± 0, p < 0.0001) and Tg4-42[hom] (One-way ANOVA, mean = 3.63, SEM ± 0.40, p < 0.0001) mice. Similarly, young TBA42[hom] mice displayed higher numbers when compared to same aged TBA42[hem] (One-way ANOVA, p < 0.0001), Tg4-42[hem] (One-way ANOVA, p < 0.0001) and Tg4-42[hom] mice (One-way ANOVA, p < 0.0001) (Fig. 19 K). Young Tg4-42[hom] mice exhibited higher numbers of Aβ immunopositive motor neurons than TBA42[hem] (One-way ANOVA, p = 0.0006) and Tg4-42[hem] mice (One-way ANOVA, p < 0.0001). No significant differences could be detected in the total number of Aβ positive motor neurons between young TBA42[hom] and TBA42/Tg4-42 mice. In aged animals, significant difference could be found only in TBA42/Tg4-42 mice (mean = 5.96, SEM ± 0.86) when compared to age-matched TBA42[hem] (One-way ANOVA, mean = 2.2, SEM ± 0.30, p = 0.0021), Tg4-42[hem] (One-way ANOVA, mean =0.46, SEM ± 0.24, p < 0.0001) and Tg4-42[hom] mice (One-way ANOVA, mean = 2.13, SEM ± 0.73, p = 0.001). Furthermore, a comprehensive and quantitative analysis of the total number of motor neurons with low, intermediate and high intracellular Aβ accumulation was performed in young and aged mice (Fig. 20). In young animals (Fig. 20 C), the results revealed a higher number of motor neurons with low Aβ accumulation in TBA42/Tg4-42 mice (mean = 3.2, SEM ± 0.33) in comparison to same-aged TBA42[hem] (One-way ANOVA, mean = 0.93, SEM ± 0.12, p = 0.0002), TBA42[hom] (One-way ANOVA, mean = 1, SEM ± 0.34, p = 0.001) and Tg4-42[hem] animals (One-way ANOVA, mean = 0, SEM ± 0, p < 0.0001). Likewise, young Tg4-42[hom] mice exhibited greater numbers than same aged TBA42[hem] (One-way ANOVA, p = 0.0009) TBA42[hom] (One-way ANOVA, p = 0.0048) and Tg4-42[hem] mice (One-way, ANOVA, p < 0.0001), while no significant differences were found between young Tg4-42[hom] and TBA42/Tg4-42 mice. Intermediate accumulation was similar in the young TBA42[hom]

(mean = 3.88, SEM ± 0.76) and TBA42/Tg4-42 (mean = 3.66, SEM ± 0.69) groups, whereas TBA42[hem] (mean = 0.46, SEM ± 0.2), Tg4-42[hem] (mean = 0.06, SEM ± 0.06) and Tg4-42[hom] mice (mean = 0.63, SEM ± 0.03) showed significantly lower overall motor neuron numbers. High intracellular Aβ accumulation was only found in the motor neurons of TBA42[hom] mice (mean = 2.66, SEM ± 0.63) (Fig.6C). In the aged mice (Fig. 20 D), no differences in the total number of motor neuron with low Aβ accumulation were found among the all the groups analyzed. Nevertheless, increased numbers of motor neurons with intermediate and high intracellular Aβ levels were found only in the TBA42/Tg4-42 mice (Fig. 20D).
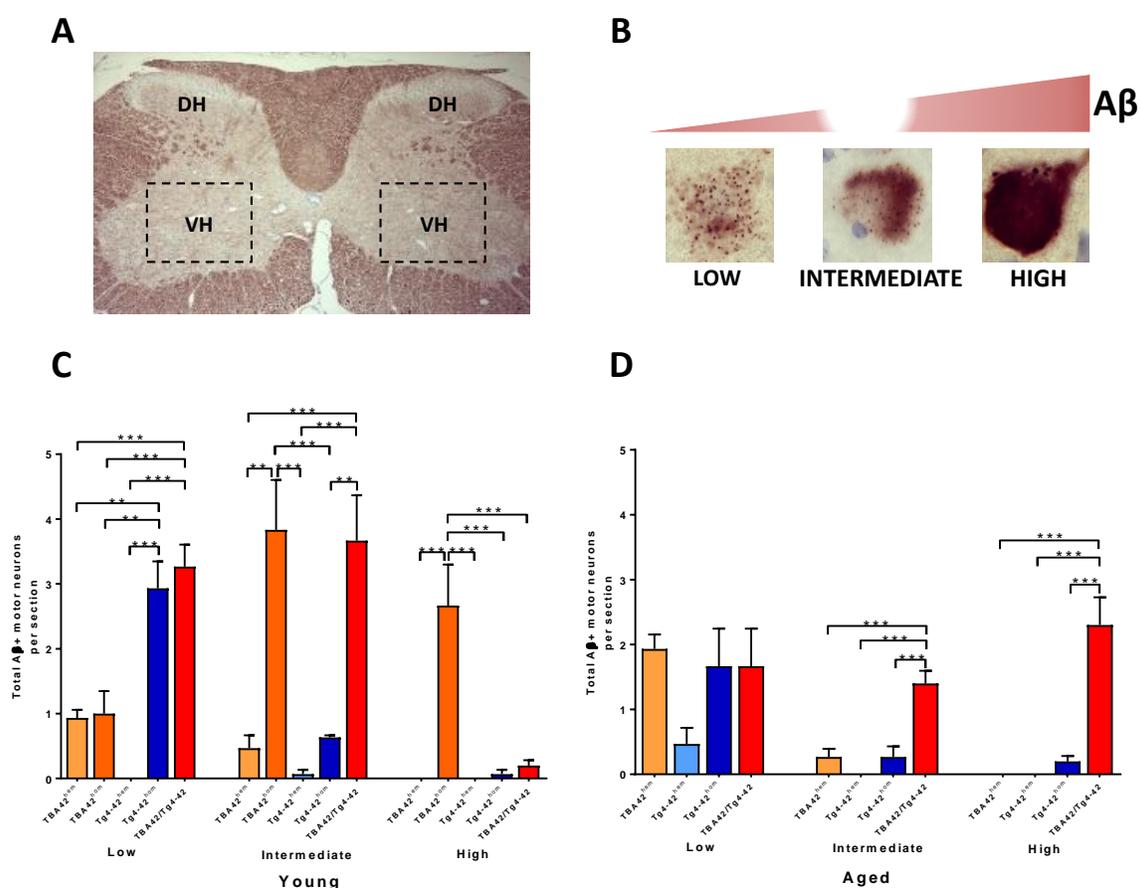


**Fig 20. Quantification of motor neurons with varying levels of intracellular Aβ accumulation.** (A) Schematic picture of the cervical region of the spinal cord showing the dorsal horn (DH) and the ventral horn (VH). (B) Three different Aβ intraneuronal accumulation levels could be found in the motor neurons located in VH and were defined as: low, intermediate and high. In young animals (C), quantification of motor neurons with low Aβ accumulation revealed a high number in the Tg4-42[hom] and TBA42/Tg4-42 mice. Intermediate accumulation was similar in young TBA42[hom] and TBA42/Tg4-42 bigenic mice. Moreover, motor neurons with high accumulation were only found in TBA42[hom] mice. In aged mice (D), no significant difference in the number of motor neurons with low Aβ accumulation could be detected

among the groups. However, motor neuron numbers with intermediate and high Aβ levels were higher in the aged TBA42/Tg4-42 mice when compared with the rest of the groups. One-way ANOVA followed by Tukey's multiple comparison test. All data were given as means ± SEM *p<0.05; **p<0.01; ***p<0.001; n = 3-5 per group (Taken from Lopez-Noguerola *et al.*, 2018).

### 3.1.6 Aggregation kinetics of the combination of Aβ$_{pE3-42}$ and Aβ$_{4-42}$

In order to assess whether the combination of Aβ$_{pE3-42}$ and Aβ$_{4-42}$ has an effect on their aggregation properties *in vitro*, the aggregation profiles of Aβ$_{pE3-42}$, Aβ$_{4-42}$ and an equimolar mixture of both peptides (50 μM final concentration) were monitored by Thioflavin-T (ThT) fluorescence under physiological conditions at pH 7.0 and 37°C.

Under the applied conditions, an initial raise in ThT-fluorescence was observed in the Aβ$_{pE3-42}$, Aβ$_{4-42}$ and equimolar mixture (Fig. 21), indicating an early rapid acceleration in the formation of intermediate assemblies, which may include oligomers and protofibrils. Interestingly, fibril formation seemed to be enhanced in the equimolar mixture of Aβ$_{pE3-42}$ and Aβ$_{4-42}$ compared to the peptides alone, as seen by the higher peaks in the equimolar mixture between the 0 and 1000 minutes. After this time, the maximum peaks were similar for the equimolar mixture and Aβ$_{pE3-42}$ with lower peaks corresponding to the Aβ$_{4-42}$ peptide.
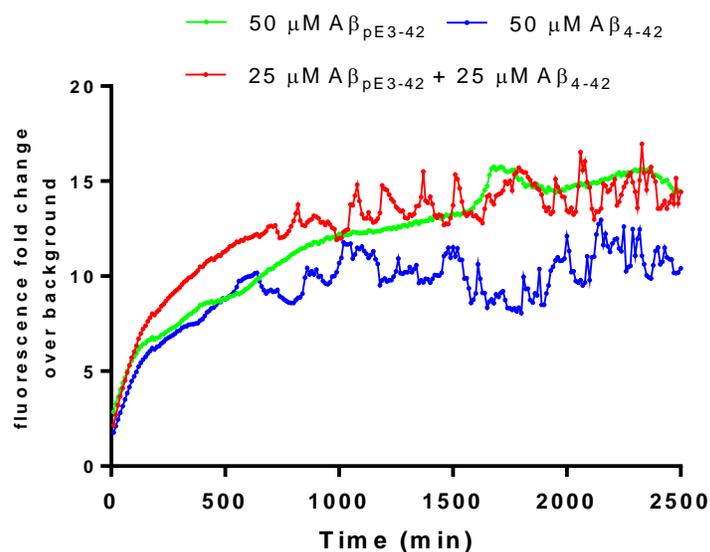


**Fig 21. Aggregation kinetics of Aβ$_{pE3-42}$, Aβ$_{4-42}$ and an equimolar mixture of both peptides were monitored by Thioflavin T fluorescence.** Aβ$_{pE3-42}$ and Aβ$_{4-42}$ displayed a similar accelerated initial fibril formation phase, which was enhanced when both peptides were combined. Each condition was measured in triplicates.

## 3.2 PROJECT II: EXPLORING THE *IN VIVO* ASSOCIATION BETWEEN Aβ PLAQUES AND SOLUBLE Aβ AGGREGATES USING THE FAD4-42 MOUSE MODEL

It has been suggested that soluble Aβ oligomers, and not fibrillar Aβ, are the main neurologically toxic Aβ species during the progression of AD. Additionally, it has been proposed that amyloid plaques may act as reservoirs for the more toxic soluble Aβ oligomeric forms and thus protect neuronal structures from their toxicity (Haass & Selkoe 2007; Brody *et al.* 2017). Therefore, the aim of the present study was to study the association of amyloid plaques and soluble Aβ oligomers. To achieve this, we crossed the well-studied 5XFAD mouse model with Tg4-42 transgenic mice to produce a novel FAD4-42 mouse model. 5XFAD mice develop extracellular amyloid deposits beginning at 2 months of age, which increase in an age-dependent fashion and spread to different brain areas (Oakley *et al.* 2006). The Tg4-42 model produces and liberates soluble toxic $A\beta_{4\text{-}42}$ oligomers that induce neuronal death in the CA1 pyramidal layer of the hippocampus in an age-dependent manner. Moreover, Tg4-42 mice do not develop extracellular amyloid plaques (Bouter *et al.* 2013). Hence, the effects on amyloid pathology and neuron loss were examined in the FAD4-42 transgenic animals.

### 3.2.1 Analysis of amyloid pathology in 5XFAD and FAD4-42 mice

In order to evaluate the impact of additional $A\beta_{4\text{-}42}$ expression on total Aβ deposition, plaque load was measured in the cortex, subiculum, dentate gyrus and thalamus of 3- and 12-month-old 5XFAD and FAD4-42 mice using the 24311 pan-Aβ antibody and the NTX-167 antibody binding to $A\beta_{pE3\text{-}x}$ and $A\beta_{4\text{-}x}$.
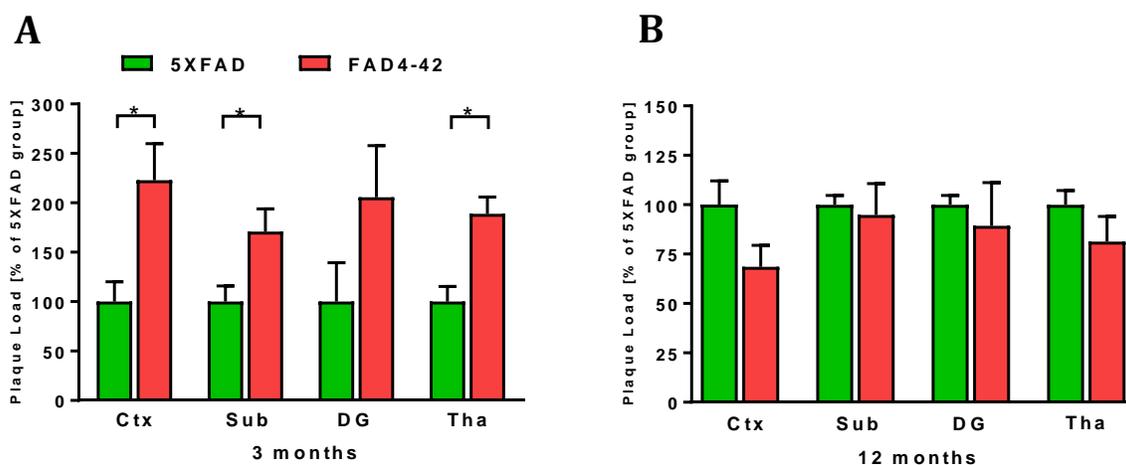
**Fig. 22. Quantification of total Aβ plaque load in 5XFAD and FAD4-42 mice.** (A) At 3 months of age, FAD4-42 showed significant higher levels of plaques reacting with the 24311 pan-Aβ antibody in the cortex, subiculum and thalamus. For the dentate gyrus a trend towards a higher plaque load deposition was detected, however, it did not reach statistical significance. (B) In the 12-month-old groups, no significant differences could be observed in the different brain regions analyzed. Abbreviations: Ctx = cortex, Sub = subiculum, DG = dentate gyrus and Tha = thalamus. Unpaired t-test; *p < 0.05. n = 5-6 per group.

At 3 months of age, a significant increase in plaque load in FAD4-42 mice using the 24311 antibody could be detected in the cortex (+123%; unpaired t-test; p = 0.01), subiculum (+71%; unpaired t-test; p = 0.02) and thalamus when compared to age-matched 5XFAD mice (+88%; unpaired t-test; p = 0.003) (Fig. 22A). Even though a trend towards higher plaque load could also be observed in the dentate gyrus of FAD4-42 mice, it did not reach a significant difference. Twelve-month-old mice did not show differences in the plaque load in any of the brain regions analyzed (Fig. 22 B).

Total $Aβ_{pE3-x}$ and $Aβ_{4-x}$ plaque area was significantly increased in the cortex (+236%; unpaired t-test; p = 0.001), subiculum (+189%; unpaired t-test; p = 0.002), dentate gyrus (+200%; unpaired t-test; p = 0.01) and thalamus (+290%; unpaired t-test; p = 0.0003) of three-month-old FAD4-42 mice (Fig. 23A) when compared to 5XFAD animals. However, no significant differences could be detected between old 5XFAD and FAD4-42 mice (Fig. 23B).
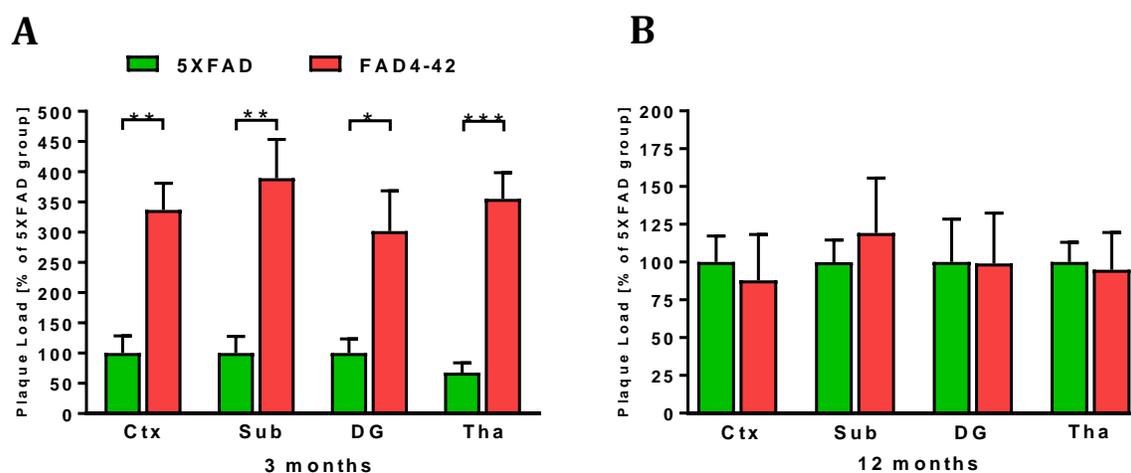
**Fig. 23. Quantification of Aβ $_{pE3-x}$ and Aβ$_{4-x}$-positive plaque load in 5XFAD and FAD4-42 mice.** (A) At 3 months of age, FAD4-42 showed significant higher levels of plaques reacting with the antibody NTX4X-167 recognizing Aβ $_{pE3-x}$ and Aβ$_{4-x}$ in the cortex, subiculum, dentate gyrus and thalamus. (B) At 12 months of age, no significant differences could be observed in the different brain regions analyzed. Abbreviations: Ctx = cortex, Sub = subiculum, DG = dentate gyrus and Tha = thalamus. Unpaired t-test; *p < 0.05; **p < 0.01; ***p < 0.001. n = 5-6 per group.

### 3.2.2   No neuron loss in the CA1 region of FAD4-42 mice

To assess whether amyloid plaques may elicit an effect on neurotoxic Aβ$_{4-42}$ soluble oligomers, unbiased designed-based stereological studies were conducted. The neurons of the CA1 pyramidal layer were quantified in 3- and 12-month-old WT, 5XFAD, Tg4-42 and FAD4-42 mice.

At three months of age, no differences in the CA1 neuron numbers could be detected between wild-type (mean = 264,386, SEM ± 9,978), 5XFAD (mean = 286,242, SEM ± 9,052), Tg4-42 (mean = 278,630, SEM ± 16,547) and FAD4-42 mice (mean = 262,938, SEM ± 14197) (Fig. 24A). Similarly, no difference in the CA1 volume could be assessed in any of the groups analyzed (Fig. 24B). At twelve months of age, a significant decrease in neuron numbers was observed in Tg4-42 mice (One-way ANOVA, mean = 201,614, SEM ± 10,646, p = 0.0063) compared to age-matched wild type mice (mean = 267,801, SEM ± 17,297) (Fig. 24C). Moreover, no neuron loss was observed in 5XFAD (mean = 235,233, SEM ± 11,548) mice compared to age-matched WT controls, which corroborates previous studies reporting no neuron loss in the CA1 region in 12-month-

old 5XFAD mice (Jawhar *et al.* 2012). Curiously, no reduction in the number of neurons was detected in the CA1 area of FAD4-42 mice (mean = 222,643, SEM ± 9,489) when compared to same-aged WT animals. Furthermore, stereological analysis of the CA1 volume revealed a significant volume reduction in 12-month-old Tg4-42 mice (mean = 2.2 x 10$^8$, SEM ± 1 x 10$^7$) when compared to same-aged WT (mean = 2.8 x 10$^8$, SEM ± 9.2 x 10$^6$, One-way ANOVA, p = 0.003) and FAD4-42 mice (mean = 2.7 x 10$^8$, SEM ± 8.5 x 10$^7$, One-way ANOVA, p = 0.02) (Fig. 24D), whereas no differences in the CA1 volume could be determined in the FAD4-42 and 5XFAD mice when compared to WT controls.
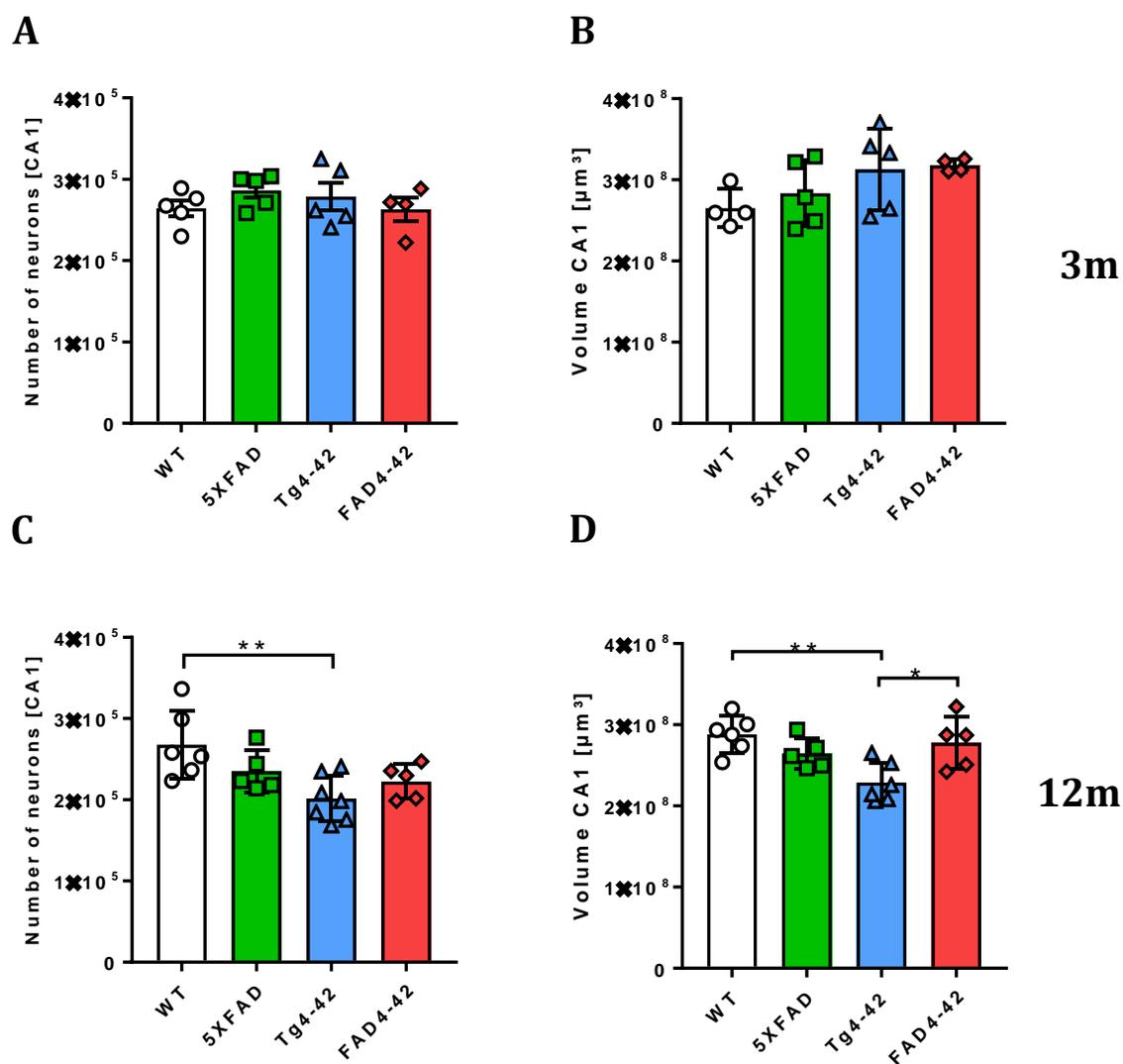
**Fig 24. No neuron loss in the CA1 pyramidal cell layer of the hippocampus in 12-month-old FAD4-42 mice.** (A) Design-based stereological analysis revealed no differences in the CA1 neuron numbers at 3 months of age in any of the groups analyzed. (B) Likewise, no reduction in the CA1 volume could be detected. (C) At 12 months of age, neuron loss was observed only in Tg4-42 mice when compared to age-matched WT controls. (D) A reduction in CA1 volume was detected in Tg4-42 mice compared to WT and FAD4-42 mice. One-way ANOVA followed by Tukey's multiple comparison test. All data were given as means ± SEM *p < 0.05; **p<0.01; m = months; n = 4-7 per group.

# 4 DISCUSSION

## 4.1 PROJECT I: STUDIES OF THE COMBINED EFFECT OF Aβ$_{pE3-42}$ AND Aβ$_{4-42}$ ON ONGOING ALZHEIMER'S DISEASE PATHOLOGY USING THE TBA42/TG4-42 BIGENIC MOUSE MODEL

Several studies have reported that N-truncated Aβ peptides account for the majority of Aβ species in AD brains (Masters *et al.* 1985; Sergeant *et al.* 2003; Portelius *et al.* 2010; Wildburger *et al.* 2017). Additionally, it has been shown that the Aβ$_{4-42}$ and Aβ$_{pE3-42}$ peptides represent the most prominent Aβ variants of these N-terminally ragged peptides(Masters *et al.* 1985; Näslund *et al.* 1994; Saido *et al.* 1995; Portelius *et al.* 2010; Moore *et al.* 2012; Rijal Upadhaya *et al.* 2014). Hence, attempts to unravel the pathogenic properties of these two N-truncated species have been carried out in the last years. *In vitro* studies from our lab and others have demonstrated that Aβ$_{pE3-42}$ and Aβ$_{4-42}$ peptides exhibit a high aggregation propensity, thus, enhancing the formation of soluble oligomers and fibrillar aggregates(Pike *et al.* 1995b; Bouter *et al.* 2013). Additionally, Russo et al. demonstrated that Aβ$_{pE3-40/42}$ species are more cytotoxic than full length Aβ (Russo *et al.* 2002). Likewise, we have corroborated these findings and also showed that Aβ$_{4-42}$ is as toxic as Aβ$_{pE3-42}$ and Aβ$_{1-42}$ *in vitro* (Antonios *et al.* 2013). In order to study the direct *in vivo* toxicity of Aβ$_{pE3-42}$ and Aβ$_{4-42}$, transgenic mouse models expressing uniquely these two N-truncated Aβ peptides have been created. The TBA42 mouse model has been utilized to study the toxic effect of Aβ$_{pE3-42}$ as this mouse line expresses Aβ starting with an N-terminal glutamine residue at position 3, to enhance the spontaneous and enzymatic conversion of Aβ$_{3-42}$ into Aβ$_{pE3-42}$ (Wittnam *et al.* 2012). The TBA42 model develops intraneuronal accumulation of Aβ in the pyramidal neurons of the CA1 region followed by a significant neuron loss as well as alterations in behavioral and motor functions, which increase in an age-dependent manner (Wittnam *et al.* 2012; Meissner *et al.* 2015). On the other hand, the Tg4-42 mouse model, previously created in our lab, exclusively generates Aβ$_{4-42}$ without any

mutations. Phenotypical characterization of this mouse model revealed that Tg4-42 mice exhibit an early accumulation of intraneuronal Aβ in the hippocampus, which coincides with a robust age-dependent pyramidal neuron loss observed in the CA1 region (Bouter *et al.* 2013). Besides, age-related behavioral impairments were detected in these mice. Altogether, it has been proven that Aβ$_{pE3-42}$ and Aβ$_{4-42}$, when individually expressed, can elicit detrimental effects in transgenic mice.

Therefore, based on the evidence that Aβ$_{pE3-42}$ and Aβ$_{4-42}$ are highly present in AD brains and have similar toxic and aggregation properties, the aim of the present study was to elucidate the pathological and behavioral impact of the expression of both Aβ$_{pE3-42}$ and Aβ$_{4-42}$ by crossing TBA42 and Tg4-42 mice to create the TBA42/Tg4-42 mouse model.

### 4.1.1 Prominent intraneuronal Aβ accumulation in the CA1 pyramidal layer of TBA42/Tg4-42 mice

Traditionally, Aβ has been viewed as mainly causing extracellular amyloid pathology in AD brains, however, increasing evidence in the past decades suggests that Aβ can be deposited intracellularly which may have a critical role in AD pathogenesis (LaFerla *et al.* 2007; Bayer & Wirths 2010; Gouras *et al.* 2010). First reports of intraneuronal Aβ come from studies of Grundke-Iqbal and colleagues back in 1989. Using monoclonal anti-Aβ antibodies, they reported on intraneuronal Aβ deposits in neurons from the cerebral and cerebellar cortices as well as in motor neurons of the spinal cord. Strikingly, the authors found strong Aβ immunoreactivity in granular and pyramidal neurons of the hippocampus. Additionally, utilizing anti-tau or anti-PHF antibodies, they showed that tangles were less frequent in those neurons than Aβ (Grundke-Iqbal *et al.* 1989). In the following years, several studies have extended these findings. Gouras and colleagues have shown that in human AD brains, intracellular accumulation of Aβ occurs in areas prone of developing early AD pathology. Such regions include the pyramidal neurons of the hippocampus and the entorhinal cortex. Moreover, intraneuronal Aβ accumulation tended to decrease with increasing cognitive impairment and extracellular Aβ deposition (Gouras *et al.* 2000). Additionally, it has been shown that the accumulation of Aβ within neurons may precede the appearance

of NFTs (Gouras *et al.* 2000; Fernandez-Vizarra *et al.* 2004). Therefore, it has been suggested that intraneuronal Aβ accumulation might be an early event in AD pathogenesis (Wirths *et al.* 2004).

In the present study, using a pan-Aβ antibody, prominent intraneuronal Aβ immunoreactivity was particularly observed in the CA1 pyramidal layer of the hippocampus in the newly created TBA42/Tg4-42 model beginning with 2-3 months of age, followed by a less pronounced staining in the TBA42$^{hom}$ and Tg4-42$^{hom}$ mice, respectively (Lopez-Noguerola *et al.* 2018). To a minor extend, intraneuronal Aβ could also be observed in TBA42$^{hem}$ and Tg4-42$^{hem}$ mice. The region-specific intraneuronal Aβ accumulation in the TBA42, Tg4-42 and TBA42/Tg4-42 models coincides with the transgene expression pattern driven by the murine Thy-1 promoter (Caroni 1997). However, Aβ immunoreactivity in the CA1 region declined with age in all groups analyzed. Furthermore, without regard of genotype and age, no extracellular amyloid plaque formation could be observed (Lopez-Noguerola *et al.* 2018). The progressive decline in Aβ immunoreactivity might be a consequence of the neurotoxic effect caused by the high expression of Aβ$_{pE3-42}$ and Aβ$_{4-42}$ in this brain region due to the Thy-1 promoter. In line with these observations, studies from patients with AD and DS suggest that intraneuronal Aβ is more abundant at early stages of the disease, yet, as the disease progresses, less intraneuronal Aβ and more extracellular Aβ can be observed (Gouras *et al.* 2000; Gyure *et al.* 2001; Mori *et al.* 2002). This inverse correlation might be a consequence of cell lysis which has been proven to occur in Aβ-burned neurons. Once the content is released, it might serve as a relevant source for amyloid plaque formation (D'Andrea *et al.* 2001). However, it cannot be ruled out that besides the intraneuronal production of Aβ, re-uptake from the extracellular space might contribute to intracellular Aβ accumulation. It has been shown that Aβ internalization can occur in a neuron-specific manner, particularly in regions susceptible to AD as reported by Bahr et al. They demonstrated that after Aβ$_{1-42}$ was exogenously applied into rat organotypic hippocampal slice cultures, progressive Aβ$_{1-42}$ accumulation was prominently detected in the CA1 field, while other regions such as the CA3 and the DG remained almost intact (Bahr *et al.* 1998). In addition, this selective internalization led to an enhanced production of amyloidogenic precursor material and a decrease of synaptic markers

(Bahr *et al.* 1998). More recently, studies combining laser capture microdissection and sensitive Aβ ELISA showed elevated levels of Aβ$_{1-42}$ and an increase in the Aβ$_{1-42}$/Aβ$_{1-40}$ ratio in CA1 pyramidal and Purkinje neurons of both sporadic and familial AD patients compared to controls. Yet, the levels of Aβ$_{1-40}$ remain unchanged between AD cases and controls, suggesting that high intraneuronal concentration of Aβ$_{42}$ correlates with increase susceptibility to AD pathology (Aoki *et al.* 2008; Hashimoto *et al.* 2010).

### 4.1.2   **Accelerated neuron loss in the TBA42/Tg4-42 mouse model**

Besides extracellular amyloid plaques and NFTs, neuron loss and brain atrophy are additional neuropathological hallmarks of AD. However, modeling neuronal loss in transgenic AD mouse models has been less successful in comparison with the vast number of transgenic mice producing Aβ deposits and tau pathology (Bayer & Wirths 2010). The first successful attempt showing prominent neurodegeneration in the hippocampus came from the APP23 mouse model, which harbors the APP Swedish mutation. This model develops significant CA1 neuron loss which is inversely correlated with the amount of extracellular Aβ deposits in the CA1 region (Calhoun *et al.* 1998). More recently, neuronal death in the APP/PS1KI mouse model could be detected at the age of 6 months with a 33% reduction of CA1 pyramidal neurons compared to PS1KI littermates (Breyhan *et al.* 2009). Next to the hippocampus, other brain regions with decreased neuronal numbers in the APP/PS1KI model were the frontal cortex (Christensen *et al.* 2008) and various cholinergic brain stem nuclei (Christensen *et al.* 2010). However, it is worth to mention that neuron loss was only detected in brain areas where intraneuronal Aβ accumulation occurred. Similarly, detailed unbiased stereological quantification in the 5XFAD mouse model revealed a reduced number of cortical layer 5 neurons, a region with robust intracellular Aβ accumulation. In contrast, no neuron loss could be detected in the CA1 region, which correlated with the absence of intraneuronal Aβ deposits (Jawhar *et al.* 2012). Moreover, studies from our lab using mass spectrometric analysis have demonstrated that 5XFAD mice show a heterogeneous population of Aβ species. In addition to the full-

length Aβ$_{1-42}$ and Aβ$_{1-40}$ peptides, Aβ$_{4-42}$ and Aβ$_{pE3-42}$ are present in high amounts (Wittnam *et al.* 2012). This data parallels observations made in the APP/PS1KI mouse model, where an age-dependent accumulation of N-truncated Aβ species was found, being Aβ$_{pE3-42}$ one of the most abundant variants (Wirths & Bayer 2010). Hence, the pathological events leading to the observed neuron loss in the APP/PS1KI and the 5XFAD model could be partially triggered by the presence of N-terminally truncated Aβ$_{x-42}$ peptides. In line with these observations, it has been shown that Aβ$_{pE3-42}$ and Aβ$_{4-42}$, respectively, are able to induce strong neurotoxic effects *in vivo*, as reported in mouse models expressing uniquely one of the aforementioned N-truncated peptides(Wirths *et al.* 2009; Alexandru *et al.* 2011; Wittnam *et al.* 2012; Bouter *et al.* 2013; Meissner *et al.* 2015). Therefore, given that Aβ$_{pE3-42}$ and Aβ$_{4-42}$ are major Aβ species in AD brains and their neurotoxic properties *in vivo* have been demonstrated, it seems plausible to study their neurotoxic effect when combined. In the current work, unbiased stereological analyses of the CA1 subfield of the hippocampus suggest that co-expression of Aβ$_{pE3-42}$ and Aβ$_{4-42}$ enhances their neurotoxicity, as seen by the accelerated neuronal death in the TBA42/Tg4-42 mice already at young ages when compared to age-matched WT mice (Lopez-Noguerola *et al.* 2018). A gene-dosage effect could be possible, as seen by the significant reduction in neuron numbers of the TBA42/Tg4-42 mice in comparison with the TBA42$^{hem}$ and Tg4-42$^{hem}$ mice. Therefore, in order to corroborate whether the neurotoxic effect observed was merely due to the higher amount of genes expressing toxic Aβ species or actually due to the combination of the two peptides, the TBA42/Tg4-42 bigenic mice were compared with TBA42$^{hom}$ and Tg4-42$^{hom}$ single transgenic mice. The results revealed a higher neuron loss in the bigenic than in the single transgenic homozygous mice, corroborating the increased neurotoxicity of a combined expression of Aβ$_{pE3-42}$ and Aβ$_{4-42}$. In addition to the neuron loss, a reduction in the CA1 volume was also observed in young TBA42/Tg4-42 mice when compared to age-matched TBA42$^{hom}$ and Tg4-42$^{hom}$ mice (Lopez-Noguerola *et al.* 2018). Neuron loss and hippocampal atrophy continued in the TBA42/Tg4-42 mice as they aged, however, only to a minor extend. Taken together, it can be assumed that Aβ$_{pE3-42}$ and Aβ$_{4-42}$, when expressed together, display enhanced neurotoxic properties.

Nevertheless, the underlying cellular and molecular mechanisms leading to neuronal death remain to be elucidated.

### 4.1.3  Reduced anxiety levels in TBA42/Tg4-42 mice

Besides cognitive symptoms, AD patients can also suffer from behavioral and psychological symptoms like dysphoria, social withdrawal and depression. However, disinhibited behavior has also been reported in AD subjects and is often accompanied by socially unacceptable behaviors and inappropriate euphoria (Frisoni *et al.* 1999; Chung & Cummings 2000; Hart *et al.* 2003). Moreover, it has been reported that anxiety has a high occurrence in patients with dementia (Ferretti *et al.* 2001).

The most common behavioral assay to investigate anxiety levels in rodents is the elevated plus maze (EPM). This task relies on the natural tendency of mice to avoid open spaces; thus, a healthy WT control mouse will tend to spend more time exploring the enclosed arms than the anxiogenic area represented by the open arms (Walf & Frye 2007). Interestingly, as observed in the AD patients, hypo- and hyper-anxious behavior has been reported in several AD mouse models. For instance, reduced anxiety levels have been described in the Tg2576, APP/PS1KI, 5XFAD and TBA42 models, just to cite a few (Lalonde *et al.* 2003; Cotel *et al.* 2012; Jawhar *et al.* 2012; Meissner *et al.* 2015). On the contrary, increased anxiety levels have been reported in the 3xTg (Pietropaolo *et al.* 2008)(Pietropaolo, 2009), APPSwe/PS1A246E (Puolivali *et al.* 2002) and APPSwe models (Savonenko *et al.* 2003).

In the present study, a reduction of anxiety levels in the TBA42/Tg4-42 bigenic mice was demonstrated by a higher time spent in the open arms of the EPM in comparison with their WT and Tg4-42[hem] littermates starting from an early age (three months). Anxiety levels decreased even more in aged TBA42/Tg4-42 compared to the rest of the groups analyzed (Lopez-Noguerola *et al.* 2018). Alterations in the connectivity between the amygdala, septum and hippocampus have been related with changes in the anxiety behavior (Lalonde *et al.* 2012). Evidence suggests that within the hippocampus, the anxiety-related behaviors are more associated with the ventral region (Bannerman *et al.* 2004; McHugh *et al.* 2004). However, several studies also

indicate that the dorsal hippocampus may be able to modulate anxiety levels (Andrews *et al.* 1994; Dos Santos *et al.* 2008; Freeman-Daniels *et al.* 2011). Taking this into account, the hypo-anxious phenotype observed in the TBA42/Tg4-42 mice might be a consequence of the massive pyramidal neuron loss observed in the CA1 region. However, a possible altered function in other circuitries of the limbic system including the septum and amygdala should not be ruled out (Lalonde *et al.* 2012). Hence, future studies comprising these cerebral areas in the TBA42/Tg4-42 mice are recommended.

### 4.1.4 **No working and spatial reference memory deficits in TBA42/Tg4-42 mice**

Besides long-term memory impairment, a wide range of studies have demonstrated that working memory is severely affected in AD. Working memory in rodents can be defined as the short-term memory for a location, stimulus or an object which is used within a test session, but typically not between different sessions (Dudchenko 2004).

The tests commonly used to asses working memory in mice are based on the natural tendency of mice to explore novel environments. Such tasks include the T-maze, Y-maze or cross maze. The spontaneous alternation rate between the different arms in these aforementioned tasks is used to measure short-term memory as well as exploratory behavior and has been shown to be very sensitive to impairments of the hippocampus. However, other brain structures besides the hippocampus might also be involved in these tasks (Lalonde 2002; Deacon & Rawlins 2006).

Age-related reduction in alternation rates has been reported in several transgenic AD animals including the Tg2576, 3xTg, 5XFAD and APP/PS1KI models(Hsiao *et al.* 1996; Holcomb *et al.* 1998; Carroll *et al.* 2007; Wirths *et al.* 2008; Jawhar *et al.* 2012). However, other studies have reported mixed results in some of these transgenic AD mice (King *et al.* 1999; Liu *et al.* 2002b).

Despite the high neuron loss observed in the hippocampus of TBA42/Tg4-42 mice, no significant differences in the spontaneous alternation rates could be detected at any age analyzed. Similarly, other transgenic mouse models including the APP/PS1(Arendash *et al.* 2001), APP23 (Lalonde 2002) and PD-APP (Karl *et al.* 2012)

did not show changes in working memory. Importantly, it has to be noted that discrepancies among the different studies may be partially explained due to differences in the transgene promoter and thus transgene expression patterns and levels in the brain, genetic background, age and sex of the animals used and/or variants in the paradigms used (e.g. number of arms). Moreover, besides the hippocampus, exploratory behavior of novel environmental stimuli also depends on the integrity of other brain areas such as the basal forebrain, thalamus, prefrontal cortex, dorsal striatum as well as the vestibular system and cerebellum (Lalonde 2002).

The Morris water maze (MWM) test (Morris 1984) is one of the most widely used paradigms to study age- and hippocampal-dependent memory deficits in rodents, hence, it represents an adequate task to assess cognitive impairment in AD mouse models (Duyckaerts *et al.* 2008). In this task, spatial learning as well as spatial memory can be examined. To this end, animals must learn to locate and swim towards a hidden platform in a circular water tank by using proximal and/or distal visual cues. Moreover, this task has demonstrated to have a high sensitivity for hippocampal lesions (Moser *et al.* 1995).

In the present study, no impairment in the spatial learning could be detected in the young TBA42/Tg4-42 mice, as they performed similarly to age-matched WT controls and single transgenic mice. Likewise, no spatial reference memory deficits were reported in the young bigenic animals. Unfortunately, due to the severe sensory-motor deficits found in the TBA42/Tg4-42 at 6 months of age, these mice could not be used in the MWM. Some studies have determined the relationship between hippocampal lesion size and acquisition of a spatial memory. Moser et al. reported that even only ~26% of the entire hippocampus can support learning in the MWM (Moser *et al.* 1995). Moreover, Broadbent and colleagues showed that spatial memory started to be impaired after bilateral dorsal hippocampal lesion comprising 30 to 50 % of the total volume (Broadbent *et al.* 2004). This might partially explain why even though the young TBA42/Tg4-42 showed a significant reduction in the CA1 neuron numbers (~36%) and total volume (~30%), they were still able to perform normally in the MWM. Furthermore, it has been shown that other brain areas such as the cerebral

cortex, striatum, basal forebrain and even the cerebellum might be involved in MWM performance (D'Hooge & De Deyn 2001).

### 4.1.5 Age-dependent motor deficits accompanied by aggravated amyloid pathology in the spinal cord of TBA42/Tg4-42 mice

Besides the typical neurobehavioral and neuropsychiatric symptoms observed in AD patients (Chung & Cummings 2000), motor impairments including rigidity and disturbances in gait or posture have also been repeatedly reported (O'Keeffe *et al.* 1996; Kluger *et al.* 1997; Scarmeas *et al.* 2004; Pettersson *et al.* 2005). Likewise, longitudinal studies have shown that motor slowing and gait disturbances are commonly present in patients with MCI and it has been suggested that the severity of motor impairment may help to distinguish those with a high risk to develop AD later on (Aggarwal *et al.* 2006; Schmidt *et al.* 2010).This suggests that motor impairment is an important aspect of cognitive decline in AD.

The string suspension, the balance beam and the inverted grid tasks, revealed age-dependent sensory-motor deficits in the TBA42/Tg4-42 model at the age of 5-6 months, compared to same-aged TBA42[hem], Tg4-42[hem] and Tg4-42[hom] mice. These results suggest that the observed motor deficits in the TBA42/Tg4-42 mice are more aggravated due the presence of both $A\beta_{pE3-42}$ and $A\beta_{4-42}$ peptides. However, motor deficits were also observed in aged TBA42[hem] mice, suggesting that the presence of $A\beta_{pE3-42}$ seems to be relevant for the observed phenotype. No motor deficits were detected in the hemi- and homozygous Tg4-42 mice regardless of age (Lopez-Noguerola *et al.* 2018). These observations are in line with other studies also showing motor dysfunction in AD mouse models only expressing $A\beta_{pE3-42}$ such as the TBA42, TBA2 and TBA2.1hom mice (Wirths *et al.* 2009; Alexandru *et al.* 2011; Wittnam *et al.* 2012; Meissner *et al.* 2015). Motor disturbances have also been reported in AD mouse models carrying APP and/or PS1 mutations like the Tg2576, 5XFAD, APP/PS1KI and APP23 mice (Lalonde *et al.* 2003; Wirths & Bayer 2008; Seo *et al.* 2010; Jawhar *et al.* 2012) among others. Moreover, the sensory-motor deficits seen in the TBA42/Tg4-42

bigenic mice nicely correlate with the significant extra- and intraneuronal Aβ deposition observed in the spinal cord of these animals. Yet, significant amyloid pathology was also found in young TBA42[hom] mice, suggesting that $Aβ_{pE3–42}$ might co-aggregate with $Aβ_{4–42}$. Interestingly, high extra- and intracellular accumulation was more pronounced in the aged bigenic mice compared to rest of the aged single transgenic mice, as reflected by the higher amount of motor neurons with high levels of intracellular Aβ (Lopez-Noguerola *et al.* 2018). This suggests that higher Aβ amounts in the spinal cord correlate better with the severity of the motor phenotype. Indeed, it has been shown that the occurrence of amyloid pathology in the spinal cord coincides with the motor deficits in the 5XFAD (Jawhar *et al.* 2012) and APP/PS1KI mice (Wirths *et al.* 2007; Wirths & Bayer 2008). Additionally, it has been also suggested that alterations in the axonal transport might be the cause of the motor impairments in the aforementioned mice, as shown by axonopathy which includes spheroids and swollen axons in the spinal cord (Wirths *et al.* 2007, 2008; Jawhar *et al.* 2012). Furthermore, Seo and colleagues reported that the motor function deficits found in the Tg2576 model might be the consequence of motor neuron loss, since histological analyses showed a severe reduction in the spinal motor neuron numbers (Seo *et al.* 2010). In contrast, very recent observations from Yuan and coworkers using TgCRND8 mice revealed that the motor deficits found in these mice are independent of axonopathy and motor neuron loss (Yuan *et al.* 2017).

Taking all together, the severe motor deficits detected in the TBA42/Tg4-42 model might be attributed to the high accumulation of Aβ in the motor neurons derived from the presence of both $Aβ_{pE3-42}$ and $Aβ_{4-42}$ in the spinal cord. However, given that motor function involves the coordination of other brains regions such as the motor cortex, basal ganglia and cerebellum (Lalonde & Strazielle 2007), additional studies involving these brain structures are advisable.

### 4.1.6   The combination of $Aβ_{pE3-42}$ and $Aβ_{4-42}$ affects their aggregation kinetics

Previous *in vitro* studies from our lab have demonstrated that $Aβ_{pE3-42}$ and $Aβ_{4-42}$ peptides are rapidly converted into soluble toxic oligomers and ThT-reactive fibrillar

aggregates (Bouter *et al.* 2013). Moreover, it was shown that this proclivity to develop aggregates is more prominent than in N-terminally intact Aβ$_{1-42}$ peptides (Bouter *et al.* 2013). Hence, to test whether the combination of Aβ$_{pE3-42}$ and Aβ$_{4-42}$ has an effect on their biochemical properties, the aggregation kinetics of both peptides were analyzed by a ThT-binding assay. The results revealed that the combination of Aβ$_{pE3-42}$ and Aβ$_{4-42}$ seems to enhance their aggregation propensity, as observed by the accelerated aggregate formation. Interestingly, the mixture of both peptides displayed a faster initial aggregation compared to the peptides alone. The lack of an initial lag phase under the applied conditions suggests the formation of seeding material, which is known to enhance fibril elongation. In good agreement with these findings, Nussbaum et al. reported that small amounts of Aβ$_{pE3-42}$ co-oligomerized with excess of full-length Aβ$_{1-42}$ *in vitro*, thus potentiating the toxicity of Aβ$_{1-42}$ by inducing the formation of toxic mixed oligomers (Nussbaum *et al.* 2012). Additionally, they showed that Aβ$_{pE3-42}$ induced tau-dependent neuronal death and template-induced misfolding of Aβ$_{1-42}$ into structurally distinct low-molecular weight oligomers that propagated by a prion-like mechanism (Nussbaum *et al.* 2012). More recently, Dammers and coworkers elucidated the co-aggregation mechanism of Aβ$_{pE3-42}$ with Aβ$_{1-42}$. They found that Aβ$_{pE3-42}$ monomers increased the primary nucleation of Aβ$_{1-42}$ and that Aβ$_{pE3-42}$ fibrils are efficient templates for Aβ$_{1-42}$ elongation. Interestingly, fibrils of Aβ$_{1-42}$ prevented Aβ$_{pE3-42}$ aggregation (Dammers *et al.* 2017). Thus, it is tempting to speculate that a similar mechanism of co-aggregation between Aβ$_{pE3-42}$ and Aβ$_{4-42}$ may partially explain the observed phenotype in TBA42/Tg4-42 mice co-expressing the two N-truncated peptides. Additional studies involving the interaction of Aβ$_{4-42}$ with other Aβ isoforms would allow us to better understand the impact of this peptide in AD.

### 4.1.7 Conclusions of Project I

Based on the results of the present study:

- Co-expression of $A\beta_{pE3-42}$ and $A\beta_{4-42}$ induces prominent intraneuronal $A\beta$ accumulation in the CA1 pyramidal region of the hippocampus in young TBA42/Tg4-42 mice compared to age-matched TBA42$^{hom}$ and Tg4-42$^{hom}$ mice.

- $A\beta_{pE3-42}$ and $A\beta_{4-42}$ have a synergistic effect on neurodegeneration as observed by the accelerated neuron loss in the CA1 pyramidal layer of young TBA42/Tg4-42 in comparison to single transgenic mice producing either $A\beta_{pE3-42}$ or $A\beta_{4-42}$.

- Under physiological conditions, when $A\beta_{pE3-42}$ and $A\beta_{4-42}$ are combined, their aggregation propensity seems to be enhanced.

- No working memory deficits could be detected in young nor aged TBA42/Tg4-42 mice.

- No spatial reference memory impairment was observed in young TBA42/Tg4-42 mice.

- Loss of anxiety is increased in an age-dependent manner in TBA42/Tg4-42 mice.

- Sensory-motor deficits in the TBA42/Tg4-42 mice strongly correlate with the strong spinal cord pathology, as demonstrated by abundant intracellular $A\beta$ accumulation within motor neurons and extracellular $A\beta$ deposition.

## 4.2 PROJECT II: EXPLORING THE *IN VIVO* ASSOCIATION BETWEEN Aβ PLAQUES AND SOLUBLE Aβ AGGREGATES USING THE FAD4-42 MOUSE MODEL

One of the pathological hallmarks of AD is the cerebral aggregation and deposition of Aβ in the form of amyloid plaques. However, the presence of Aβ plaques has also been found in cognitively normal elderly subjects (Katzman *et al.* 1988; Hulette *et al.* 1998; Price & Morris 1999; Aizenstein *et al.* 2008). This observation has raised the question of whether fibrillar Aβ plaques really play a pivotal role in the pathogenesis of AD. Moreover, several studies have demonstrated the presence of soluble Aβ oligomeric forms in post mortem tissue from AD patients (Kuo *et al.* 1996; Roher *et al.* 1996; Shankar *et al.* 2008; Tomic *et al.* 2009). Additionally, accumulated evidence from AD brains suggests that the levels of soluble Aβ oligomers correlate better with the risk and severity of the disease than insoluble amyloid plaques (McLean *et al.* 1999; Wang *et al.* 1999; Mc Donald *et al.* 2010; Esparza *et al.* 2013). Therefore, it has been proposed that rather than insoluble fibrillar Aβ, soluble Aβ oligomers may be the crucial players in AD etiology.

The association of soluble Aβ oligomers and fibrillar plaques have been studied in detail by several groups. For instance, in two independent experiments, Shankar and colleagues extracted soluble Aβ oligomers and insoluble amyloid cores from the temporal and frontal cortices of AD brains (Shankar *et al.* 2008). In the first experiment, the extracted Aβ oligomers inhibited long-term potentiation (LTP), enhanced long-term depression (LTD), reduced spine density and impaired the memory learning behavior in normal rats. Interestingly, in the second experiment, the insoluble amyloid plaques isolated from the same AD brain cortices did not impair LTP, however, once they were solubilized, the amyloid plaques released Aβ dimers that did so (Shankar *et al.* 2008). In line with this, using array tomography, Koffie et al. examined synaptic loss as a function of distance from amyloid plaques in APP transgenic mice and human AD brains. They found that synaptic density progressively decreased near plaques but raised towards normal at distances further than 50 μm (Koffie *et al.* 2009, 2012). Taken together, these and other studies suggest that the insoluble and relatively inactive amyloid plaques might serve as a reservoir of the soluble 'toxic Aβ oligomers', but once

the reservoir is saturated, the excess oligomers can diffuse and bind other targets, resulting in local neurotoxicity, which might trigger inflammatory responses and ultimately result in neuronal death (Haass & Selkoe 2007; Benilova *et al.* 2012; Selkoe & Hardy 2016; Brody *et al.* 2017).

The current study aimed to explore the *in vivo* association of soluble Aβ oligomers and insoluble amyloid plaques. For this purpose, we crossed the two well-characterized AD models 5XFAD and Tg4-42 in order to create the novel FAD4-42 line. The 5XFAD model develops extracellular amyloid deposition beginning at 2 months of age which increases in an age-dependent fashion and spreads to different brain areas (Oakley *et al.* 2006). Tg4-42 mice produce and liberate soluble toxic Aβ$_{4\text{-}42}$ oligomers that induce neuronal death in the CA1 pyramidal layer of the hippocampus in an age-dependent manner. Moreover, these mice do not develop extracellular amyloid plaques (Bouter *et al.* 2013). Hence, the effects on amyloid plaque deposition and neuron loss were examined in the FAD4-42 transgenic animals, which are characterized by both amyloid plaque deposition and Aβ oligomer generation, at young (3 months) and old (12 months) ages.

### 4.2.1  Amyloid-beta deposition in young and old FAD4-42 mice

In order to assess whether additional soluble Aβ$_{4\text{-}42}$ production may influence the Aβ deposition profile in 3- and 12-month-old FAD4-42 mice, quantification of extracellular Aβ plaque load was performed using the 24311 and NT4X-167antibodies against total Aβ and Aβ$_{pE3/4\text{-}x}$, respectively. At 3 months of age, total Aβ plaque load levels in the cortex, subiculum and thalamus were significantly increased in FAD4-42 compared to 5XFAD mice. The total Aβ plaque load in the dentate gyrus of FAD4-42 mice showed a trend towards higher plaque burden, however, it did not reach statistical significance. Furthermore, Aβ$_{pE\text{-}3/4\text{-}x}$ plaque load was significantly higher in the FAD4-42 mice in all regions analyzed. On the other hand, analysis of the total Aβ and Aβ$_{pE/4\text{-}x}$ plaque burden in 12-month-old 5XFAD and FAD4-42 mice did not show significant differences in any of the brain regions studied. Taking these results together, the high elevation of total

Aβ and Aβ$_{p3/4-x}$ positive plaques observed at 3 months of age in FAD4-42 mice coincides with the strong intraneuronal Aβ$_{4-42}$ immunoreactivity observed in the Tg4-42 model beginning at 2 months of age(Bouter *et al.* 2013). Therefore, it can be hypothesized that the Aβ$_{4-42}$ produced by the expression of the Tg4-42 transgene might diffuse and bind to newly formed amyloid plaques and probably even accelerates their formation at young ages. However, at 12 months of age, this effect is not seen anymore, probably due to a plaque saturation effect. In fact, it has been previously reported that amyloid plaque deposition in the 5XFAD mice starts ~2 months of age and increases rapidly, reaching plateau levels around 10-14 months of age, depending on the sex of the mice (Oakley *et al.* 2006; Bhattacharya *et al.* 2014; Richard *et al.* 2015). This phenomenon has also been reported for other AD double transgenic animals carrying both APP and PS1 mutations(Holcomb *et al.* 1998; Gordon *et al.* 2002).

### 4.2.2 Potential protective effect of amyloid plaques against neurotoxic N-truncated Aβ$_{4-42}$ oligomers

The aim of this part of the project was to test whether the amyloid plaques may have an effect on the toxicity of soluble Aβ$_{4-42}$ oligomers. To this end, we took advantage of the Tg4-42 mouse model, which develops age- and dose-dependent neuron loss in the CA1 region of the hippocampus (Bouter *et al.* 2013; Antonios *et al.* 2015). Moreover, this model does not express human APP and does not develop extracellular amyloid plaques; hence, the loss of neurons reported in the CA1 can be attributed to the expression and intraneuronal accumulation of Aβ$_{4-42}$ in this brain region. In the 5XFAD mouse model, neuron death has been reported in the fifth cortical layer at 9 and 12 months of age (Jawhar *et al.* 2012; Eimer & Vassar 2013), while no neuron loss has been detected in the CA1 region at any age studied (Shao *et al.* 2011; Jawhar *et al.* 2012). Interestingly, the loss of neurons in the cortical layer 5 strongly correlates with intraneuronal Aβ$_{x-42}$ accumulation (Jawhar *et al.* 2012; Eimer & Vassar 2013).

Unbiased stereological analyses of the hippocampal CA1 region revealed no differences in the pyramidal neuron numbers between 3-month-old WT, 5XFAD, Tg4-42 and FAD4-42 mice. Likewise, no changes in the CA1 volume could be observed. This

means that the elevated plaque burden observed at 3 months of age in the FAD4-42 mice had no neurotoxic effect on the CA1 region of the hippocampus. At 12 months of age, Tg4-42 mice exhibited profound neuron loss compared to wild type controls, which was expected since neuron death in these animals can be detected already at 8 months of age (Bouter *et al.* 2013). However, surprisingly, 12-month-old FAD4-42 mice displayed no difference in the number of neurons when compared to same-aged WT, 5XFAD and Tg4-42 mice, respectively. In addition, old FAD4-42 mice showed a higher CA1 volume loss than Tg4-42 mice.

Altogether, it can be assumed that the elevated amyloid deposition observed in FAD4-42 mice might be the result of the binding of soluble $A\beta_{4-42}$ oligomers to the newly formed amyloid plaques. Furthermore, it is tempting to speculate that as the mice aged, more $A\beta_{4-42}$ bound to the amyloid plaques, thus preventing their toxicity. This is partially supported by the fact that no differences in CA1 neuron numbers were observed between old FAD4-42 and WT controls and supports the hypothesis that $A\beta$ plaques can function as buffers for soluble toxic $A\beta$ oligomers. However, no difference in the CA1 neuron numbers between old Tg4-42 and old FAD4-42 could be detected. This raised the question whether amyloid plaques might have a limited buffering capacity. In fact, it has been proposed that initially amyloid plaques may serve as "reservoirs" for the soluble toxic $A\beta$ oligomers, but once they have reached their capacity, they might release the soluble toxic $A\beta$ oligomers which are able to freely diffuse and exert their toxicity (Hong *et al.* 2014; Brody *et al.* 2017). So, it might be possible that the buffering capacity of the amyloid plaques was reached before 12 months. If this is the case, this might partially explain why no differences in neuron loss could be detected between FAD4-42 and Tg4-42 at 12 months of age. Therefore, further studies are required to determine the relationship between insoluble amyloid plaques and soluble $A\beta$ oligomeric forms.

### 4.2.3 Conclusions of project II

Based on the results of the present study:

- Additional $A\beta_{4\text{-}42}$ production in FAD4-42 mice via the Tg4-42 transgene increased the amyloid plaque load in all brain regions studied at 3 months of age, compared to age-matched 5XFAD mice.

- At 12 months of age, no differences in amyloid deposition could be detected between FAD4-42 and 5XFAD mice, suggesting a saturation effect.

- The absence of neuron loss in the FAD4-42 mice at 12 months of age suggests a potential protective effect of amyloid plaques against soluble toxic $A\beta$ oligomers, which might be limited once the plaques are saturated.

# 5 SUMMARY AND CONCLUSIONS

The brain of Alzheimer's disease (AD) patients contains a heterogeneous mixture of amyloid beta (Aβ) isoforms. Besides Aβ peptide isoforms possessing different C-termini, several N-terminally truncated Aβ species have been identified. From these, the $Aβ_{pE3-42}$ and $Aβ_{4-42}$ peptides are known to be the most prominent Aβ variants. Hence, transgenic mouse models have been created to study their direct effect *in vivo*, showing that when individually expressed, $Aβ_{pE3-42}$ and $Aβ_{4-42}$ can exert pathological and behavioral alterations.

The aim of the first part of the present thesis was to investigate the *in vivo* effect of $Aβ_{pE3-42}$ and $Aβ_{4-42}$ when concurrently expressed. Therefore, the TBA42 and the Tg4-42 mouse models expressing $Aβ_{pE3-42}$ and $Aβ_{4-42}$, respectively, were crossed. The resulting TBA42/Tg4-42 bigenic line showed prominent intracellular Aβ accumulation in the CA1 pyramidal neurons of the hippocampus at a young age, which was reduced in older animals. The decline of intraneuronal Aβ accumulation can be attributed to the early robust neuron loss detected in this area in the young TBA42/Tg4-42 mice compared to age-matched TBA42$^{hom}$ and Tg4-42$^{hom}$ mice, respectively. This suggests that $Aβ_{pE3-42}$ and $Aβ_{4-42}$ might have a synergistic effect on neurodegeneration. Additionally, aggregation kinetics analysis indicates that under physiological conditions, when $Aβ_{pE3-42}$ and $Aβ_{4-42}$ peptides are combined, their aggregation propensity is enhanced, as observed by the faster initial aggregation compared to the individual peptides alone.

Behavioral analysis of TBA42/Tg4-42 mice revealed reduced anxiety levels at an early age when compared to WT controls, which was not the case for TBA42 and Tg4-42 mice. Furthermore, TBA42/Tg4-42 anxiety levels decreased further in an age-dependent manner. Interestingly, no working and spatial reference memory deficits were detected in TBA42/Tg4-42 mice at any age studied. Additionally, the TBA42/Tg4-42 model displayed sever sensory-motor deficits when compared to WT and single transgenic mice, which strongly correlated with significant extra- and intraneuronal Aβ deposition in the spinal cord of these mice. However, significant amyloid pathology was

also found in young TBA42$^{hom}$ mice, suggesting that Aβ$_{pE3-42}$ might co-aggregate with Aβ$_{4-42}$.

In sum, the effect on neuron loss, neuropathological alteration and neurological deficits was enhanced when Aβ$_{pE3-42}$ and Aβ$_{4-42}$ were simultaneously expressed. This suggest a possible *in vivo* interaction between these two N-truncated Aβ peptides, which seems plausible, as both peptides are two of the most abundant Aβ isoforms in AD brains. Therefore, their potential role in AD pathogenesis should be further studied in order to generate better therapeutic strategies to fight AD.

The second part of the current work aimed to explore the *in vivo* association between soluble Aβ oligomers and insoluble fibrillar plaques. To this end, the 5XFAD and Tg4-42 mouse models were crossed to produce the FAD4-42 model. The well-studied 5XFAD mouse model rapidly develops extracellular Aβ deposition which increases in an age-dependent manner spreading to different brain areas. On the other hand, the Tg4-42 mouse model does not generate extracellular Aβ deposits, however, the expression of Aβ$_{4-42}$ induces progressive neuron loss in the pyramidal neurons of the CA1 region. FAD4-42 mice showed increased amyloid plaque burden in all regions studied at 3 months of age, compared to same-aged 5XFAD mice, indicating that Aβ$_{4-42}$ might bind to the amyloid plaques. However, at 12 months of age, no differences in amyloid plaque deposition between the FAD4-42 and 5XFAD model could be detected anymore. This might be caused by a saturation effect, meaning that no more Aβ$_{4-42}$ can bind to the amyloid plaques if the plaques are already saturated. Next, in order to test whether amyloid plaques have an effect on the toxicity of soluble Aβ$_{4-42}$ aggregates, neuron counting was performed in the CA1 region of FAD4-42 mice. Interestingly, no neuron loss could be detected in FAD4-42 mice compared to WT controls at any age analyzed. Likewise, no differences between FAD4-42 and Tg4-42 could be seen. However, at 12 months of age, Tg4-42 mice showed a significant loss of neurons in comparison with age-mated WT mice. The absence of neuron loss in the FAD4-42 model suggests that the binding of Aβ$_{4-42}$ to amyloid plaques reduced its toxicity, however, this potential protective effect might be decreased when more Aβ$_{4-42}$ binds during aging. It can be speculated that once the plaques reach their binding capacity, free Aβ$_{4-42}$ is free to diffuse onto the surrounding exerting its toxicity.

Based on the results from the second project, it can be concluded that binding of soluble Aβ$_{4-42}$ to amyloid plaques seems to result in a reduction of Aβ$_{4-42}$ toxicity, suggesting a potential protective effect of amyloid plaques against soluble toxic Aβ oligomers. However, further work is necessary to clarify the relationship between plaques and soluble Aβ aggregates.

# 6 REFERENCES

Aggarwal, N.T., Wilson, R.S., Beck, T.L., Bienias, J.L. & Bennett, D.A. (2006) Motor Dysfunction in Mild Cognitive Impairment and the Risk of Incident Alzheimer Disease. *Arch Neurol* **63**, 1763.

Aizenstein, H.J., Nebes, R.D., Saxton, J.A., Price, J.C., Mathis, C.A., Tsopelas, N.D., Ziolko, S.K., James, J.A., Snitz, B.E., Houck, P.R., Bi, W., Cohen, A.D., Lopresti, B.J., DeKosky, S.T., Halligan, E.M. & Klunk, W.E. (2008) Frequent amyloid deposition without significant cognitive impairment among the elderly. *Arch Neurol* **65**, 1509–1517.

Alexandru, A., Jagla, W., Graubner, S., Becker, A., Bauscher, C., Kohlmann, S., Sedlmeier, R., Raber, K., Cynis, H., Ronicke, R., Reymann, K., Petrasch-Parwez, E., Hartlage-Rubsamen, M., Waniek, A., Rossner, S., Schilling, S., Osmand, A., Demuth, H. & von Horsten, S. (2011) Selective hippocampal neurodegeneration in transgenic mice expressing small amounts of truncated Abeta is induced by pyroglutamate-Abeta formation. *J Neurosci* **31**, 12790–12801.

Allinson, T.M.J., Parkin, E.T., Turner, A.J. & Hooper, N.M. (2003) ADAMs family members as amyloid precursor protein alpha-secretases. *J Neurosci Res* **74**, 342–352.

Almeida, C.G., Takahashi, R.H. & Gouras, G.K. (2006) Beta-amyloid accumulation impairs multivesicular body sorting by inhibiting the ubiquitin-proteasome system. *J Neurosci* **26**, 4277–4288.

Alzheimer's Association. (2015). Alzheimers disease facts and figures 2015. *Alzheimers Dement* **11**, 104–105.

Alzheimer, A. (1907) "Über eine eigenartige Erkankung der Himrinde." *Allg Z Psychiatr* **64**, 146–148.

Andrews, N., Hogg, S., Gonzalez, L.E. & File, S.E. (1994) 5-HT1A receptors in the median raphe nucleus and dorsal hippocampus may mediate anxiolytic and anxiogenic behaviours respectively. *Eur J Pharmacol* **264**, 259–264.

Anstey, K.J., Cherbuin, N., Budge, M. & Young, J. (2011) Body mass index in midlife and late-life as a risk factor for dementia: A meta-analysis of prospective studies. *Obes Rev* **12**, 426–437.

Antonios, G., Borgers, H., Richard, B.C., Brauß, A., Meißner, J., Weggen, S., Pena, V., Pillot, T., Davies, S.L., Bakrania, P., Matthews, D., Brownlees, J., Bouter, Y. & Bayer, T.A. (2015) Alzheimer therapy with an antibody against N-terminal Abeta 4-X and pyroglutamate Abeta 3-X. *Sci Rep* **5**, 17338.

Antonios, G., Saiepour, N., Bouter, Y., Richard, B.C., Paetau, A., Verkkoniemi-Ahola, A., Lannfelt, L., Ingelsson, M., Kovacs, G.G., Pillot, T., Wirths, O. & Bayer, T.A. (2013) N-truncated Abeta starting with position four: early intraneuronal accumulation and rescue of toxicity using NT4X-167, a novel monoclonal antibody. *Acta Neuropathol Commun* **1**, 56.

Aoki, M., Volkmann, I., Tjernberg, L.O., Winblad, B. & Bogdanovic, N. (2008) Amyloid beta-peptide levels in laser capture microdissected cornu ammonis 1 pyramidal neurons of Alzheimer's brain. *Neuroreport* **19**, 1085–1089.

Arai, T., Akiyama, H., Ikeda, K., Kondo, H. & Mori, H. (1999) Immunohistochemical localization of amyloid beta-protein with amino-terminal aspartate in the cerebral cortex of patients

with Alzheimer's disease. *Brain Res* **823**, 202–206.

Arendash, G.W., King, D.L., Gordon, M.N., Morgan, D., Hatcher, J.M., Hope, C.E. & Diamond, D.M. (2001) Progressive, age-related behavioral impairments in transgenic mice carrying both mutant amyloid precursor protein and presenilin-1 transgenes. *Brain Res* **891**, 42–53.

Arnold, S.E., Hyman, B.T., Flory, J., Damasio, A.R. & Van Hoesen, G.W. (1991) The topographical and neuroanatomical distribution of neurofibrillary tangles and neuritic plaques in the cerebral cortex of patients with Alzheimer's disease. *Cereb Cortex* **1**, 103–116.

Arriagada, P. V, Growdon, J.H., Hedley-Whyte, E.T. & Hyman, B.T. (1992) Neurofibrillary tangles but not senile plaques parallel duration and severity of Alzheimer's disease. *Neurology* **42**, 631–639.

Augustinack, J.C., Schneider, A., Mandelkow, E.-M. & Hyman, B.T. (2002) Specific tau phosphorylation sites correlate with severity of neuronal cytopathology in Alzheimer's disease. *Acta Neuropathol* **103**, 26–35.

Bahr, B.A., Hoffman, K.B., Yang, A.J., Hess, U.S., Glabe, C.G. & Lynch, G. (1998) Amyloid beta protein is internalized selectively by hippocampal field CA1 and causes neurons to accumulate amyloidogenic carboxyterminal fragments of the amyloid precursor protein. *J Comp Neurol* **397**, 139–147.

Bannerman, D.M., Rawlins, J.N.P., McHugh, S.B., Deacon, R.M.J., Yee, B.K., Bast, T., Zhang, W.-N., Pothuizen, H.H.J. & Feldon, J. (2004) Regional dissociations within the hippocampus--memory and anxiety. *Neurosci Biobehav Rev* **28**, 273–283.

Barnes, D.E., Yaffe, K., Byers, A.L., McCormick, M., Schaefer, C. & Whitmer, R.A. (2012) Mid-life versus late-life depressive symptoms and risk of dementia: Differential effects for Alzheimer's disease and vascular dementia. *Arch Gen Psychiatry* **69**, 493–498.

Bayer, T.A., Cappai, R., Masters, C.L., Beyreuther, K. & Multhaup, G. (1999) It all sticks together--the APP-related family of proteins and Alzheimer's disease. *Mol Psychiatry* **4**, 524–528.

Bayer, T.A. & Wirths, O. (2010) Intracellular Accumulation of Amyloid-Beta – A Predictor for Synaptic Dysfunction and Neuron Loss in Alzheimer's Disease. *Front Aging Neurosci* **2**, 1-10.

Bayer, T.A. & Wirths, O. (2011) Intraneuronal Aβ as a trigger for neuron loss: can this be translated into human pathology? *Biochem Soc Trans* **39**, 857–61.

Bayer, T.A. & Wirths, O. (2014) Focusing the amyloid cascade hypothesis on N-truncated Abeta peptides as drug targets against Alzheimer's disease. *Acta Neuropathol* **127**, 787–801.

Benilova, I., Karran, E. & De Strooper, B. (2012) The toxic Abeta oligomer and Alzheimer's disease: an emperor in need of clothes. *Nat Neurosci* **15**, 349–357.

Bertram, L., Lange, C., Mullin, K., Parkinson, M., Hsiao, M., Hogan, M.F., Schjeide, B.M.M., Hooli, B., Divito, J., Ionita, I., Jiang, H., Laird, N., Moscarillo, T., Ohlsen, K.L., Elliott, K., Wang, X., Hu-Lince, D., Ryder, M., Murphy, A., Wagner, S.L., Blacker, D., Becker, K.D. & Tanzi, R.E. (2008) Genome-wide association analysis reveals putative Alzheimer's disease susceptibility loci in addition to APOE. *Am J Hum Genet* **83**, 623–632.

Bertram, L., Lill, C.M. & Tanzi, R.E. (2010) The genetics of Alzheimer disease: back to the future. *Neuron* **68**, 270–81.

Beyreuther, K. & Masters, C.L. (1991) Amyloid precursor protein (APP) and beta A4 amyloid in the etiology of Alzheimer's disease: precursor-product relationships in the derangement

of neuronal function. *Brain Pathol* **1**, 241–251.

Bhattacharya, R., Barren, C. & Kovacs, D.M. (2013) Palmitoylation of Amyloid Precursor Protein Regulates Amyloidogenic Processing in Lipid Rafts. *J Neurosci* **33** 11169-11183.

Bhattacharya, S., Haertel, C., Maelicke, A. & Montag, D. (2014) Galantamine slows down plaque formation and behavioral decline in the 5XFAD mouse model of Alzheimer's disease. *PLoS One* **9**, e89454.

Bi, X., Gall, C.M., Zhou, J. & Lynch, G. (2002) Uptake and pathogenic effects of amyloid beta peptide 1-42 are enhanced by integrin antagonists and blocked by NMDA receptor antagonists. *Neuroscience* **112**, 827–840.

Bien, J., Jefferson, T., Causevic, M., Jumpertz, T., Munter, L., Multhaup, G., Weggen, S., Becker-Pauly, C. & Pietrzik, C.U. (2012) The metalloprotease meprin beta generates amino terminal-truncated amyloid beta peptide species. *J Biol Chem* **287**, 33304–33313.

Blennow, K., de Leon, M.J. & Zetterberg, H. (2006) Alzheimer's disease. *Lancet* **368**, 387–403.

Borchelt, D.R., Thinakaran, G., Eckman, C.B., Lee, M.K., Davenport, F., Ratovitsky, T., Prada, C.M., Kim, G., Seekins, S., Yager, D., Slunt, H.H., Wang, R., Seeger, M., Levey, A.I., Gandy, S.E., Copeland, N.G., Jenkins, N.A., Price, D.L., Younkin, S.G. & Sisodia, S.S. (1996) Familial Alzheimer's disease-linked presenilin 1 variants elevate Abeta1-42/1-40 ratio in vitro and in vivo. *Neuron* **17**, 1005–1013.

Bouter, Y., Dietrich, K., Wittnam, J.L., Rezaei-Ghaleh, N., Pillot, T., Papot-Couturier, S., Lefebvre, T., Sprenger, F., Wirths, O., Zweckstetter, M. & Bayer, T.A. (2013) N-truncated amyloid beta (Abeta) 4-42 forms stable aggregates and induces acute and long-lasting behavioral deficits. *Acta Neuropathol* **126**, 189–205.

Bouter, Y., Kacprowski, T., Weissmann, R., Dietrich, K., Borgers, H., Brauß, A., Sperling, C., Wirths, O., Albrecht, M., Jensen, L.R., Kuss, A.W. & Bayer, T.A. (2014) Deciphering the molecular profile of plaques, memory decline and neuron loss in two mouse models for Alzheimer's disease by deep sequencing. *Front Aging Neurosci* **6**, 1–28.

Braak, E., Braak, H. & Mandelkow, E.M. (1994) A sequence of cytoskeleton changes related to the formation of neurofibrillary tangles and neuropil threads. *Acta Neuropathol* **87**, 554–567.

Braak, H., Alafuzoff, I., Arzberger, T., Kretzschmar, H. & Del Tredici, K. (2006) Staging of Alzheimer disease-associated neurofibrillary pathology using paraffin sections and immunocytochemistry. *Acta Neuropathol* **112** 389-404.

Braak, H. & Braak, E. (1991) Neuropathological stageing of Alzheimer-related changes. *Acta Neuropathol* **82**, 239–259.

Brenowitz, W.D., Nelson, P.T., Besser, L.M., Heller, K.B. & Kukull, W.A. (2015) Cerebral amyloid angiopathy and its co-occurrence with Alzheimer's disease and other cerebrovascular neuropathologic changes. *Neurobiol Aging* **36** 2702-2708.

Breyhan, H., Wirths, O., Duan, K., Marcello, A., Rettig, J. & Bayer, T.A. (2009) APP/PS1KI bigenic mice develop early synaptic deficits and hippocampus atrophy. *Acta Neuropathol* **117**, 677–685.

Broadbent, N.J., Squire, L.R. & Clark, R.E. (2004) Spatial memory, recognition memory, and the hippocampus. *Proc Natl Acad Sci U S A* **101**, 14515–14520.

Brody, D.L., Jiang, H., Wildburger, N. & Esparza, T.J. (2017) Non-canonical soluble amyloid-beta

aggregates and plaque buffering: controversies and future directions for target discovery in Alzheimer's disease. *Alzheimers Res Ther* **9** 62.

Van Broeck, B., Vanhoutte, G., Pirici, D., Van Dam, D., Wils, H., Cuijt, I., Vennekens, K., Zabielski, M., Michalik, A., Theuns, J., De Deyn, P.P., Van der Linden, A., Van Broeckhoven, C. & Kumar-Singh, S. (2008) Intraneuronal amyloid beta and reduced brain volume in a novel APP T714I mouse model for Alzheimer's disease. *Neurobiol Aging* **29**, 241–252.

Bu, G., Cam, J. & Zerbinatti, C. (2006) LRP in amyloid-beta production and metabolism. *Ann N Y Acad Sci* **1086**, 35–53.

Calhoun, M.E., Wiederhold, K.H., Abramowski, D., Phinney, A.L., Probst, A., Sturchler-Pierrat, C., Staufenbiel, M., Sommer, B. & Jucker, M. (1998) Neuron loss in APP transgenic mice. *Nature* **395** 755-756.

Campos, A.C., Fogaca, M. V, Aguiar, D.C. & Guimaraes, F.S. (2013) Animal models of anxiety disorders and stress. *Rev Bras Psiquiatr* **35 Suppl 2**, S101-11.

Cao, X. & Sudhof, T.C. (2001) A transcriptionally [correction of transcriptively] active complex of APP with Fe65 and histone acetyltransferase Tip60. *Science* **293**, 115–120.

Caroni, P. (1997) Overexpression of growth-associated proteins in the neurons of adult transgenic mice. *J Neurosci Methods* **71**, 3–9.

Carroll, J.C., Rosario, E.R., Chang, L., Stanczyk, F.Z., Oddo, S., LaFerla, F.M. & Pike, C.J. (2007) Progesterone and estrogen regulate Alzheimer-like neuropathology in female 3xTg-AD mice. *J Neurosci* **27**, 13357–13365.

Casas, C., Sergeant, N., Itier, J.-M., Blanchard, V., Wirths, O., van der Kolk, N., Vingtdeux, V., van de Steeg, E., Ret, G., Canton, T., Drobecq, H., Clark, A., Bonici, B., Delacourte, A., Benavides, J., Schmitz, C., Tremp, G., Bayer, T.A., Benoit, P. & Pradier, L. (2004) Massive CA1/2 neuronal loss with intraneuronal and N-terminal truncated Abeta42 accumulation in a novel Alzheimer transgenic model. *Am J Pathol* **165**, 1289–1300.

Castellano, J.M., Kim, J., Stewart, F.R., Jiang, H., DeMattos, R.B., Patterson, B.W., Fagan, A.M., Morris, J.C., Mawuenyega, K.G., Cruchaga, C., Goate, A.M., Bales, K.R., Paul, S.M., Bateman, R.J. & Holtzman, D.M. (2011) Human apoE isoforms differentially regulate brain amyloid-beta peptide clearance. *Sci Transl Med* **3**, 89ra57.

Cataldo, A.M., Petanceska, S., Terio, N.B., Peterhoff, C.M., Durham, R., Mercken, M., Mehta, P.D., Buxbaum, J., Haroutunian, V. & Nixon, R.A. (2004) Abeta localization in abnormal endosomes: association with earliest Abeta elevations in AD and Down syndrome. *Neurobiol Aging* **25**, 1263–1272.

Christensen, D.Z., Bayer, T.A. & Wirths, O. (2010) Intracellular Aβ triggers neuron loss in the cholinergic system of the APP/PS1KI mouse model of Alzheimer's disease. *Neurobiol Aging* **31**, 1153–1163.

Christensen, D.Z., Kraus, S.L., Flohr, A., Cotel, M.-C., Wirths, O. & Bayer, T.A. (2008) Transient intraneuronal A beta rather than extracellular plaque pathology correlates with neuron loss in the frontal cortex of APP/PS1KI mice. *Acta Neuropathol* **116**, 647–655.

Chung, J.A. & Cummings, J.L. (2000) Neurobehavioral and neuropsychiatric symptoms in Alzheimer's disease: Characteristics and treatment. *Neurol Clin* **18** 829-846.

Cleary, J.P., Walsh, D.M., Hofmeister, J.J., Shankar, G.M., Kuskowski, M.A., Selkoe, D.J. & Ashe, K.H. (2005) Natural oligomers of the amyloid-beta protein specifically disrupt cognitive

function. *Nat Neurosci* **8**, 79–84.

Corder, E.H., Saunders, A.M., Risch, N.J., Strittmatter, W.J., Schmechel, D.E., Gaskell, P.C.J., Rimmler, J.B., Locke, P.A., Conneally, P.M. & Schmader, K.E. (1994) Protective effect of apolipoprotein E type 2 allele for late onset Alzheimer disease. *Nat Genet* **7**, 180–184.

Corder, E.H., Saunders, A.M., Strittmatter, W.J., Schmechel, D.E., Gaskell, P.C., Small, G.W., Roses, A.D., Haines, J.L. & Pericak-Vance, M.A. (1993) Gene dose of apolipoprotein E type 4 allele and the risk of Alzheimer's disease in late onset families. *Science* **261**, 921–923.

Cotel, M.-C., Jawhar, S., Christensen, D.Z., Bayer, T.A. & Wirths, O. (2012) Environmental enrichment fails to rescue working memory deficits, neuron loss, and neurogenesis in APP/PS1KI mice. *Neurobiol Aging* **33**, 96–107.

Cras, P., Smith, M.A., Richey, P.L., Siedlak, S.L., Mulvihill, P. & Perry, G. (1995) Extracellular neurofibrillary tangles reflect neuronal loss and provide further evidence of extensive protein cross-linking in Alzheimer disease. *Acta Neuropathol* **89**, 291–295.

Cruchaga, C., Karch, C.M., Jin, S.C., Benitez, B.A., Cai, Y., Guerreiro, R., Harari, O., Norton, J., Budde, J., Bertelsen, S., Jeng, A.T., Cooper, B., Skorupa, T., Carrell, D., Levitch, D., Hsu, S., Choi, J., Ryten, M., Sassi, C., Bras, J., Gibbs, R.J., Hernandez, D.G., Lupton, M.K., Powell, J., Forabosco, P., Ridge, P.G., Corcoran, C.D., Tschanz, J.T., Norton, M.C., Munger, R.G., Schmutz, C., Leary, M., Demirci, F.Y., Bamne, M.N., Wang, X., Lopez, O.L., Ganguli, M., Medway, C., Turton, J., Lord, J., Braae, A., Barber, I., Brown, K., Pastor, P., Lorenzo-Betancor, O., Brkanac, Z., Scott, E., Topol, E., Morgan, K., Rogaeva, E., Singleton, A., Hardy, J., Kamboh, M.I., George-Hyslop, P.S., Cairns, N., Morris, J.C., Kauwe, J.S.K. & Goate, A.M. (2014) Rare coding variants in the phospholipase D3 gene confer risk for Alzheimer's disease. *Nature* **505**, 550–554.

Cruts, M., Theuns, J. & Van Broeckhoven, C. (2012) Locus-specific mutation databases for neurodegenerative brain diseases. *Hum Mutat* **33**, 1340–1344.

Cynis, H., Schilling, S., Bodnár, M., Hoffmann, T., Heiser, U., Saido, T.C. & Demuth, H.-U. (2006) Inhibition of glutaminyl cyclase alters pyroglutamate formation in mammalian cells. *Biochim Biophys Acta - Proteins Proteomics* **1764**, 1618–1625.

D'Andrea, M.R., Nagele, R.G., Wang, H.Y., Peterson, P.A. & Lee, D.H. (2001) Evidence that neurones accumulating amyloid can undergo lysis to form amyloid plaques in Alzheimer's disease. *Histopathology* **38**, 120–134.

D'Hooge, R. & De Deyn, P.P. (2001) Applications of the Morris water maze in the study of learning and memory. *Brain Res Brain Res Rev* **36**, 60–90.

Dahlgren, K.N., Manelli, A.M., Stine, W.B.J., Baker, L.K., Krafft, G.A. & LaDu, M.J. (2002) Oligomeric and fibrillar species of amyloid-beta peptides differentially affect neuronal viability. *J Biol Chem* **277**, 32046–32053.

Dammers, C., Schwarten, M., Buell, A.K. & Willbold, D. (2017) Pyroglutamate-modified Aβ(3-42) affects aggregation kinetics of Aβ(1-42) by accelerating primary and secondary pathways. *Chem Sci* **8**, 4996–5004.

Dawkins, E. & Small, D.H. (2014) Insights into the physiological function of the β-amyloid precursor protein: beyond Alzheimer's disease. *J Neurochem* **129** 756-769.

Deacon, R.M.J. & Rawlins, J.N.P. (2006) T-maze alternation in the rodent. *Nat Protoc* **1**, 7–12.

Delaère, P., Duyckaerts, C., Masters, C., Beyreuther, K., Piette, F. & Hauw, J.-J. (1990) Large amounts of neocortical βA4 deposits without neuritic plaques nor tangles in a

psychometrically assessed, non-demented person. *Neurosci Lett* **116**, 87–93.

Devi, L. & Ohno, M. (2010) Genetic reductions of beta-site amyloid precursor protein-cleaving enzyme 1 and amyloid-beta ameliorate impairment of conditioned taste aversion memory in 5XFAD Alzheimer's disease model mice. *Eur J Neurosci* **31**, 110–118.

Dickerson, B.C., Stoub, T.R., Shah, R.C., Sperling, R.A., Killiany, R.J., Albert, M.S., Hyman, B.T., Blacker, D. & Detoledo-Morrell, L. (2011) Alzheimer-signature MRI biomarker predicts AD dementia in cognitively normal adults. *Neurology* **76**, 1395–1402.

Dickson, D.W., Crystal, H.A., Mattiace, L.A., Masur, D.M., Blau, A.D., Davies, P., Yen, S.H. & Aronson, M.K. (1992) Identification of normal and pathological aging in prospectively studied nondemented elderly humans. *Neurobiol Aging* **13**, 179–189.

Dominguez, D., Tournoy, J., Hartmann, D., Huth, T., Cryns, K., Deforce, S., Serneels, L., Camacho, I.E., Marjaux, E., Craessaerts, K., Roebroek, A.J.M., Schwake, M., D'Hooge, R., Bach, P., Kalinke, U., Moechars, D., Alzheimer, C., Reiss, K., Saftig, P. & De Strooper, B. (2005) Phenotypic and biochemical analyses of BACE1- and BACE2-deficient mice. *J Biol Chem* **280**, 30797–30806.

Drew, S.C., Masters, C.L. & Barnham, K.J. (2009) Alanine-2 carbonyl is an oxygen ligand in Cu2+ coordination of Alzheimer's disease amyloid-beta peptide--relevance to N-terminally truncated forms. *J Am Chem Soc* **131**, 8760–8761.

Dudchenko, P.A. (2004) An overview of the tasks used to test working memory in rodents. *Neurosci Biobehav Rev* **28**, 699–709.

Duyckaerts, C., Delatour, B. & Potier, M.C. (2009) Classification and basic pathology of Alzheimer disease. *Acta Neuropathol* **118**, 5–36.

Duyckaerts, C., Potier, M.-C. & Delatour, B. (2008) Alzheimer disease models and human neuropathology: similarities and differences. *Acta Neuropathol* **115** 5-38.

Eimer, W.A. & Vassar, R. (2013) Neuron loss in the 5XFAD mouse model of Alzheimer's disease correlates with intraneuronal Abeta42 accumulation and Caspase-3 activation. *Mol Neurodegener* **8**, 2.

Erbel-Sieler, C., Dudley, C., Zhou, Y., Wu, X., Estill, S.J., Han, T., Diaz-Arrastia, R., Brunskill, E.W., Potter, S.S. & McKnight, S.L. (2004) Behavioral and regulatory abnormalities in mice deficient in the NPAS1 and NPAS3 transcription factors. *Proc Natl Acad Sci U S A* **101**, 13648 LP-13653.

Esch, F.S., Keim, P.S., Beattie, E.C., Blacher, R.W., Culwell, A.R., Oltersdorf, T., McClure, D. & Ward, P.J. (1990) Cleavage of amyloid beta peptide during constitutive processing of its precursor. *Science* **248**, 1122–1124.

Esh, C., Patton, L., Kalback, W., Kokjohn, T.A., Lopez, J., Brune, D., Newell, A.J., Beach, T., Schenk, D., Games, D., Paul, S., Bales, K., Ghetti, B., Castaño, E.M. & Roher, A.E. (2005) Altered APP Processing in PDAPP (Val717 → Phe) Transgenic Mice Yields Extended-Length Aβ Peptides. *Biochemistry* **44**, 13807–13819.

Esparza, T.J., Zhao, H., Cirrito, J.R., Cairns, N.J., Bateman, R.J., Holtzman, D.M. & Brody, D.L. (2013) Amyloid-beta oligomerization in Alzheimer dementia versus high-pathology controls. *Ann Neurol* **73**, 104–119.

Fagan, A.M., Watson, M., Parsadanian, M., Bales, K.R., Paul, S.M. & Holtzman, D.M. (2002) Human and murine ApoE markedly alters A beta metabolism before and after plaque formation in

a mouse model of Alzheimer's disease. *Neurobiol Dis* **9**, 305–318.

Fernandez-Vizarra, P., Fernandez, A.P., Castro-Blanco, S., Serrano, J., Bentura, M.L., Martinez-Murillo, R., Martinez, A. & Rodrigo, J. (2004) Intra- and extracellular Abeta and PHF in clinically evaluated cases of Alzheimer's disease. *Histol Histopathol* **19**, 823–844.

Ferretti, L., McCurry, S.M., Logsdon, R., Gibbons, L. & Teri, L. (2001) Anxiety and Alzheimer's disease. *J Geriatr Psychiatry Neurol* **14**, 52–58.

Francis, R., McGrath, G., Zhang, J., Ruddy, D.A., Sym, M., Apfeld, J., Nicoll, M., Maxwell, M., Hai, B., Ellis, M.C., Parks, A.L., Xu, W., Li, J., Gurney, M., Myers, R.L., Himes, C.S., Hiebsch, R., Ruble, C., Nye, J.S. & Curtis, D. (2002) aph-1 and pen-2 are required for Notch pathway signaling, gamma-secretase cleavage of betaAPP, and presenilin protein accumulation. *Dev Cell* **3**, 85–97.

Franklin, K. & G., P. (2012) The mouse brain in stereotaxic coordinates. 4th edn. *Academic Press*.

Fratiglioni, L., Paillard-Borg, S. & Winblad, B. (2004) An active and socially integrated lifestyle in late life might protect against dementia. *Lancet Neurol* **3**, 343–53.

Fratiglioni, L. & Wang, H.-X. (2007) Brain reserve hypothesis in dementia. *J Alzheimers Dis* **12**, 11–22.

Freeman-Daniels, E., Beck, S.G. & Kirby, L.G. (2011) Cellular correlates of anxiety in CA1 hippocampal pyramidal cells of 5-HT(1A) receptor knockout mice. *Psychopharmacology (Berl)* **213** 453-463.

Frisoni, G.B., Rozzini, L., Gozzetti, A., Binetti, G., Zanetti, O., Bianchetti, A., Trabucchi, M. & Cummings, J.L. (1999) Behavioral syndromes in Alzheimer's disease: description and correlates. *Dement Geriatr Cogn Disord* **10**, 130–138.

Genin, E., Hannequin, D., Wallon, D., Sleegers, K., Hiltunen, M., Combarros, O., Bullido, M.J., Engelborghs, S., De Deyn, P., Berr, C., Pasquier, F., Dubois, B., Tognoni, G., Fievet, N., Brouwers, N., Bettens, K., Arosio, B., Coto, E., Del Zompo, M., Mateo, I., Epelbaum, J., Frank-Garcia, A., Helisalmi, S., Porcellini, E., Pilotto, A., Forti, P., Ferri, R., Scarpini, E., Siciliano, G., Solfrizzi, V., Sorbi, S., Spalletta, G., Valdivieso, F., Vepsalainen, S., Alvarez, V., Bosco, P., Mancuso, M., Panza, F., Nacmias, B., Bossu, P., Hanon, O., Piccardi, P., Annoni, G., Seripa, D., Galimberti, D., Licastro, F., Soininen, H., Dartigues, J.-F., Kamboh, M.I., Van Broeckhoven, C., Lambert, J.C., Amouyel, P. & Campion, D. (2011) APOE and Alzheimer disease: a major gene with semi-dominant inheritance. *Mol Psychiatry* **16**, 903–907.

Giannakopoulos, P., Herrmann, F.R., Bussière, T., Bouras, C., Kövari, E., Perl, D.P., Morrison, J.H., Gold, G. & Hof, P.R. (2003) Tangle and neuron numbers, but not amyloid load, predict cognitive status in Alzheimer's disease. *Neurology* **60**, 1495 LP-1500.

Giunta, B., Deng, J., Jin, J. & Sadic, E. (2012) Evaluation of How Cigarette Smoke Is a Direct Risk Factor for Alzheimer'S Disease. *Technol Innov* **14**, 39–48.

Glenner, G.G. & Wong, C.W. (1984a) Alzheimer's disease: initial report of the purification and characterization of a novel cerebrovascular amyloid protein. *Biochem Biophys Res Commun* **120**, 885–890.

Glenner, G.G. & Wong, C.W. (1984b) Alzheimer's disease and Down's syndrome: sharing of a unique cerebrovascular amyloid fibril protein. *Biochem Biophys Res Commun* **122**, 1131–1135.

Goate, A., Chartier-Harlin, M.C., Mullan, M., Brown, J., Crawford, F., Fidani, L., Giuffra, L., Haynes,

A., Irving, N. & James, L. (1991) Segregation of a missense mutation in the amyloid precursor protein gene with familial Alzheimer's disease. *Nature* **349**, 704–706.

Goedert, M. & Spillantini, M.G. (2000) Tau mutations in frontotemporal dementia FTDP-17 and their relevance for Alzheimer's disease. *Biochim Biophys Acta - Mol Basis Dis* **1502**, 110–121.

Goedert, M., Spillantini, M.G., Jakes, R., Rutherford, D. & Crowther, R.A. (1989) Multiple isoforms of human microtubule-associated protein tau: sequences and localization in neurofibrillary tangles of Alzheimer's disease. *Neuron* **3**, 519–526.

Goldgaber, D., Lerman, M.I., McBride, O.W., Saffiotti, U. & Gajdusek, D.C. (1987) Characterization and chromosomal localization of a cDNA encoding brain amyloid of Alzheimer's disease. *Science* **235**, 877–880.

Gomez-Isla, T., Hollister, R., West, H., Mui, S., Growdon, J.H., Petersen, R.C., Parisi, J.E. & Hyman, B.T. (1997) Neuronal loss correlates with but exceeds neurofibrillary tangles in Alzheimer's disease. *Ann Neurol* **41**, 17–24.

Gomez-Isla, T., Price, J.L., McKeel, D.W.J., Morris, J.C., Growdon, J.H. & Hyman, B.T. (1996) Profound loss of layer II entorhinal cortex neurons occurs in very mild Alzheimer's disease. *J Neurosci* **16**, 4491–4500.

Gordon, M.N., Holcomb, L.A., Jantzen, P.T., DiCarlo, G., Wilcock, D., Boyett, K.W., Connor, K., Melachrino, J., O'Callaghan, J.P. & Morgan, D. (2002) Time course of the development of Alzheimer-like pathology in the doubly transgenic PS1+APP mouse. *Exp Neurol* **173**, 183–195.

Gouras, G.K., Tampellini, D., Takahashi, R.H. & Capetillo-Zarate, E. (2010) Intraneuronal β-amyloid accumulation and synapse pathology in Alzheimer's disease. *Acta Neuropathol* **119** 523-541.

Gouras, G.K., Tsai, J., Naslund, J., Vincent, B., Edgar, M., Checler, F., Greenfield, J.P., Haroutunian, V., Buxbaum, J.D., Xu, H., Greengard, P. & Relkin, N.R. (2000) Intraneuronal Abeta42 accumulation in human brain. *Am J Pathol* **156**, 15–20.

Grignon, Y., Duyckaerts, C., Bennecib, M. & Hauw, J.J. (1998) Cytoarchitectonic alterations in the supramarginal gyrus of late onset Alzheimer's disease. *Acta Neuropathol* **95**, 395–406.

Grundke-Iqbal, I., Iqbal, K., George, L., Tung, Y.C., Kim, K.S. & Wisniewski, H.M. (1989) Amyloid protein and neurofibrillary tangles coexist in the same neuron in Alzheimer disease. *Proc Natl Acad Sci U S A* **86**, 2853–2857.

Grundke-Iqbal, I., Iqbal, K., Tung, Y.C., Quinlan, M., Wisniewski, H.M. & Binder, L.I. (1986) Abnormal phosphorylation of the microtubule-associated protein tau (tau) in Alzheimer cytoskeletal pathology. *Proc Natl Acad Sci U S A* **83**, 4913–4917.

Gu, Y., Misonou, H., Sato, T., Dohmae, N., Takio, K. & Ihara, Y. (2001) Distinct intramembrane cleavage of the beta-amyloid precursor protein family resembling gamma-secretase-like cleavage of Notch. *J Biol Chem* **276**, 35235–8.

Gu, Y., Nieves, J.W., Stern, Y., Luchsinger, J.A. & Scarmeas, N. (2010) Food combination and Alzheimer disease risk: a protective diet. *Arch Neurol* **67**, 699–706.

Guerreiro, R., Wojtas, A., Bras, J., Carrasquillo, M., Rogaeva, E., Majounie, E., Cruchaga, C., Sassi, C., Kauwe, J.S.K., Younkin, S., Hazrati, L., Collinge, J., Pocock, J., Lashley, T., Williams, J., Lambert, J.-C., Amouyel, P., Goate, A., Rademakers, R., Morgan, K., Powell, J., St George-

Hyslop, P., Singleton, A. & Hardy, J. (2013) TREM2 variants in Alzheimer's disease. *N Engl J Med* **368**, 117–127.

Guntert, A., Dobeli, H. & Bohrmann, B. (2006) High sensitivity analysis of amyloid-beta peptide composition in amyloid deposits from human and PS2APP mouse brain. *Neuroscience* **143**, 461–475.

Gyure, K.A., Durham, R., Stewart, W.F., Smialek, J.E. & Troncoso, J.C. (2001) Intraneuronal abeta-amyloid precedes development of amyloid plaques in Down syndrome. *Arch Pathol Lab Med* **125**, 489–492.

Haass, C. (2004) Take five—BACE and the γ-secretase quartet conduct Alzheimer's amyloid β-peptide generation. *EMBO J* **23** 483-488.

Haass, C., Hung, A.Y., Schlossmacher, M.G., Teplow, D.B. & Selkoe, D.J. (1993) beta-Amyloid peptide and a 3-kDa fragment are derived by distinct cellular mechanisms. *J Biol Chem* **268**, 3021–3024.

Haass, C., Kaether, C., Thinakaran, G. & Sisodia, S. (2012) Trafficking and Proteolytic Processing of APP. *Cold Spring Harb Perspect Med* **2** a006270.

Haass, C., Koo, E.H., Mellon, A., Hung, A.Y. & Selkoe, D.J. (1992) Targeting of cell-surface beta-amyloid precursor protein to lysosomes: alternative processing into amyloid-bearing fragments. *Nature* **357**, 500–503.

Haass, C. & Selkoe, D.J. (2007) Soluble protein oligomers in neurodegeneration: Lessons from the Alzheimer's amyloid β-peptide. *Nat Rev Mol Cell Biol* **8**, 101–112.

Halliday, G.M., Double, K.L., Macdonald, V. & Kril, J.J. (2003) Identifying severely atrophic cortical subregions in Alzheimer's disease. *Neurobiol Aging* **24**, 797–806.

Hardy, J.A. & Higgins, G.A. (1992) Alzheimer's disease: the amyloid cascade hypothesis. *Science* **256**, 184–185.

Hardy, J. & Allsop, D. (1991) Amyloid deposition as the central event in the aetiology of Alzheimer's disease. *Trends Pharmacol Sci* **12** 383-388.

Harigaya, Y., Saido, T.C., Eckman, C.B., Prada, C.M., Shoji, M. & Younkin, S.G. (2000) Amyloid beta protein starting pyroglutamate at position 3 is a major component of the amyloid deposits in the Alzheimer's disease brain. *Biochem Biophys Res Commun* **276** 422-427.

Harold, D., Abraham, R., Hollingworth, P., Sims, R., Gerrish, A., Hamshere, M.L., Pahwa, J.S., Moskvina, V., Dowzell, K., Williams, A., Jones, N., Thomas, C., Stretton, A., Morgan, A.R., Lovestone, S., Powell, J., Proitsi, P., Lupton, M.K., Brayne, C., Rubinsztein, D.C., Gill, M., Lawlor, B., Lynch, A., Morgan, K., Brown, K.S., Passmore, P.A., Craig, D., McGuinness, B., Todd, S., Holmes, C., Mann, D., Smith, A.D., Love, S., Kehoe, P.G., Hardy, J., Mead, S., Fox, N., Rossor, M., Collinge, J., Maier, W., Jessen, F., Schurmann, B., Heun, R., van den Bussche, H., Heuser, I., Kornhuber, J., Wiltfang, J., Dichgans, M., Frolich, L., Hampel, H., Hull, M., Rujescu, D., Goate, A.M., Kauwe, J.S.K., Cruchaga, C., Nowotny, P., Morris, J.C., Mayo, K., Sleegers, K., Bettens, K., Engelborghs, S., De Deyn, P.P., Van Broeckhoven, C., Livingston, G., Bass, N.J., Gurling, H., McQuillin, A., Gwilliam, R., Deloukas, P., Al-Chalabi, A., Shaw, C.E., Tsolaki, M., Singleton, A.B., Guerreiro, R., Muhleisen, T.W., Nothen, M.M., Moebus, S., Jockel, K.-H., Klopp, N., Wichmann, H.-E., Carrasquillo, M.M., Pankratz, V.S., Younkin, S.G., Holmans, P.A., O'Donovan, M., Owen, M.J. & Williams, J. (2009) Genome-wide association study identifies variants at CLU and PICALM associated with Alzheimer's disease. *Nat Genet* **41**, 1088–1093.

Harrison, S.M., Harper, A.J., Hawkins, J., Duddy, G., Grau, E., Pugh, P.L., Winter, P.H., Shilliam, C.S., Hughes, Z.A., Dawson, L.A., Gonzalez, M.I., Upton, N., Pangalos, M.N. & Dingwall, C. (2003) BACE1 (beta-secretase) transgenic and knockout mice: identification of neurochemical deficits and behavioral changes. *Mol Cell Neurosci* **24**, 646–655.

Hart, D.J., Craig, D., Compton, S.A., Critchlow, S., Kerrigan, B.M., McIlroy, S.P. & Passmore, A.P. (2003) A retrospective study of the behavioural and psychological symptoms of mid and late phase Alzheimer's disease. *Int J Geriatr Psychiatry* **18**, 1037–1042.

Hashimoto, M., Bogdanovic, N., Volkmann, I., Aoki, M., Winblad, B. & Tjernberg, L.O. (2010) Analysis of microdissected human neurons by a sensitive ELISA reveals a correlation between elevated intracellular concentrations of Abeta42 and Alzheimer's disease neuropathology. *Acta Neuropathol* **119**, 543–554.

He, W. & Barrow, C.J. (1999) The A beta 3-pyroglutamyl and 11-pyroglutamyl peptides found in senile plaque have greater beta-sheet forming and aggregation propensities in vitro than full-length A beta. *Biochemistry* **38**, 10871–10877.

Himmler, A., Drechsel, D., Kirschner, M.W. & Martin, D.W.J. (1989) Tau consists of a set of proteins with repeated C-terminal microtubule-binding domains and variable N-terminal domains. *Mol Cell Biol* **9**, 1381–1388.

Holcomb, L., Gordon, M.N., McGowan, E., Yu, X., Benkovic, S., Jantzen, P., Wright, K., Saad, I., Mueller, R., Morgan, D., Sanders, S., Zehr, C., O'Campo, K., Hardy, J., Prada, C.M., Eckman, C., Younkin, S., Hsiao, K. & Duff, K. (1998) Accelerated Alzheimer-type phenotype in transgenic mice carrying both mutant amyloid precursor protein and presenilin 1 transgenes. *Nat Med* **4**, 97–100.

Hollingworth, P., Harold, D., Sims, R., Gerrish, A., Lambert, J.-C., Carrasquillo, M.M., Abraham, R., Hamshere, M.L., Pahwa, J.S., Moskvina, V., Dowzell, K., Jones, N., Stretton, A., Thomas, C., Richards, A., Ivanov, D., Widdowson, C., Chapman, J., Lovestone, S., Powell, J., Proitsi, P., Lupton, M.K., Brayne, C., Rubinsztein, D.C., Gill, M., Lawlor, B., Lynch, A., Brown, K.S., Passmore, P.A., Craig, D., McGuinness, B., Todd, S., Holmes, C., Mann, D., Smith, A.D., Beaumont, H., Warden, D., Wilcock, G., Love, S., Kehoe, P.G., Hooper, N.M., Vardy, E.R.L.C., Hardy, J., Mead, S., Fox, N.C., Rossor, M., Collinge, J., Maier, W., Jessen, F., Ruther, E., Schurmann, B., Heun, R., Kolsch, H., van den Bussche, H., Heuser, I., Kornhuber, J., Wiltfang, J., Dichgans, M., Frolich, L., Hampel, H., Gallacher, J., Hull, M., Rujescu, D., Giegling, I., Goate, A.M., Kauwe, J.S.K., Cruchaga, C., Nowotny, P., Morris, J.C., Mayo, K., Sleegers, K., Bettens, K., Engelborghs, S., De Deyn, P.P., Van Broeckhoven, C., Livingston, G., Bass, N.J., Gurling, H., McQuillin, A., Gwilliam, R., Deloukas, P., Al-Chalabi, A., Shaw, C.E., Tsolaki, M., Singleton, A.B., Guerreiro, R., Muhleisen, T.W., Nothen, M.M., Moebus, S., Jockel, K.-H., Klopp, N., Wichmann, H.-E., Pankratz, V.S., Sando, S.B., Aasly, J.O., Barcikowska, M., Wszolek, Z.K., Dickson, D.W., Graff-Radford, N.R., Petersen, R.C., van Duijn, C.M., Breteler, M.M.B., Ikram, M.A., DeStefano, A.L., Fitzpatrick, A.L., Lopez, O., Launer, L.J., Seshadri, S., Berr, C., Campion, D., Epelbaum, J., Dartigues, J.-F., Tzourio, C., Alperovitch, A., Lathrop, M., Feulner, T.M., Friedrich, P., Riehle, C., Krawczak, M., Schreiber, S., Mayhaus, M., Nicolhaus, S., Wagenpfeil, S., Steinberg, S., Stefansson, H., Stefansson, K., Snaedal, J., Bjornsson, S., Jonsson, P. V, Chouraki, V., Genier-Boley, B., Hiltunen, M., Soininen, H., Combarros, O., Zelenika, D., Delepine, M., Bullido, M.J., Pasquier, F., Mateo, I., Frank-Garcia, A., Porcellini, E., Hanon, O., Coto, E., Alvarez, V., Bosco, P., Siciliano, G., Mancuso, M., Panza, F., Solfrizzi, V., Nacmias, B., Sorbi, S., Bossu, P., Piccardi, P., Arosio, B., Annoni, G., Seripa, D., Pilotto, A., Scarpini, E., Galimberti, D., Brice, A., Hannequin, D., Licastro, F., Jones, L., Holmans, P.A., Jonsson, T., Riemenschneider, M., Morgan, K., Younkin, S.G., Owen, M.J., O'Donovan, M., Amouyel, P. &

Williams, J. (2011) Common variants at ABCA7, MS4A6A/MS4A4E, EPHA1, CD33 and CD2AP are associated with Alzheimer's disease. *Nat Genet* **43**, 429–435.

Holtzman, D.M., Bales, K.R., Tenkova, T., Fagan, A.M., Parsadanian, M., Sartorius, L.J., Mackey, B., Olney, J., McKeel, D., Wozniak, D. & Paul, S.M. (2000) Apolipoprotein E isoform-dependent amyloid deposition and neuritic degeneration in a mouse model of Alzheimer's disease. *Proc Natl Acad Sci U S A* **97**, 2892–2897.

Holtzman, D.M., Morris, J.C. & Goate, A.M. (2011) Alzheimer's disease: the challenge of the second century. *Sci Transl Med* **3**, 77sr1.

Hong, L., Koelsch, G., Lin, X., Wu, S., Terzyan, S., Ghosh, A.K., Zhang, X.C. & Tang, J. (2000) Structure of the protease domain of memapsin 2 (beta-secretase) complexed with inhibitor. *Science* **290**, 150–153.

Hong, S., Ostaszewski, B.L., Yang, T., O'Malley, T.T., Jin, M., Yanagisawa, K., Li, S., Bartels, T. & Selkoe, D.J. (2014) Soluble Aβ Oligomers Are Rapidly Sequestered from Brain ISF In Vivo and Bind GM1 Ganglioside on Cellular Membranes. *Neuron* **82**, 308–319.

Howell, S., Nalbantoglu, J. & Crine, P. (1995) Neutral endopeptidase can hydrolyze beta-amyloid(1-40) but shows no effect on beta-amyloid precursor protein metabolism. *Peptides* **16**, 647–652.

Hsia, A.Y., Masliah, E., McConlogue, L., Yu, G.Q., Tatsuno, G., Hu, K., Kholodenko, D., Malenka, R.C., Nicoll, R.A. & Mucke, L. (1999) Plaque-independent disruption of neural circuits in Alzheimer's disease mouse models. *Proc Natl Acad Sci U S A* **96**, 3228–3233.

Hsiao, K., Chapman, P., Nilsen, S., Eckman, C., Harigaya, Y., Younkin, S., Yang, F. & Cole, G. (1996) Correlative memory deficits, Abeta elevation, and amyloid plaques in transgenic mice. *Science* **274**, 99–102.

Hu, J., Igarashi, A., Kamata, M. & Nakagawa, H. (2001) Angiotensin-converting enzyme degrades Alzheimer amyloid beta-peptide (A beta ); retards A beta aggregation, deposition, fibril formation; and inhibits cytotoxicity. *J Biol Chem* **276**, 47863–47868.

Hu, X., Hicks, C.W., He, W., Wong, P., Macklin, W.B., Trapp, B.D. & Yan, R. (2006) Bace1 modulates myelination in the central and peripheral nervous system. *Nat Neurosci* **9**, 1520–1525.

Hulette, C.M., Welsh-Bohmer, K.A., Murray, M.G., Saunders, A.M., Mash, D.C. & McIntyre, L.M. (1998) Neuropathological and neuropsychological changes in "normal" aging: evidence for preclinical Alzheimer disease in cognitively normal individuals. *J Neuropathol Exp Neurol* **57**, 1168–1174.

Hüttenrauch, M., Brauß, A., Kurdakova, A., Borgers, H., Klinker, F., Liebetanz, D., Salinas-Riester, G., Wiltfang, J., Klafki, H.W. & Wirths, O. (2016) Physical activity delays hippocampal neurodegeneration and rescues memory deficits in an Alzheimer disease mouse model. *Transl Psychiatry* **6** e800.

Hutton, M., Lendon, C.L., Rizzu, P., Baker, M., Froelich, S., Houlden, H., Pickering-Brown, S., Chakraverty, S., Isaacs, A., Grover, A., Hackett, J., Adamson, J., Lincoln, S., Dickson, D., Davies, P., Petersen, R.C., Stevens, M., de Graaff, E., Wauters, E., van Baren, J., Hillebrand, M., Joosse, M., Kwon, J.M., Nowotny, P., Che, L.K., Norton, J., Morris, J.C., Reed, L.A., Trojanowski, J., Basun, H., Lannfelt, L., Neystat, M., Fahn, S., Dark, F., Tannenberg, T., Dodd, P.R., Hayward, N., Kwok, J.B., Schofield, P.R., Andreadis, A., Snowden, J., Craufurd, D., Neary, D., Owen, F., Oostra, B.A., Hardy, J., Goate, A., van Swieten, J., Mann, D., Lynch, T. & Heutink, P. (1998) Association of missense and 5'-splice-site mutations in tau with the inherited dementia

FTDP-17. *Nature* **393**, 702–705.

Ingelsson, M., Fukumoto, H., Newell, K.L., Growdon, J.H., Hedley-Whyte, E.T., Frosch, M.P., Albert, M.S., Hyman, B.T. & Irizarry, M.C. (2004) Early Abeta accumulation and progressive synaptic loss, gliosis, and tangle formation in AD brain. *Neurology* **62**, 925–931.

Iqbal, K., Liu, F., Gong, C.-X. & Grundke-Iqbal, I. (2010) Tau in Alzheimer Disease and Related Tauopathies. *Curr Alzheimer Res* **7** 656-664.

Itagaki, S., McGeer, P.L., Akiyama, H., Zhu, S. & Selkoe, D. (1989) Relationship of microglia and astrocytes to amyloid deposits of Alzheimer disease. *J Neuroimmunol* **24**, 173–182.

Iwatsubo, T., Odaka, A., Suzuki, N., Mizusawa, H., Nukina, N. & Ihara, Y. (1994) Visualization of A beta 42(43) and A beta 40 in senile plaques with end-specific  A beta monoclonals: evidence that an initially deposited species is A beta 42(43). *Neuron* **13**, 45–53.

Jan, A., Gokce, O., Luthi-Carter, R. & Lashuel, H.A. (2008) The ratio of monomeric to aggregated forms of Abeta40 and Abeta42 is an important determinant of amyloid-beta aggregation, fibrillogenesis, and toxicity. *J Biol Chem* **283**, 28176–28189.

Jarrett, J.T., Berger, E.P. & Lansbury, P.T.J. (1993) The carboxy terminus of the beta amyloid protein is critical for the seeding of amyloid formation: implications for the pathogenesis of Alzheimer's disease. *Biochemistry* **32**, 4693–4697.

Jawhar, S., Trawicka, A., Jenneckens, C., Bayer, T.A. & Wirths, O. (2012) Motor deficits, neuron loss, and reduced anxiety coinciding with axonal degeneration and intraneuronal Abeta aggregation in the 5XFAD mouse model of Alzheimer's disease. *Neurobiol Aging* **33**, 196.e29-40.

Jawhar, S., Wirths, O., Schilling, S., Graubner, S., Demuth, H.U. & Bayer, T.A. (2011) Overexpression of glutaminyl cyclase, the enzyme responsible for pyroglutamate Aβ formation, induces behavioral deficits, and glutaminyl cyclase knock-out rescues the behavioral phenotype in 5XFAD mice. *J Biol Chem* **286**, 4454–4460.

Jonsson, T., Stefansson, H., Steinberg, S., Jonsdottir, I., Jonsson, P. V, Snaedal, J., Bjornsson, S., Huttenlocher, J., Levey, A.I., Lah, J.J., Rujescu, D., Hampel, H., Giegling, I., Andreassen, O.A., Engedal, K., Ulstein, I., Djurovic, S., Ibrahim-Verbaas, C., Hofman, A., Ikram, M.A., van Duijn, C.M., Thorsteinsdottir, U., Kong, A. & Stefansson, K. (2013) Variant of TREM2 associated with the risk of Alzheimer's disease. *N Engl J Med* **368**, 107–116.

Kang, J., Lemaire, H.G., Unterbeck, A., Salbaum, J.M., Masters, C.L., Grzeschik, K.H., Multhaup, G., Beyreuther, K. & Muller-Hill, B. (1987) The precursor of Alzheimer's disease amyloid A4 protein resembles a cell-surface  receptor. *Nature* **325**, 733–736.

Karch, C.M. & Goate, A.M. (2015) Alzheimer's disease risk genes and mechanisms of disease pathogenesis. *Biol Psychiatry* **77**, 43–51.

Karl, T., Bhatia, S., Cheng, D., Kim, W.S. & Garner, B. (2012) Cognitive phenotyping of amyloid precursor protein transgenic J20 mice. *Behav Brain Res* **228**, 392–397.

Karl, T., Pabst, R. & von Horsten, S. (2003) Behavioral phenotyping of mice in pharmacological and toxicological research. *Exp Toxicol Pathol* **55**, 69–83.

Katzman, R., Terry, R., DeTeresa, R., Brown, T., Davies, P., Fuld, P., Renbing, X. & Peck, A. (1988) Clinical, pathological, and neurochemical changes in dementia: a subgroup with preserved mental status and numerous neocortical plaques. *Ann Neurol* **23**, 138–144.

Kennelly, S.P., Lawlor, B.A. & Kenny, R.A. (2009) Blood pressure and dementia - a

comprehensive review. *Ther Adv Neurol Disord* **2**, 241–260.

Kidd, M. (1963) Paired Helical Filaments in Electron Microscopy of Alzheimer's Disease. *Nature* **197**, 192.

Kim, J., Basak, J.M. & Holtzman, D.M. (2009) The role of apolipoprotein E in Alzheimer's disease. *Neuron* **63**, 287–303.

Kimberly, W.T., LaVoie, M.J., Ostaszewski, B.L., Ye, W., Wolfe, M.S. & Selkoe, D.J. (2003) Gamma-secretase is a membrane protein complex comprised of presenilin, nicastrin, Aph-1, and Pen-2. *Proc Natl Acad Sci U S A* **100**, 6382–6387.

King, D.L., Arendash, G.W., Crawford, F., Sterk, T., Menendez, J. & Mullan, M.J. (1999) Progressive and gender-dependent cognitive impairment in the APP(SW) transgenic mouse model for Alzheimer's disease. *Behav Brain Res* **103**, 145–162.

Kitaguchi, N., Takahashi, Y., Tokushima, Y., Shiojiri, S. & Ito, H. (1988) Novel precursor of Alzheimer's disease amyloid protein shows protease inhibitory activity. *Nature* **331**, 530.

Kivipelto, M., Helkala, E., Laakso, M.P., Hänninen, T., Hallikainen, M., Alhainen, K., Soininen, H., Tuomilehto, J. & Nissien, A. (2001) Midlife vascular risk factors and Alzheimer's Disease in later life: Longitudinal, population based study. *BMJ* **322**, 1447–1451.

Kivipelto, M., Ngandu, T., Fratiglioni, L., Viitanen, M., Kareholt, I., Winblad, B., Helkala, E.L., Tuomilehto, J., Soininen, H. & Nissinen, A. (2005) Obesity and vascular risk factors at midlife and the risk of dementia and Alzheimer disease. *Arch Neurol* **62**, 1556–1560.

Kluger, A., Gianutsos, J.G., Golomb, J., Ferris, S.H., George, a. E., Franssen, E. & Reisberg, B. (1997) Patterns of Motor Impairment in Normal Aging, Mild Cognitive Decline, and Early Alzheimer' Disease. *Journals Gerontol Ser B Psychol Sci Soc Sci* **52B**, P28–P39.

Knowles, R.B., Wyart, C., Buldyrev, S. V, Cruz, L., Urbanc, B., Hasselmo, M.E., Stanley, H.E. & Hyman, B.T. (1999) Plaque-induced neurite abnormalities: implications for disruption of neural networks in Alzheimer's disease. *Proc Natl Acad Sci U S A* **96**, 5274–5279.

Koffie, R.M., Hashimoto, T., Tai, H.-C., Kay, K.R., Serrano-Pozo, A., Joyner, D., Hou, S., Kopeikina, K.J., Frosch, M.P., Lee, V.M., Holtzman, D.M., Hyman, B.T. & Spires-Jones, T.L. (2012) Apolipoprotein E4 effects in Alzheimer's disease are mediated by synaptotoxic oligomeric amyloid-beta. *Brain* **135**, 2155–2168.

Koffie, R.M., Meyer-Luehmann, M., Hashimoto, T., Adams, K.W., Mielke, M.L., Garcia-Alloza, M., Micheva, K.D., Smith, S.J., Kim, M.L., Lee, V.M., Hyman, B.T. & Spires-Jones, T.L. (2009) Oligomeric amyloid beta associates with postsynaptic densities and correlates with excitatory synapse loss near senile plaques. *Proc Natl Acad Sci U S A* **106**, 4012–4017.

Koistinaho, M., Lin, S., Wu, X., Esterman, M., Koger, D., Hanson, J., Higgs, R., Liu, F., Malkani, S., Bales, K.R. & Paul, S.M. (2004) Apolipoprotein E promotes astrocyte colocalization and degradation of deposited amyloid-beta peptides. *Nat Med* **10**, 719–726.

Komada, M., Takao, K. & Miyakawa, T. (2008) Elevated Plus Maze for Mice. *J Vis Exp* **22** e1088.

Koo, E.H., Squazzo, S.L., Selkoe, D.J. & Koo, C.H. (1996) Trafficking of cell-surface amyloid beta-protein precursor. I. Secretion, endocytosis and recycling as detected by labeled monoclonal antibody. *J Cell Sci* **109**, 991 LP-998.

Kosik, K.S., Joachim, C.L. & Selkoe, D.J. (1986) Microtubule-associated protein tau (tau) is a major antigenic component of paired helical filaments in Alzheimer disease. *Proc Natl Acad Sci U S A* **83**, 4044–4048.

Kril, J.J., Hodges, J. & Halliday, G. (2004) Relationship between hippocampal volume and CA1 neuron loss in brains of humans with and without Alzheimer's disease. *Neurosci Lett* **361**, 9–12.

Kuhn, P.-H., Wang, H., Dislich, B., Colombo, A., Zeitschel, U., Ellwart, J.W., Kremmer, E., Rossner, S. & Lichtenthaler, S.F. (2010) ADAM10 is the physiologically relevant, constitutive alpha-secretase of the amyloid precursor protein in primary neurons. *EMBO J* **29**, 3020–3032.

Kummer, M.P. & Heneka, M.T. (2014) Truncated and modified amyloid-beta species. *Alzheimers Res Ther* **6**, 28.

Kuo, Y.M., Emmerling, M.R., Vigo-Pelfrey, C., Kasunic, T.C., Kirkpatrick, J.B., Murdoch, G.H., Ball, M.J. & Roher, A.E. (1996) Water-soluble Abeta (N-40, N-42) oligomers in normal and Alzheimer disease brains. *J Biol Chem* **271**, 4077–4081.

LaFerla, F.M., Green, K.N. & Oddo, S. (2007) Intracellular amyloid-beta in Alzheimer's disease. *Nat Rev Neurosci* **8**, 499–509.

Lai, A., Sisodia, S.S. & Trowbridge, I.S. (1995) Characterization of sorting signals in the beta-amyloid precursor protein cytoplasmic domain. *J Biol Chem* **270**, 3565–3573.

Lalonde, R. (2002) The neurobiological basis of spontaneous alternation. *Neurosci Biobehav Rev* **26**, 91–104.

Lalonde, R., Fukuchi, K. & Strazielle, C. (2012) APP transgenic mice for modelling behavioural and psychological symptoms of dementia (BPSD). *Neurosci Biobehav* **36**, 1357–1375.

Lalonde, R., Lewis, T.L., Strazielle, C., Kim, H. & Fukuchi, K. (2003) Transgenic mice expressing the betaAPP695SWE mutation: effects on exploratory activity, anxiety, and motor coordination. *Brain Res* **977**, 38–45.

Lalonde, R. & Strazielle, C. (2007) Brain regions and genes affecting postural control. *Prog Neurobiol* **81**, 45–60.

Lamb, B.T., Sisodia, S.S., Lawler, A.M., Slunt, H.H., Kitt, C.A., Kearns, W.G., Pearson, P.L., Price, D.L. & Gearhart, J.D. (1993) Introduction and expression of the 400 kilobase amyloid precursor protein gene in transgenic mice [corrected]. *Nat Genet* **5**, 22–30.

Lambert, J.C., Ibrahim-Verbaas, C.A., Harold, D., Naj, A.C., Sims, R., Bellenguez, C., DeStafano, A.L., Bis, J.C., Beecham, G.W., Grenier-Boley, B., Russo, G., Thorton-Wells, T.A., Jones, N., Smith, A. V, Chouraki, V., Thomas, C., Ikram, M.A., Zelenika, D., Vardarajan, B.N., Kamatani, Y., Lin, C.F., Gerrish, A., Schmidt, H., Kunkle, B., Dunstan, M.L., Ruiz, A., Bihoreau, M.T., Choi, S.H., Reitz, C., Pasquier, F., Cruchaga, C., Craig, D., Amin, N., Berr, C., Lopez, O.L., De Jager, P.L., Deramecourt, V., Johnston, J.A., Evans, D., Lovestone, S., Letenneur, L., Moron, F.J., Rubinsztein, D.C., Eiriksdottir, G., Sleegers, K., Goate, A.M., Fievet, N., Huentelman, M.W., Gill, M., Brown, K., Kamboh, M.I., Keller, L., Barberger-Gateau, P., McGuiness, B., Larson, E.B., Green, R., Myers, A.J., Dufouil, C., Todd, S., Wallon, D., Love, S., Rogaeva, E., Gallacher, J., St George-Hyslop, P., Clarimon, J., Lleo, A., Bayer, A., Tsuang, D.W., Yu, L., Tsolaki, M., Bossu, P., Spalletta, G., Proitsi, P., Collinge, J., Sorbi, S., Sanchez-Garcia, F., Fox, N.C., Hardy, J., Deniz Naranjo, M.C., Bosco, P., Clarke, R., Brayne, C., Galimberti, D., Mancuso, M., Matthews, F., Moebus, S., Mecocci, P., Del Zompo, M., Maier, W., Hampel, H., Pilotto, A., Bullido, M., Panza, F., Caffarra, P., Nacmias, B., Gilbert, J.R., Mayhaus, M., Lannefelt, L., Hakonarson, H., Pichler, S., Carrasquillo, M.M., Ingelsson, M., Beekly, D., Alvarez, V., Zou, F., Valladares, O., Younkin, S.G., Coto, E., Hamilton-Nelson, K.L., Gu, W., Razquin, C., Pastor, P., Mateo, I., Owen, M.J., Faber, K.M., Jonsson, P. V, Combarros, O., O'Donovan, M.C., Cantwell, L.B., Soininen, H., Blacker, D., Mead, S., Mosley, T.H.J., Bennett, D.A., Harris, T.B., Fratiglioni,

L., Holmes, C., de Bruijn, R.F., Passmore, P., Montine, T.J., Bettens, K., Rotter, J.I., Brice, A., Morgan, K., Foroud, T.M., Kukull, W.A., Hannequin, D., Powell, J.F., Nalls, M.A., Ritchie, K., Lunetta, K.L., Kauwe, J.S., Boerwinkle, E., Riemenschneider, M., Boada, M., Hiltuenen, M., Martin, E.R., Schmidt, R., Rujescu, D., Wang, L.S., Dartigues, J.F., Mayeux, R., Tzourio, C., Hofman, A., Nothen, M.M., Graff, C., Psaty, B.M., Jones, L., Haines, J.L., Holmans, P.A., Lathrop, M., Pericak-Vance, M.A., Launer, L.J., Farrer, L.A., van Duijn, C.M., Van Broeckhoven, C., Moskvina, V., Seshadri, S., Williams, J., Schellenberg, G.D. & Amouyel, P. (2013) Meta-analysis of 74,046 individuals identifies 11 new susceptibility loci for Alzheimer's disease. *Nat Genet* **45**, 1452–1458.

Lambert, M.P., Barlow, A.K., Chromy, B.A., Edwards, C., Freed, R., Liosatos, M., Morgan, T.E., Rozovsky, I., Trommer, B., Viola, K.L., Wals, P., Zhang, C., Finch, C.E., Krafft, G.A. & Klein, W.L. (1998) Diffusible, nonfibrillar ligands derived from Abeta1-42 are potent central nervous system neurotoxins. *Proc Natl Acad Sci U S A* **95**, 6448–6453.

Lee, V.M., Balin, B.J., Otvos, L.J. & Trojanowski, J.Q. (1991) A68: a major subunit of paired helical filaments and derivatized forms of normal Tau. *Science* **251**, 675–678.

Leibson, C.L., Rocca, W.A., Hanson, V.A., Cha, R., Kokmen, E., O'Brien, P.C. & Palumbo, P.J. (1997) The risk of dementia among persons with diabetes mellitus: a population-based cohort study. *Ann N Y Acad Sci* **826**, 422–427.

Leissring, M.A., Lu, A., Condron, M.M., Teplow, D.B., Stein, R.L., Farris, W. & Selkoe, D.J. (2003) Kinetics of amyloid beta-protein degradation determined by novel fluorescence- and fluorescence polarization-based assays. *J Biol Chem* **278**, 37314–37320.

Lesne, S., Koh, M.T., Kotilinek, L., Kayed, R., Glabe, C.G., Yang, A., Gallagher, M. & Ashe, K.H. (2006) A specific amyloid-beta protein assembly in the brain impairs memory. *Nature* **440**, 352–357.

Levy-Lahad, E., Wasco, W., Poorkaj, P., Romano, D.M., Oshima, J., Pettingell, W.H., Yu, C.E., Jondro, P.D., Schmidt, S.D. & Wang, K. (1995) Candidate gene for the chromosome 1 familial Alzheimer's disease locus. *Science* **269**, 973–977.

Lewis, H., Beher, D., Cookson, N., Oakley, A., Piggott, M., Morris, C.M., Jaros, E., Perry, R., Ince, P., Kenny, R.A., Ballard, C.G., Shearman, M.S. & Kalaria, R.N. (2006) Quantification of Alzheimer pathology in ageing and dementia: age-related accumulation of amyloid-beta(42) peptide in vascular dementia. *Neuropathol Appl Neurobiol* **32**, 103–118.

Lewis, J., Dickson, D.W., Lin, W.L., Chisholm, L., Corral, A., Jones, G., Yen, S.H., Sahara, N., Skipper, L., Yager, D., Eckman, C., Hardy, J., Hutton, M. & McGowan, E. (2001) Enhanced neurofibrillary degeneration in transgenic mice expressing mutant tau and APP. *Science* **293**, 1487–1491.

Li, S., Hong, S., Shepardson, N.E., Walsh, D.M., Shankar, G.M. & Selkoe, D. (2009) Soluble Oligomers of Amyloid β Protein Facilitate Hippocampal Long-Term Depression by Disrupting Neuronal Glutamate Uptake. *Neuron* **62**, 788–801.

Lichtenthaler, S.F., Haass, C. & Steiner, H. (2011) Regulated intramembrane proteolysis--lessons from amyloid precursor protein processing. *J Neurochem* **117**, 779–796.

Liu, K., Doms, R.W. & Lee, V.M.-Y. (2002a) Glu11 Site Cleavage and N-Terminally Truncated Aβ Production upon BACE Overexpression. *Biochemistry* **41**, 3128–3136.

Liu, L., Ikonen, S., Heikkinen, T., Heikkila, M., Puolivali, J., van Groen, T. & Tanila, H. (2002b) Effects of fimbria-fornix lesion and amyloid pathology on spatial learning and memory in

transgenic APP+PS1 mice. *Behav Brain Res* **134**, 433–445.

Liu, R.-Q., Zhou, Q.-H., Ji, S.-R., Zhou, Q., Feng, D., Wu, Y. & Sui, S.-F. (2010) Membrane Localization of β-Amyloid 1–42 in Lysosomes: a possible mechanism for lysosome labilization. *J Biol Chem* **285** 19986-19996.

Lopez-Noguerola, J.S., Giessen, N.M.E., Ueberück, M., Meißner, J.N., Pelgrim, C.E., Adams, J., Wirths, O., Bouter, Y. & Bayer, T.A. (2018) Synergistic Effect on Neurodegeneration by N-Truncated Aβ4–42 and Pyroglutamate Aβ3–42 in a Mouse Model of Alzheimer's Disease . *Front Aging Neurosci* **10** 64.

Ludewig, S. & Korte, M. (2016) Novel Insights into the Physiological Function of the APP (Gene) Family and Its Proteolytic Fragments in Synaptic Plasticity. *Front Mol Neurosci* **9** 161.

Luo, Y., Bolon, B., Kahn, S., Bennett, B.D., Babu-Khan, S., Denis, P., Fan, W., Kha, H., Zhang, J., Gong, Y., Martin, L., Louis, J.C., Yan, Q., Richards, W.G., Citron, M. & Vassar, R. (2001) Mice deficient in BACE1, the Alzheimer's beta-secretase, have normal phenotype and abolished beta-amyloid generation. *Nat Neurosci* **4**, 231–232.

Marquez-Sterling, N.R., Lo, A.C., Sisodia, S.S. & Koo, E.H. (1997) Trafficking of cell-surface beta-amyloid precursor protein: evidence that a sorting intermediate participates in synaptic vesicle recycling. *J Neurosci* **17**, 140–151.

Masliah, E., Mallory, M., Hansen, L., DeTeresa, R., Alford, M. & Terry, R. (1994) Synaptic and neuritic alterations during the progression of Alzheimer's disease. *Neurosci Lett* **174**, 67–72.

Masters, C., Simms, G., Weinman, N., Multhaup, G., McDonald, B. & Beyreuther, K. (1985) Amyloid plaque core protein in Alzheimer disease and Down syndrome. *Proc Natl Acad Sci U S A* **82**, 4245–4249.

Mc Donald, J.M., Savva, G.M., Brayne, C., Welzel, A.T., Forster, G., Shankar, G.M., Selkoe, D.J., Ince, P.G. & Walsh, D.M. (2010) The presence of sodium dodecyl sulphate-stable Abeta dimers is strongly associated with Alzheimer-type dementia. *Brain* **133**, 1328–1341.

McHugh, S.B., Deacon, R.M.J., Rawlins, J.N.P. & Bannerman, D.M. (2004) Amygdala and ventral hippocampus contribute differentially to mechanisms of fear  and anxiety. *Behav Neurosci* **118**, 63–78.

McLean, C.A., Cherny, R.A., Fraser, F.W., Fuller, S.J., Smith, M.J., Beyreuther, K., Bush, A.I. & Masters, C.L. (1999) Soluble pool of Abeta amyloid as a determinant of severity of neurodegeneration in Alzheimer's disease. *Ann Neurol* **46**, 860–866.

Meissner, J.N., Bouter, Y. & Bayer, T.A. (2015) Neuron Loss and Behavioral Deficits in the TBA42 Mouse Model Expressing N-Truncated Pyroglutamate Amyloid-beta3-42. *J Alzheimers Dis* **45**, 471–482.

Miller, D.L., Papayannopoulos, I.A., Styles, J., Bobin, S.A., Lin, Y.Y., Biemann, K. & Iqbal, K. (1993) Peptide Compositions of the Cerebrovascular and Senile Plaque Core Amyloid Deposits of Alzheimer's Disease. *Arch Biochem Biophys* **301** 41-52.

Moore, B.D., Chakrabarty, P., Levites, Y., Kukar, T.L., Baine, A.-M., Moroni, T., Ladd, T.B., Das, P., Dickson, D.W. & Golde, T.E. (2012) Overlapping profiles of Aβ peptides in the Alzheimer's disease and pathological aging brains. *Alzheimers Res Ther* **4**, 18.

Moran, P.M., Higgins, L.S., Cordell, B. & Moser, P.C. (1995) Age-related learning deficits in transgenic mice expressing the 751-amino acid isoform of human beta-amyloid precursor

protein. *Proc Natl Acad Sci U S A* **92** 5341-5345.

Mori, C., Spooner, E.T., Wisniewsk, K.E., Wisniewski, T.M., Yamaguch, H., Saido, T.C., Tolan, D.R., Selkoe, D.J. & Lemere, C.A. (2002) Intraneuronal Abeta42 accumulation in Down syndrome brain. *Amyloid* **9**, 88–102.

Mori, H., Takio, K., Ogawara, M. & Selkoe, D.J. (1992) Mass spectrometry of purified amyloid beta protein in Alzheimer's disease. *J Biol Chem* **267**, 17082–17086.

Morris, R. (1984) Developments of a water-maze procedure for studying spatial learning in the rat. *J Neurosci Methods* **11**, 47–60.

Moser, M.B., Moser, E.I., Forrest, E., Andersen, P. & Morris, R.G. (1995) Spatial learning with a minislab in the dorsal hippocampus. *Proc Natl Acad Sci U S A* **92** 9697-9701.

Mucke, L., Masliah, E., Yu, G.Q., Mallory, M., Rockenstein, E.M., Tatsuno, G., Hu, K., Kholodenko, D., Johnson-Wood, K. & McConlogue, L. (2000) High-level neuronal expression of abeta 1-42 in wild-type human amyloid protein precursor transgenic mice: synaptotoxicity without plaque formation. *J Neurosci* **20**, 4050–4058.

Müller, U.C., Deller, T. & Korte, M. (2017) Not just amyloid: physiological functions of the amyloid precursor protein family. *Nat Rev Neurosci* **18**, 281.

Myers, R.H., Schaefer, E.J., Wilson, P.W., D'Agostino, R., Ordovas, J.M., Espino, A., Au, R., White, R.F., Knoefel, J.E., Cobb, J.L., McNulty, K.A., Beiser, A. & Wolf, P.A. (1996) Apolipoprotein E epsilon4 association with dementia in a population-based study: The Framingham study. *Neurology* **46**, 673–677.

Nagele, R.G., D'Andrea, M.R., Anderson, W.J. & Wang, H.-Y. (2002) Intracellular accumulation of beta-amyloid(1-42) in neurons is facilitated by the alpha 7 nicotinic acetylcholine receptor in Alzheimer's disease. *Neuroscience* **110**, 199–211.

Nagele, R.G., D'Andrea, M.R., Lee, H., Venkataraman, V. & Wang, H.-Y. (2003) Astrocytes accumulate A beta 42 and give rise to astrocytic amyloid plaques in Alzheimer disease brains. *Brain Res* **971**, 197–209.

Naj, A.C., Jun, G., Beecham, G.W., Wang, L.-S., Vardarajan, B.N., Buros, J., Gallins, P.J., Buxbaum, J.D., Jarvik, G.P., Crane, P.K., Larson, E.B., Bird, T.D., Boeve, B.F., Graff-Radford, N.R., De Jager, P.L., Evans, D., Schneider, J.A., Carrasquillo, M.M., Ertekin-Taner, N., Younkin, S.G., Cruchaga, C., Kauwe, J.S.K., Nowotny, P., Kramer, P., Hardy, J., Huentelman, M.J., Myers, A.J., Barmada, M.M., Demirci, F.Y., Baldwin, C.T., Green, R.C., Rogaeva, E., St George-Hyslop, P., Arnold, S.E., Barber, R., Beach, T., Bigio, E.H., Bowen, J.D., Boxer, A., Burke, J.R., Cairns, N.J., Carlson, C.S., Carney, R.M., Carroll, S.L., Chui, H.C., Clark, D.G., Corneveaux, J., Cotman, C.W., Cummings, J.L., DeCarli, C., DeKosky, S.T., Diaz-Arrastia, R., Dick, M., Dickson, D.W., Ellis, W.G., Faber, K.M., Fallon, K.B., Farlow, M.R., Ferris, S., Frosch, M.P., Galasko, D.R., Ganguli, M., Gearing, M., Geschwind, D.H., Ghetti, B., Gilbert, J.R., Gilman, S., Giordani, B., Glass, J.D., Growdon, J.H., Hamilton, R.L., Harrell, L.E., Head, E., Honig, L.S., Hulette, C.M., Hyman, B.T., Jicha, G.A., Jin, L.-W., Johnson, N., Karlawish, J., Karydas, A., Kaye, J.A., Kim, R., Koo, E.H., Kowall, N.W., Lah, J.J., Levey, A.I., Lieberman, A.P., Lopez, O.L., Mack, W.J., Marson, D.C., Martiniuk, F., Mash, D.C., Masliah, E., McCormick, W.C., McCurry, S.M., McDavid, A.N., McKee, A.C., Mesulam, M., Miller, B.L., Miller, C.A., Miller, J.W., Parisi, J.E., Perl, D.P., Peskind, E., Petersen, R.C., Poon, W.W., Quinn, J.F., Rajbhandary, R.A., Raskind, M., Reisberg, B., Ringman, J.M., Roberson, E.D., Rosenberg, R.N., Sano, M., Schneider, L.S., Seeley, W., Shelanski, M.L., Slifer, M.A., Smith, C.D., Sonnen, J.A., Spina, S., Stern, R.A., Tanzi, R.E., Trojanowski, J.Q., Troncoso, J.C., Van Deerlin, V.M., Vinters, H. V, Vonsattel, J.P., Weintraub,

S., Welsh-Bohmer, K.A., Williamson, J., Woltjer, R.L., Cantwell, L.B., Dombroski, B.A., Beekly, D., Lunetta, K.L., Martin, E.R., Kamboh, M.I., Saykin, A.J., Reiman, E.M., Bennett, D.A., Morris, J.C., Montine, T.J., Goate, A.M., Blacker, D., Tsuang, D.W., Hakonarson, H., Kukull, W.A., Foroud, T.M., Haines, J.L., Mayeux, R., Pericak-Vance, M.A., Farrer, L.A. & Schellenberg, G.D. (2011) Common variants at MS4A4/MS4A6E, CD2AP, CD33 and EPHA1 are associated with late-onset Alzheimer's disease. *Nat Genet* **43**, 436–441.

Naj, A.C., Schellenberg, G.D. & (ADGC), for the A.D.G.C. (2017) Genomic variants, genes, and pathways of Alzheimer's disease: An overview. *Am J Med Genet B Neuropsychiatr Genet* **174**, 5–26.

Näslund, J., Schierhorn, A., Hellman, U., Lannfelt, L., Roses, A.D., Tjernberg, L.O., Silberring, J., Gandy, S.E., Winblad, B. & Greengard, P. (1994) Relative abundance of Alzheimer A beta amyloid peptide variants in Alzheimer disease and normal aging. *Proc Natl Acad Sci U S A* **91** 8378-8382.

Neumann, H. & Takahashi, K. (2007) Essential role of the microglial triggering receptor expressed on myeloid cells-2 (TREM2) for central nervous tissue immune homeostasis. *J Neuroimmunol* **184**, 92–99.

Nicoll, J.A.R., Barton, E., Boche, D., Neal, J.W., Ferrer, I., Thompson, P., Vlachouli, C., Wilkinson, D., Bayer, A., Games, D., Seubert, P., Schenk, D. & Holmes, C. (2006) Abeta species removal after abeta42 immunization. *J Neuropathol Exp Neurol* **65**, 1040–1048.

Nixon, R.A. (2005) Endosome function and dysfunction in Alzheimer's disease and other neurodegenerative diseases. *Neurobiol Aging* **26**, 373–382.

Van Nostrand, W.E., Wagner, S.L., Suzuki, M., Choi, B.H., Farrow, J.S., Geddes, J.W., Cotman, C.W. & Cunningham, D.D. (1989) Protease nexin-II, a potent antichymotrypsin, shows identity to amyloid beta-protein precursor. *Nature* **341**, 546–549.

Nussbaum, J.M., Schilling, S., Cynis, H., Silva, A., Swanson, E., Wangsanut, T., Tayler, K., Wiltgen, B., Hatami, A., Rönicke, R., Hutter-paier, B., Alexandru, A., Jagla, W., Graubner, S., Glabe, C.G., Demuth, H. & Bloom, G.S. (2012) Prion-Like Behavior and Tau-dependent Cytotoxicity of Pyroglutamylated β-Amyloid. *Nature* **485**, 651–655.

O'Keeffe, S.T., Kazeem, H., Philpott, R.M., Playfer, J.R., Gosney, M. & Lye, M. (1996) Gait disturbance in Alzheimer's disease: A clinical study. *Age Ageing* **25**, 313–316.

Oakley, H., Cole, S.L., Logan, S., Maus, E., Shao, P., Craft, J., Guillozet-Bongaarts, A., Ohno, M., Disterhoft, J., Van Eldik, L., Berry, R. & Vassar, R. (2006) Intraneuronal beta-amyloid aggregates, neurodegeneration, and neuron loss in transgenic mice with five familial Alzheimer's disease mutations: potential factors in amyloid plaque formation. *J Neurosci* **26**, 10129–10140.

Oddo, S., Caccamo, A., Green, K.N., Liang, K., Tran, L., Chen, Y., Leslie, F.M. & LaFerla, F.M. (2005) Chronic nicotine administration exacerbates tau pathology in a transgenic model of Alzheimer's disease. *Proc Natl Acad Sci U S A* **102**, 3046–3051.

Oh, S., Hong, H.S., Hwang, E., Sim, H.J., Lee, W., Shin, S.J. & Mook-Jung, I. (2005) Amyloid peptide attenuates the proteasome activity in neuronal cells. *Mech Ageing Dev* **126**, 1292—1299.

Ohno, M., Cole, S.L., Yasvoina, M., Zhao, J., Citron, M., Berry, R., Disterhoft, J.F. & Vassar, R. (2007) BACE1 gene deletion prevents neuron loss and memory deficits in 5XFAD APP/PS1 transgenic mice. *Neurobiol Dis* **26**, 134–145.

Pastor, P., Roe, C.M., Villegas, A., Bedoya, G., Chakraverty, S., Garcia, G., Tirado, V., Norton, J., Rios,

S., Martinez, M., Kosik, K.S., Lopera, F. & Goate, A.M. (2003) Apolipoprotein Eepsilon4 modifies Alzheimer's disease onset in an E280A PS1 kindred. *Ann Neurol* **54**, 163–169.

Perl, D.P. (2010) Neuropathology of Alzheimer's Disease. *Mt Sinai J Med* **77** 32-42.

Pettersson, A.F., Olsson, E. & Wahlund, L.-O. (2005) Motor Function in Subjects with Mild Cognitive Impairment and Early Alzheimer's Disease. *Dement Geriatr Cogn Disord* **19**, 299–304.

Piccini, A., Russo, C., Gliozzi, A., Relini, A., Vitali, A., Borghi, R., Giliberto, L., Armirotti, A., D'Arrigo, C., Bachi, A., Cattaneo, A., Canale, C., Torrassa, S., Saido, T.C., Markesbery, W., Gambetti, P. & Tabaton, M. (2005) beta-amyloid is different in normal aging and in Alzheimer disease. *J Biol Chem* **280**, 34186–34192.

Pietropaolo, S., Feldon, J. & Yee, B.K. (2008) Age-dependent phenotypic characteristics of a triple transgenic mouse model of Alzheimer disease. *Behav Neurosci* **122**, 733–747.

Pike, C.J., Cummings, B.J. & Cotman, C.W. (1995a) Early association of reactive astrocytes with senile plaques in Alzheimer's disease. *Exp Neurol* **132**, 172–179.

Pike, C.J., Overman, M.J. & Cotman, C.W. (1995b) Amino-terminal deletions enhance aggregation of β-amyloid peptides in vitro. *J Biol Chem* **270**, 23895–23898.

Poorkaj, P., Bird, T.D., Wijsman, E., Nemens, E., Garruto, R.M., Anderson, L., Andreadis, A., Wiederholt, W.C., Raskind, M. & Schellenberg, G.D. (1998) Tau is a candidate gene for chromosome 17 frontotemporal dementia. *Ann Neurol* **43**, 815–825.

Portelius, E., Gustavsson, M.K., Volkmann, I. & Zetterberg, H. (2010) Mass spectrometric characterization of brain amyloid beta isoform signatures in familial and sporadic Alzheimer's disease. *Acta Neuropathol* **120**, 185–193.

Portelius, E., Lashley, T., Westerlund, A., Persson, R., Fox, N.C., Blennow, K., Revesz, T. & Zetterberg, H. (2015) Brain amyloid-beta fragment signatures in pathological ageing and alzheimer's disease by hybrid immunoprecipitation mass spectrometry. *Neurodegener Dis* **15**, 50–57.

Portelius, E., Price, E., Brinkmalm, G., Stiteler, M., Olsson, M., Persson, R., Westman-Brinkmalm, A., Zetterberg, H., Simon, A.J. & Blennow, K. (2011) A novel pathway for amyloid precursor protein processing. *Neurobiol Aging* **32**, 1090–1098.

Price, J.L. & Morris, J.C. (1999) Tangles and plaques in nondemented aging and "preclinical" Alzheimer's disease. *Ann Neurol* **45**, 358–368.

Prox, J., Bernreuther, C., Altmeppen, H., Grendel, J., Glatzel, M., D'Hooge, R., Stroobants, S., Ahmed, T., Balschun, D., Willem, M., Lammich, S., Isbrandt, D., Schweizer, M., Horre, K., De Strooper, B. & Saftig, P. (2013) Postnatal disruption of the disintegrin/metalloproteinase ADAM10 in brain causes epileptic seizures, learning deficits, altered spine morphology, and defective synaptic functions. *J Neurosci* **33**, 12915–28, 12928a.

Puolivali, J., Wang, J., Heikkinen, T., Heikkila, M., Tapiola, T., van Groen, T. & Tanila, H. (2002) Hippocampal A beta 42 levels correlate with spatial memory deficit in APP and PS1 double transgenic mice. *Neurobiol Dis* **9**, 339–347.

Qi-Takahara, Y., Morishima-Kawashima, M., Tanimura, Y., Dolios, G., Hirotani, N., Horikoshi, Y., Kametani, F., Maeda, M., Saido, T.C., Wang, R. & Ihara, Y. (2005) Longer forms of amyloid beta protein: implications for the mechanism of intramembrane cleavage by gamma-secretase. *J Neurosci* **25**, 436–445.

Radde, R., Duma, C., Goedert, M. & Jucker, M. (2008) The value of incomplete mouse models of Alzheimer's disease. *Eur J Nucl Med Mol Imaging* **35 Suppl 1**, S70-4.

Reinert, J., Richard, B.C., Klafki, H.W., Friedrich, B., Bayer, T.A., Wiltfang, J., Kovacs, G.G., Ingelsson, M., Lannfelt, L., Paetau, A., Bergquist, J. & Wirths, O. (2016) Deposition of C-terminally truncated Aβ species Aβ37 and Aβ39 in Alzheimer's disease and transgenic mouse models. *Acta Neuropathol Commun* **4**, 24.

Reitz, C. & Mayeux, R. (2014) Alzheimer disease: epidemiology, diagnostic criteria, risk factors and biomarkers. *Biochem Pharmacol* **88**, 640–651.

Richard, B.C., Kurdakova, A., Baches, S., Bayer, T.A., Weggen, S. & Wirths, O. (2015) Gene Dosage Dependent Aggravation of the Neurological Phenotype in the 5XFAD Mouse Model of Alzheimer's Disease. *J Alzheimers Dis* **45**, 1223–1236.

Rijal Upadhaya, A., Kosterin, I., Kumar, S., von Arnim, C.A.F., Yamaguchi, H., Fandrich, M., Walter, J. & Thal, D.R. (2014) Biochemical stages of amyloid-beta peptide aggregation and accumulation in the human brain and their association with symptomatic and pathologically preclinical Alzheimer's disease. *Brain* **137**, 887–903.

Robakis, N.K., Ramakrishna, N., Wolfe, G. & Wisniewski, H.M. (1987) Molecular cloning and characterization of a cDNA encoding the cerebrovascular and the neuritic plaque amyloid peptides. *Proc Natl Acad Sci U S A* **84** 4190-4194.

Rogaev, E.I., Sherrington, R., Rogaeva, E.A., Levesque, G., Ikeda, M., Liang, Y., Chi, H., Lin, C., Holman, K. & Tsuda, T. (1995) Familial Alzheimer's disease in kindreds with missense mutations in a gene on chromosome 1 related to the Alzheimer's disease type 3 gene. *Nature* **376**, 775–778.

Roher, A.E., Chaney, M.O., Kuo, Y.M., Webster, S.D., Stine, W.B., Haverkamp, L.J., Woods, A.S., Cotter, R.J., Tuohy, J.M., Krafft, G.A., Bonnell, B.S. & Emmerling, M.R. (1996) Morphology and toxicity of Abeta-(1-42) dimer derived from neuritic and vascular amyloid deposits of Alzheimer's disease. *J Biol Chem* **271**, 20631–20635.

von Rotz, R.C., Kohli, B.M., Bosset, J., Meier, M., Suzuki, T., Nitsch, R.M. & Konietzko, U. (2004) The APP intracellular domain forms nuclear multiprotein complexes and regulates the transcription of its own precursor. *J Cell Sci* **117**, 4435–4448.

Rovelet-Lecrux, A., Hannequin, D., Raux, G., Le Meur, N., Laquerriere, A., Vital, A., Dumanchin, C., Feuillette, S., Brice, A., Vercelletto, M., Dubas, F., Frebourg, T. & Campion, D. (2006) APP locus duplication causes autosomal dominant early-onset Alzheimer disease with cerebral amyloid angiopathy. *Nat Genet* **38**, 24–26.

Runz, H., Rietdorf, J., Tomic, I., de Bernard, M., Beyreuther, K., Pepperkok, R. & Hartmann, T. (2002) Inhibition of intracellular cholesterol transport alters presenilin localization and amyloid precursor protein processing in neuronal cells. *J Neurosci* **22**, 1679–1689.

Russo, C., Violani, E., Salis, S., Venezia, V., Dolcini, V., Damonte, G., Benatti, U., D'Arrigo, C., Patrone, E., Carlo, P. & Schettini, G. (2002) Pyroglutamate-modified amyloid β-peptides - AβN3(pE) - strongly affect cultured neuron and astrocyte survival. *J Neurochem* **82**, 1480–1489.

Saido, T.C., Iwatsubo, T., Mann, D.M., Shimada, H., Ihara, Y. & Kawashima, S. (1995) Dominant and differential deposition of distinct beta-amyloid peptide species, A beta N3(pE), in senile plaques. *Neuron* **14**, 457–466.

Saido, T.C., Yamao-Harigaya, W., Iwatsubo, T. & Kawashima, S. (1996) Amino- and carboxyl-

terminal heterogeneity of β-amyloid peptides deposited in human brain. *Neurosci Lett* **215**, 173–176.

Dos Santos, L., de Andrade, T.G.C.S. & Zangrossi Junior, H. (2008) 5-HT1A receptors in the dorsal hippocampus mediate the anxiogenic effect induced by the stimulation of 5-HT neurons in the median raphe nucleus. *Eur Neuropsychopharmacol* **18**, 286–294.

Sastre, M., Steiner, H., Fuchs, K., Capell, A., Multhaup, G., Condron, M.M., Teplow, D.B. & Haass, C. (2001) Presenilin-dependent gamma-secretase processing of beta-amyloid precursor protein at a site corresponding to the S3 cleavage of Notch. *EMBO Rep* **2**, 835–841.

Savonenko, A. V, Xu, G.M., Price, D.L., Borchelt, D.R. & Markowska, A.L. (2003) Normal cognitive behavior in two distinct congenic lines of transgenic mice hyperexpressing mutant APP SWE. *Neurobiol Dis* **12**, 194–211.

Scarmeas, N., Hadjigeorgiou, G.M., Papadimitriou, A., Dubois, B., Sarazin, M., Brandt, J., Albert, M., Marder, K., Bell, K., Honig, L.S., Wegesin, D. & Stern, Y. (2004) Motor signs during the course of Alzheimer disease. *Neurology* **63**, 975–982.

Scheff, S.W., Price, D.A., Schmitt, F.A., DeKosky, S.T. & Mufson, E.J. (2007) Synaptic alterations in CA1 in mild Alzheimer disease and mild cognitive impairment. *Neurology* **68**, 1501–1508.

Schilling, S., Hoffmann, T., Manhart, S., Hoffmann, M. & Demuth, H.U. (2004) Glutaminyl cyclases unfold glutamyl cyclase activity under mild acid conditions. *FEBS Lett* **563**, 191–196.

Schilling, S., Zeitschel, U., Hoffmann, T., Heiser, U., Francke, M., Kehlen, A., Holzer, M., Hutter-Paier, B., Prokesch, M., Windisch, M., Jagla, W., Schlenzig, D., Lindner, C., Rudolph, T., Reuter, G., Cynis, H., Montag, D., Demuth, H.-U. & Rossner, S. (2008) Glutaminyl cyclase inhibition attenuates pyroglutamate Abeta and Alzheimer's disease-like pathology. *Nat Med* **14**, 1106–1111.

Schmidt, C., Redyk, K., Meissner, B., Krack, L., von Ahsen, N., Roeber, S., Kretzschmar, H. & Zerr, I. (2010) Clinical features of rapidly progressive Alzheimer's disease. *Dement Geriatr Cogn Disord* **29**, 371–378.

Schmittgen, T.D. & Livak, K.J. (2008) Analyzing real-time PCR data by the comparative CT method. *Nat Protoc* **3**, 1101.

Schmitz, C. & Hof, P.R. (2005) Design-based stereology in neuroscience. *Neuroscience* **130**, 813–831.

Schmitz, C., Rutten, B.P.F., Pielen, A., Schafer, S., Wirths, O., Tremp, G., Czech, C., Blanchard, V., Multhaup, G., Rezaie, P., Korr, H., Steinbusch, H.W.M., Pradier, L. & Bayer, T.A. (2004) Hippocampal neuron loss exceeds amyloid plaque load in a transgenic mouse model of Alzheimer's disease. *Am J Pathol* **164**, 1495–1502.

Schonherr, C., Bien, J., Isbert, S., Wichert, R., Prox, J., Altmeppen, H., Kumar, S., Walter, J., Lichtenthaler, S.F., Weggen, S., Glatzel, M., Becker-Pauly, C. & Pietrzik, C.U. (2016) Generation of aggregation prone N-terminally truncated amyloid beta peptides by meprin beta depends on the sequence specificity at the cleavage site. *Mol Neurodegener* **11**, 19.

Selkoe, D.J. (1991) The molecular pathology of Alzheimer's disease. *Neuron* **6**, 487–498.

Selkoe, D.J. (2001) Alzheimer's disease: genes, proteins, and therapy. *Physiol Rev* **81**, 741–766.

Selkoe, D.J. & Hardy, J. (2016) The amyloid hypothesis of Alzheimer's disease at 25 years. *EMBO Mol Med* **8**, 595–608.

Seo, J.-S., Leem, Y.-H., Lee, K.-W., Kim, S.-W., Lee, J.-K. & Han, P.-L. (2010) Severe motor neuron degeneration in the spinal cord of the Tg2576 mouse model of Alzheimer disease. *J Alzheimers Dis* **21**, 263–276.

Sergeant, N., Bombois, S., Ghestem, A., Drobecq, H., Kostanjevecki, V., Missiaen, C., Wattez, A., David, J.P., Vanmechelen, E., Sergheraert, C. & Delacourte, A. (2003) Truncated beta-amyloid peptide species in pre-clinical Alzheimer's disease as new targets for the vaccination approach. *J Neurochem* **85**, 1581–1591.

Serrano-Pozo, A., Frosch, M.P., Masliah, E. & Hyman, B.T. (2011a) Neuropathological alterations in Alzheimer disease. *Cold Spring Harb Perspect Med* **1**, a006189.

Serrano-Pozo, A., Mielke, M.L., Gomez-Isla, T., Betensky, R.A., Growdon, J.H., Frosch, M.P. & Hyman, B.T. (2011b) Reactive glia not only associates with plaques but also parallels tangles in Alzheimer's disease. *Am J Pathol* **179**, 1373–1384.

Sevalle, J., Amoyel, A., Robert, P., Fournie-Zaluski, M.-C., Roques, B. & Checler, F. (2009) Aminopeptidase A contributes to the N-terminal truncation of amyloid beta-peptide. *J Neurochem* **109**, 248–256.

Shankar, G.M., Li, S., Mehta, T.H., Garcia-Munoz, A., Shepardson, N.E., Smith, I., Brett, F.M., Farrell, M.A., Rowan, M.J., Lemere, C.A., Regan, C.M., Walsh, D.M., Sabatini, B.L. & Selkoe, D.J. (2008) Amyloid-beta protein dimers isolated directly from Alzheimer's brains impair synaptic plasticity and memory. *Nat Med* **14**, 837–842.

Shao, C.Y., Mirra, S.S., Sait, H.B.R., Sacktor, T.C. & Sigurdsson, E.M. (2011) Postsynaptic degeneration as revealed by PSD-95 reduction occurs after advanced Abeta and tau pathology in transgenic mouse models of Alzheimer's disease. *Acta Neuropathol* **122**, 285–292.

Sherrington, R., Rogaev, E.I., Liang, Y., Rogaeva, E.A., Levesque, G., Ikeda, M., Chi, H., Lin, C., Li, G., Holman, K., Tsuda, T., Mar, L., Foncin, J.F., Bruni, A.C., Montesi, M.P., Sorbi, S., Rainero, I., Pinessi, L., Nee, L., Chumakov, I., Pollen, D., Brookes, A., Sanseau, P., Polinsky, R.J., Wasco, W., Da Silva, H.A., Haines, J.L., Perkicak-Vance, M.A., Tanzi, R.E., Roses, A.D., Fraser, P.E., Rommens, J.M. & St George-Hyslop, P.H. (1995) Cloning of a gene bearing missense mutations in early-onset familial Alzheimer's disease. *Nature* **375**, 754–760.

Shimojo, M., Sahara, N., Mizoroki, T., Funamoto, S., Morishima-Kawashima, M., Kudo, T., Takeda, M., Ihara, Y., Ichinose, H. & Takashima, A. (2008) Enzymatic characteristics of I213T mutant presenilin-1/gamma-secretase in cell models and knock-in mouse brains: familial Alzheimer disease-linked mutation impairs gamma-site cleavage of amyloid precursor protein C-terminal fragment beta. *J Biol Chem* **283**, 16488–96.

Siest, G., Pillot, T., Regis-Bailly, A., Leininger-Muller, B., Steinmetz, J., Galteau, M.M. & Visvikis, S. (1995) Apolipoprotein E: an important gene and protein to follow in laboratory medicine. *Clin Chem* **41**, 1068–1086.

Sinha, S., Anderson, J.P., Barbour, R., Basi, G.S., Caccavello, R., Davis, D., Doan, M., Dovey, H.F., Frigon, N., Hong, J., Jacobson-Croak, K., Jewett, N., Keim, P., Knops, J., Lieberburg, I., Power, M., Tan, H., Tatsuno, G., Tung, J., Schenk, D., Seubert, P., Suomensaari, S.M., Wang, S., Walker, D., Zhao, J., McConlogue, L. & John, V. (1999) Purification and cloning of amyloid precursor protein beta-secretase from human brain. *Nature* **402**, 537–540.

Sisodia, S.S., Koo, E.H., Beyreuther, K., Unterbeck, A. & Price, D.L. (1990) Evidence that beta-amyloid protein in Alzheimer's disease is not derived by normal processing. *Science* **248**, 492–495.

Slunt, H.H., Thinakaran, G., Von Koch, C., Lo, A.C., Tanzi, R.E. & Sisodia, S.S. (1994) Expression of a ubiquitous, cross-reactive homologue of the mouse beta-amyloid precursor protein (APP). *J Biol Chem* **269**, 2637–2644.

Smith, E.E. & Greenberg, S.M. (2009) Beta-amyloid, blood vessels, and brain function. *Stroke* **40**, 2601–2606.

Smith, R.P., Higuchi, D.A. & Broze, G.J. (1990) Platelet Coagulation Factor XIa-Inhibitor, a Form of Alzheimer Amyloid Precursor Protein. *Science* **248**, 1126–1128.

Sola, C., Mengod, G., Probst, A. & Palacios, J.M. (1993) Differential regional and cellular distribution of beta-amyloid precursor protein messenger RNAs containing and lacking the Kunitz protease inhibitor domain in the brain of human, rat and mouse. *Neuroscience* **53**, 267–295.

Solans, A., Estivill, X. & de La Luna, S. (2000) A new aspartyl protease on 21q22.3, BACE2, is highly similar to Alzheimer's amyloid precursor protein beta-secretase. *Cytogenet Cell Genet* **89**, 177–184.

Steiner, H., Fluhrer, R. & Haass, C. (2008) Intramembrane proteolysis by gamma-secretase. *J Biol Chem* **283**, 29627–29631.

Stirland, L.E., O'Shea, C.I. & Russ, T.C. (2017) Passive smoking as a risk factor for dementia and cognitive impairment: systematic review of observational studies. *Int Psychogeriatrics* **18** 1–11.

De Strooper, B., Iwatsubo, T. & Wolfe, M.S. (2012) Presenilins and γ-Secretase: Structure, Function, and Role in Alzheimer Disease. *Cold Spring Harb Perspect Med* **2** a006304.

Suzuki, N., Iwatsubo, T., Odaka, A., Ishibashi, Y., Kitada, C. & Ihara, Y. (1994) High tissue content of soluble beta 1-40 is linked to cerebral amyloid angiopathy. *Am J Pathol* **145** 452-460.

Takahashi, R.H., Almeida, C.G., Kearney, P.F., Yu, F., Lin, M.T., Milner, T.A. & Gouras, G.K. (2004) Oligomerization of Alzheimer's beta-amyloid within processes and synapses of cultured neurons and brain. *J Neurosci* **24**, 3592–3599.

Takahashi, R.H., Milner, T.A., Li, F., Nam, E.E., Edgar, M.A., Yamaguchi, H., Beal, M.F., Xu, H., Greengard, P. & Gouras, G.K. (2002) Intraneuronal Alzheimer Aβ42 Accumulates in Multivesicular Bodies and Is Associated with Synaptic Pathology. *Am J Pathol* **161** 1869-1879.

Takuma, K., Fang, F., Zhang, W., Yan, S., Fukuzaki, E., Du, H., Sosunov, A., McKhann, G., Funatsu, Y., Nakamichi, N., Nagai, T., Mizoguchi, H., Ibi, D., Hori, O., Ogawa, S., Stern, D.M., Yamada, K. & Yan, S.S. (2009) RAGE-mediated signaling contributes to intraneuronal transport of amyloid-beta and neuronal dysfunction. *Proc Natl Acad Sci U S A* **106**, 20021–20026.

Tanaka, S., Shiojiri, S., Takahashi, Y., Kitaguchi, N., Ito, H., Kameyama, M., Kimura, J., Nakamura, S. & Ueda, K. (1989) Tissue-specific expression of three types of beta-protein precursor mRNA: enhancement of protease inhibitor-harboring types in Alzheimer's disease brain. *Biochem Biophys Res Commun* **165**, 1406—1414.

Tanzi, R.E., Gusella, J.F., Watkins, P.C., Bruns, G.A., St George-Hyslop, P., Van Keuren, M.L., Patterson, D., Pagan, S., Kurnit, D.M. & Neve, R.L. (1987) Amyloid beta protein gene: cDNA, mRNA distribution, and genetic linkage near the Alzheimer locus. *Science* **235**, 880–884.

Tanzi, R.E., McClatchey, A.I., Lamperti, E.D., Villa-Komaroff, L., Gusella, J.F. & Neve, R.L. (1988) Protease inhibitor domain encoded by an amyloid protein precursor mRNA associated

with Alzheimer&#39;s disease. *Nature* **331**, 528.

Terry, R.D., Masliah, E., Salmon, D.P., Butters, N., DeTeresa, R., Hill, R., Hansen, L.A. & Katzman, R. (1991) Physical basis of cognitive alterations in Alzheimer's disease: synapse loss is the major correlate of cognitive impairment. *Ann Neurol* **30**, 572–580.

Thal, D.R., Rüb, U., Orantes, M. & Braak, H. (2002) Phases of Aβ-deposition in the human brain and its relevance for the development of AD. *Neurology* **58**, 1791 LP-1800.

Thinakaran, G. & Koo, E.H. (2008) Amyloid precursor protein trafficking, processing, and function. *J Biol Chem* **283**, 29615–29619.

Tomic, J.L., Pensalfini, A., Head, E. & Glabe, C.G. (2009) Soluble fibrillar oligomer levels are elevated in Alzheimer's disease brain and correlate with cognitive dysfunction. *Neurobiol Dis* **35**, 352–358.

Tomiyama, T., Matsuyama, S., Iso, H., Umeda, T., Takuma, H., Ohnishi, K., Ishibashi, K., Teraoka, R., Sakama, N., Yamashita, T., Nishitsuji, K., Ito, K., Shimada, H., Lambert, M.P., Klein, W.L. & Mori, H. (2010) A mouse model of amyloid beta oligomers: their contribution to synaptic alteration, abnormal tau phosphorylation, glial activation, and neuronal loss in vivo. *J Neurosci* **30**, 4845–4856.

Topiwala, A. & Ebmeier, K.P. (2017) Effects of drinking on late-life brain and cognition *Evid Based Ment Health* **21**, 2–6.

Tseng, B.P., Green, K.N., Chan, J.L., Blurton-Jones, M. & LaFerla, F.M. (2008) Abeta inhibits the proteasome and enhances amyloid and tau accumulation. *Neurobiol Aging* **29**, 1607–1618.

Urbanc, B., Cruz, L., Le, R., Sanders, J., Ashe, K.H., Duff, K., Stanley, H.E., Irizarry, M.C. & Hyman, B.T. (2002) Neurotoxic effects of thioflavin S-positive amyloid deposits in transgenic mice and Alzheimer's disease. *Proc Natl Acad Sci U S A* **99**, 13990–5.

Vassar, R., Bennett, B.D., Babu-Khan, S., Kahn, S., Mendiaz, E.A., Denis, P., Teplow, D.B., Ross, S., Amarante, P., Loeloff, R., Luo, Y., Fisher, S., Fuller, J., Edenson, S., Lile, J., Jarosinski, M.A., Biere, A.L., Curran, E., Burgess, T., Louis, J.C., Collins, F., Treanor, J., Rogers, G. & Citron, M. (1999) Beta-secretase cleavage of Alzheimer's amyloid precursor protein by the transmembrane aspartic protease BACE. *Science* **286**, 735–41.

Vassar, R., Kovacs, D.M., Yan, R. & Wong, P.C. (2009) The β-Secretase Enzyme BACE in Health and Alzheimer's Disease: Regulation, Cell Biology, Function, and Therapeutic Potential. *J Neurosci* **29** 12787-12794.

Vehmas, A.K., Kawas, C.H., Stewart, W.F. & Troncoso, J.C. (2003) Immune reactive cells in senile plaques and cognitive decline in Alzheimer's disease. *Neurobiol Aging* **24**, 321–331.

Vereecken, T.H., Vogels, O.J. & Nieuwenhuys, R. (1994) Neuron loss and shrinkage in the amygdala in Alzheimer's disease. *Neurobiol Aging* **15**, 45–54.

Verghese, P.B., Castellano, J.M., Garai, K., Wang, Y., Jiang, H., Shah, A., Bu, G., Frieden, C. & Holtzman, D.M. (2013) ApoE influences amyloid-beta (Abeta) clearance despite minimal apoE/Abeta association in physiological conditions. *Proc Natl Acad Sci U S A* **110**, E1807-16.

Van Vickle, G.D., Esh, C.L., Kokjohn, T.A., Patton, R.L., Kalback, W.M., Luehrs, D.C., Beach, T.G., Newel, A.J., Lopera, F., Ghetti, B., Vidal, R., Castaño, E.M. & Roher, A.E. (2008) Presenilin-1 280Glu→Ala Mutation Alters C-Terminal APP Processing Yielding Longer Aβ Peptides: Implications for Alzheimer's Disease. *Mol Med* **14** 184-194.

Vinters, H. V. (1987) Cerebral amyloid angiopathy. A critical review. *Stroke* **18**, 311–324.

Walf, A.A. & Frye, C.A. (2007) The use of the elevated plus maze as an assay of anxiety-related behavior in rodents. *Nat Protoc* **2**, 322.

Walsh, D.M., Klyubin, I., Fadeeva, J. V, Cullen, W.K., Anwyl, R., Wolfe, M.S., Rowan, M.J. & Selkoe, D.J. (2002) Naturally secreted oligomers of amyloid beta protein potently inhibit hippocampal long-term potentiation in vivo. *Nature* **416**, 535–539.

Wang, H.-W., Pasternak, J.F., Kuo, H., Ristic, H., Lambert, M.P., Chromy, B., Viola, K.L., Klein, W.L., Stine, W.B., Krafft, G.A. & Trommer, B.L. (2002) Soluble oligomers of beta amyloid (1-42) inhibit long-term potentiation but not long-term depression in rat dentate gyrus. *Brain Res* **924**, 133–140.

Wang, H.-X., Xu, W. & Pei, J.-J. (2012) Leisure activities, cognition and dementia. *Biochim Biophys Acta - Mol Basis Dis* **1822**, 482–491.

Wang, J., Dickson, D.W., Trojanowski, J.Q. & Lee, V.M. (1999) The levels of soluble versus insoluble brain Abeta distinguish Alzheimer's disease from normal and pathologic aging. *Exp Neurol* **158**, 328–337.

Wasco, W., Bupp, K., Magendantz, M., Gusella, J.F., Tanzi, R.E. & Solomon, F. (1992) Identification of a mouse brain cDNA that encodes a protein related to the Alzheimer disease-associated amyloid beta protein precursor. *Proc Natl Acad Sci U S A* **89** 10758-10762.

Wasco, W., Gurubhagavatula, S., Paradis, M.D., Romano, D.M., Sisodia, S.S., Hyman, B.T., Neve, R.L. & Tanzi, R.E. (1993) Isolation and characterization of APLP2 encoding a homologue of the Alzheimer's associated amyloid beta protein precursor. *Nat Genet* **5**, 95–100.

Weiner, M.W., Veitch, D.P., Hayes, J., Neylan, T., Grafman, J., Aisen, P.S., Petersen, R.C., Jack, C., Jagust, W., Trojanowski, J.Q., Shaw, L.M., Saykin, A.J., Green, R.C., Harvey, D., Toga, A.W., Friedl, K.E., Pacifico, A., Sheline, Y., Yaffe, K. & Mohlenoff, B. (2014) Effects of traumatic brain injury and posttraumatic stress disorder on Alzheimer's disease in veterans, using the Alzheimer's Disease Neuroimaging Initiative. *Alzheimers Dement* **10**, S226–S235.

Welander, H., Franberg, J., Graff, C., Sundstrom, E., Winblad, B. & Tjernberg, L.O. (2009) Abeta43 is more frequent than Abeta40 in amyloid plaque cores from Alzheimer disease brains. *J Neurochem* **110**, 697–706.

West, M.J., Coleman, P.D., Flood, D.G. & Troncoso, J.C. (1994) Differences in the pattern of hippocampal neuronal loss in normal ageing and Alzheimer's disease. *Lancet* **344**, 769–772.

West, M.J., Slomianka, L. & Gundersen, H.J.G. (1991) Unbiased stereological estimation of the total number of neurons in the subdivisions of the rat hippocampus using the optical fractionator. *Anat Rec* **231**, 482–497.

Wildburger, N.C., Esparza, T.J., Leduc, R.D., Fellers, R.T., Thomas, P.M., Cairns, N.J., Kelleher, N.L., Bateman, R.J. & Brody, D.L. (2017) Diversity of Amyloid-beta Proteoforms in the Alzheimer's Disease Brain. *Sci Rep* **7**, 1–9.

Wiltfang, J., Esselmann, H., Bibl, M., Smirnov, A., Otto, M., Paul, S., Schmidt, B., Klafki, H.-W., Maler, M., Dyrks, T., Bienert, M., Beyermann, M., Ruther, E. & Kornhuber, J. (2002) Highly conserved and disease-specific patterns of carboxyterminally truncated Abeta peptides 1-37/38/39 in addition to 1-40/42 in Alzheimer's disease and in patients with chronic neuroinflammation. *J Neurochem* **81**, 481–496.

Wiltfang, J., Esselmann, H., Cupers, P., Neumann, M., Kretzschmar, H., Beyermann, M., Schleuder, D., Jahn, H., Ruther, E., Kornhuber, J., Annaert, W., De Strooper, B. & Saftig, P. (2001) Elevation of beta-amyloid peptide 2-42 in sporadic and familial Alzheimer's disease and its generation in PS1 knockout cells. *J Biol Chem* **276**, 42645–42657.

Wirths, O. & Bayer, T.A. (2008) Motor impairment in Alzheimer's disease and transgenic Alzheimer's disease mouse models. *Genes, Brain Behav* **7**, 1–5.

Wirths, O. & Bayer, T.A. (2010) Neuron Loss in Transgenic Mouse Models of Alzheimer's Disease. *Int J Alzheimers Dis* **2010**, 1–6.

Wirths, O., Breyhan, H., Cynis, H., Schilling, S., Demuth, H.U. & Bayer, T.A. (2009) Intraneuronal pyroglutamate-Abeta 3-42 triggers neurodegeneration and lethal neurological deficits in a transgenic mouse model. *Acta Neuropathol* **118**, 487–496.

Wirths, O., Breyhan, H., Schäfer, S., Roth, C. & Bayer, T.A. (2008) Deficits in working memory and motor performance in the APP/PS1ki mouse model for Alzheimer's disease. *Neurobiol Aging* **29**, 891–901.

Wirths, O., Erck, C., Martens, H., Harmeier, A., Geumann, C., Jawhar, S., Kumar, S., Multhaup, G., Walter, J., Ingelsson, M., Degerman-Gunnarsson, M., Kalimo, H., Huitinga, I., Lannfelt, L. & Bayer, T.A. (2010) Identification of low molecular weight pyroglutamate Aβ oligomers in Alzheimer disease: A novel tool for therapy and diagnosis. *J Biol Chem* **285**, 41517–41524.

Wirths, O., Multhaup, G. & Bayer, T.A. (2004) A modified beta-amyloid hypothesis: intraneuronal accumulation of the beta-amyloid peptide--the first step of a fatal cascade. *J Neurochem* **91**, 513–520.

Wirths, O., Weis, J., Kayed, R., Saido, T.C. & Bayer, T.A. (2007) Age-dependent axonal degeneration in an Alzheimer mouse model. *Neurobiol Aging* **28**, 1689–1699.

Wisniewski, K.E., Dalton, A.J., McLachlan, C., Wen, G.Y. & Wisniewski, H.M. (1985) Alzheimer's disease in Down's syndrome: clinicopathologic studies. *Neurology* **35**, 957–961.

Wittnam, J.L. (2012) The contribution of N-terminally modified amyloid beta to the etiology of Alzheimer's disease. PhD thesis Georg-August-Universität Göttingen. https://ediss.uni-goettingen.de/handle/11858/00-1735-0000-000D-F0BC-7

Wittnam, J.L., Portelius, E., Zetterberg, H., Gustavsson, M.K., Schilling, S., Koch, B., Demuth, H.-U., Blennow, K., Wirths, O. & Bayer, T.A. (2012) Pyroglutamate amyloid beta (Abeta) aggravates behavioral deficits in transgenic amyloid mouse model for Alzheimer disease. *J Biol Chem* **287**, 8154–8162.

Wolfe, M.S., Xia, W., Ostaszewski, B.L., Diehl, T.S., Kimberly, W.T. & Selkoe, D.J. (1999) Two transmembrane aspartates in presenilin-1 required for presenilin endoproteolysis and gamma-secretase activity. *Nature* **398**, 513–517.

Wood, J.G., Mirra, S.S., Pollock, N.J. & Binder, L.I. (1986) Neurofibrillary tangles of Alzheimer disease share antigenic determinants with the axonal microtubule-associated protein tau (tau). *Proc Natl Acad Sci* **83**.

Wu, H.-Y., Hudry, E., Hashimoto, T., Kuchibhotla, K., Rozkalne, A., Fan, Z., Spires-Jones, T., Xie, H., Arbel-Ornath, M., Grosskreutz, C.L., Bacskai, B.J. & Hyman, B.T. (2010) Amyloid Beta (Aβ) Induces the Morphological Neurodegenerative Triad of Spine Loss, Dendritic Simplification, and Neuritic Dystrophies through Calcineurin (CaN) Activation. *J Neurosci* **30** 2636-2649.

Wyss-Coray, T., Loike, J.D., Brionne, T.C., Lu, E., Anankov, R., Yan, F., Silverstein, S.C. & Husemann, J. (2003) Adult mouse astrocytes degrade amyloid-beta in vitro and in situ. *Nat Med* **9**, 453–457.

Wyss-Coray, T. & Rogers, J. (2012) Inflammation in Alzheimer disease-a brief review of the basic science and clinical literature. *Cold Spring Harb Perspect Med* **2**, a006346.

Yagishita, S., Morishima-Kawashima, M., Tanimura, Y., Ishiura, S. & Ihara, Y. (2006) DAPT-induced intracellular accumulations of longer amyloid beta-proteins: further implications for the mechanism of intramembrane cleavage by gamma-secretase. *Biochemistry* **45**, 3952–3960.

Yan, R., Bienkowski, M.J., Shuck, M.E., Miao, H., Tory, M.C., Pauley, A.M., Brashier, J.R., Stratman, N.C., Mathews, W.R., Buhl, A.E., Carter, D.B., Tomasselli, A.G., Parodi, L.A., Heinrikson, R.L. & Gurney, M.E. (1999) Membrane-anchored aspartyl protease with Alzheimer's disease beta-secretase activity. *Nature* **402**, 533–537.

Yan, R., Munzner, J.B., Shuck, M.E. & Bienkowski, M.J. (2001) BACE2 functions as an alternative alpha-secretase in cells. *J Biol Chem* **276**, 34019–34027.

Yoshikai, S., Sasaki, H., Doh-ura, K., Furuya, H. & Sakaki, Y. (1991) Genomic organization of the human-amyloid beta-protein precursor gene. *Gene* **102** 291-292.

Yu, G., Nishimura, M., Arawaka, S., Levitan, D., Zhang, L., Tandon, A., Song, Y.Q., Rogaeva, E., Chen, F., Kawarai, T., Supala, A., Levesque, L., Yu, H., Yang, D.S., Holmes, E., Milman, P., Liang, Y., Zhang, D.M., Xu, D.H., Sato, C., Rogaev, E., Smith, M., Janus, C., Zhang, Y., Aebersold, R., Farrer, L.S., Sorbi, S., Bruni, A., Fraser, P. & St George-Hyslop, P. (2000) Nicastrin modulates presenilin-mediated notch/glp-1 signal transduction and betaAPP processing. *Nature* **407**, 48–54.

Yuan, Q., Yang, J., Wu, W. & Lin, Z.-X. (2017) Motor deficits are independent of axonopathy in an Alzheimer's disease mouse model of TgCRND8 mice. *Oncotarget* **8**, 97900–97912.

Zhang, J., Chen, C., Hua, S., Liao, H., Wang, M., Xiong, Y. & Cao, F. (2017) An updated meta-analysis of cohort studies: Diabetes and risk of Alzheimer's disease. *Diabetes Res Clin Pract* **124**, 41–47.

# 7 ACKNOWLEDGEMENTS

First of all, I would like to thank my supervisor Prof. Dr. Thomas Bayer for giving me the opportunity to perform my PhD thesis in his lab. I gratefully acknowledge your scientific guidance and support throughout my entire doctoral studies. Thank you for patience, the numerous scientific discussions and your encouragement.

Furthermore, I thank Prof. Dr. Oliver Wirths for all his help, patience and experimental advices.

I further gratefully thank the members of my thesis committee: Thank you Prof. Dr. Dr. Hannelore Ehrenreich for agreeing to be the second reviewer of my thesis and your helpful scientific advices during the thesis committee meetings. Thank you, Prof. Dr. Silvio Rizolli for your support, your time and also for agreeing to be part of my thesis committee.

Many thanks also go to the GGNB office, specially to Prof. Dr. Michael Hörner, Dr. Kirsten Pöhlker and Franziska Kühne.

To the Universidad Autonoma de Estado de Hidalgo (UAEH) and the Programa para el mejoramiento del profesorado (PROMEP) for providing me with the stipend during the time of my doctoral studies.

To Petra Tucolla for her technical support.

To the current and former lab members, specially to, Adriana, Bernhard, Meike, Sidar, Martina N, Martina S, Silvia and Yvonne for the nice time in and outside the lab, the scientific and non-scientific discussions.

To my beloved family, thanks for your motivation and support during all this time.

Specially I would like to thank one person, Melli, words are missing to express how much I appreciate your support and encouragement through the good and the bad times. Without you it would not have been the same. I am thankful that our paths in life crossed. For that and more, I will be always grateful.

# 8 APPENDIX

## 8.1 LIST OF FIGURES

## 8.2 LIST OF TABLES

Table 1. Reaction mixture for 5XFAD and FAD/4-42 genotyping

Table 2. Reaction mixture for Tg4-42 and TBA42 genotyping

Table 3. Thermal cycling program for Tg4-42, TBA42, 5XFAD and FAD/4-42 genotyping

Table 4. Reaction mixture for TBA42/Tg4-42 genotyping

Table 5. Thermal cycling program for TBA42/Tg4-42 genotyping

Table 6. List of primers used for mouse genotyping

Table 7. Stereological parameters used for neuron counting analysis in the CA1

Table 8. Primary antibodies for immunohistochemistry

Table 9. Secondary antibodies used for immunohistochemistry

## 8.3   LIST OF ABBREVIATIONS

| Abbreviation | Description |
| --- | --- |
| ABC | Avidin-biotin complex |
| ACE | Angiotensin-converting enzyme |
| AD | Alzheimer's disease |
| ADAM | A disintegrin and metalloproteinase |
| AICD | Amyloid precursor protein intracellular domain |
| ANOVA | Analysis of variance |
| APA | Aminopeptidase A |
| APH | Anterior pharynx defective |
| APLP | APP-like protein |
| ApoE | Apolipoprotein E |
| APP | Amyloid precursor protein |
| Aβ | Amyloid beta |
| BACE1 | Beta-site cleaving enzyme 1 |
| CA1-3 | Cornu ammonis area 1-3 |
| CAA | Cerebral amyloid angiopathy |
| cDNA | Complementary DNA |
| CTF | C-terminal fragment |
| Ctx | Cortex |
| DAB | 3,3'-diaminobenzidine |
| DCX | Doublecortin X |
| DG | Dentate gyrus |
| DH | Dorsal horn |
| DNA | Deoxyribonucleic acid |
| DS | Down Syndrome |
| ELISA | Enzyme-linked immunosorbent assay |
| EOAD | Early-onset Alzheimer's disease |
| EPM | Elevated plus maze |
| ESI | Electrospray-ionization |
| FAD | Familial Alzheimer's disease |
| FCS | Fetal calf serum |
| GWAS | Genome-wide association studies |

| | |
|---|---|
| Het | Heterozygous |
| Hom | Homozygous |
| LDLR | LDL receptor family |
| LOAD | Late-onset Alzheimer's disease |
| LTD | Long-term depression |
| LTP | Long-term potentiation |
| MALDI-TOF | Matrix-assisted laser-desorption/ionization-time-of-flight |
| MBP | Myelin basic protein |
| MCI | Mild cognitive impairment |
| MRI | Magnetic resonance imaging |
| mTRH | Murine Thyrotropin-releasing hormone |
| MVB | Multivesicular bodies |
| MWM | Morris water maze |
| NCT | Nicastrin |
| NEP | Neprilysin |
| NFT | Neurofibrillary tangle |
| NMDA | N-methyl-D-aspartate |
| PA | Pathological aging |
| PBS | Phosphate buffered saline |
| PCR | Polymerase chain reaction |
| PEN2 | Presenilin enhancer 2 |
| PFA | Paraformaldehyde |
| PHF | Paired helical filament |
| PLD3 | Phospholipase D3 |
| PSEN 1/2 | Presenilin 1/2 |
| QC | Glutaminyl cyclase |
| qRT-PCR | Quantitative real-time PCR |
| RAGE | Receptor for advanced glycation end products |
| RIP | Regulated intramembrane proteolysis |
| RM | Repeated measures |
| RNA | Ribonucleic acid |
| rpm | Rounds per minute |
| RT | Room temperature |
| SAD | Sporadic Alzheimer's disease |

| | |
|---|---|
| sAPP | soluble APP |
| SDS | Sodium dodecyl sulfate |
| SEM | Standard error of the mean |
| SNP | Single nucleotide polymorphisms |
| Sub | Subiculum |
| TAE buffer | Tris base/acetic acid buffer |
| TBE buffer | Tris/borate/EDTA buffer |
| Thal | Thalamus |
| ThT | Thioflavin-T |
| TREM2 | Triggering receptor expressed on myeloid cells 2 |
| v/v | Volume/volume |
| VH | Ventral horn |
| w/v | Weight/volume |
| WHO | World Health Organization |
| WT | Wildtype |

## 8.4 CURRICULUM VITAE

José Sócrates López Noguerola.

City of birth: Pachuca de Soto, Hidalgo. México.

Nationality: Mexican. Date of birth: February 6th, 1986.

E-mail: josolono@gmail.com

**EDUCATION**

| | |
|---|---|
| October/14-June/18 | Doctoral studies.<br>University Medicine Göttingen, Dept. of Molecular Psychiatry (Germany).<br>Thesis: The role of N-truncated Aβ peptides in Alzheimer's Disease.<br>Advisor: Prof. Dr. Thomas A. Bayer. |
| August/09 - July/11: | Master studies (Neurobiology).<br>National Autonomous University of Mexico (UNAM. Institute of Neurobiology (Mexico).<br>Thesis: Characterization of ectopic catecholaminergic neurons in rat embryonic dorsal mesencephalon.<br>Advisor: Prof. Dr. Alfredo Varela Echeverría. |
| September/03 - June/08: | Bachelor studies (Experimental Biology).<br>Metropolitan Autonomous University (UAM) (Mexico).<br>Thesis: Effect of the implantation of a semi-conductive polymer and a neuroprotector on the motor functions of adult rats with traumatic spinal cord injury.<br>Advisor: Hermelinda Salgado Ceballos MD/PhD. |

**MEMBERSHIPS AND STIPENDS**

| | |
|---|---|
| October/14-Present | Göttingen Graduate School for Neurosciences, Biophysics and Molecular Biosciences (GGNB), PhD Program: Molecular Physiology of the Brain (CMPB). |
| October/17-December/17 | GGNB Bridging Fund in order to complete the doctoral studies. |
| July/17 | Travel grant for the Alzheimer's Association International Conference (AAIC) in London, England given by the Alzheimer Forschung Initiative e.V. (AFI). |

| | |
|---|---|
| March/17 | Travel grant for the 13th International Conference on Alzheimer's & Parkinson's Diseases (AD/PD) in Vienna, Austria given by the GGNB. |
| October/14-September/17 | Three-year stipend for doctoral studies abroad as part of the Program for the Improvement of the Professorship (PROMEP) given by the Mexican Ministry of Education (SEP). |
| October/13-Oct/14 | One-year stipend for young scientists as part of the Program for the Improvement of the Professorship (PROMEP) given by the Mexican Ministry of Education (SEP). |
| August/09-July/11 | Enrolled in the International Master Program of Neurobiology at the National Autonomous University of Mexico (UNAM). |
| August/09 - July/11: | Two-year stipend for master studies given by the National Council on Science and Technology (CONACYT). |

**WORKING AND TEACHING EXPERIENCE**

| | |
|---|---|
| October/14-December/17 | Training and supervision of bachelor, master and medical students during the doctoral studies. Dept. of Molecular Psychiatry, University Medicine Göttingen (Germany). |
| January/13-July/14 | Coordinator of the Undergraduate program in Gerontology. Autonomous University of Hidalgo State (UAEH) (Mexico). |
| January/12-September/14 | Lecturer in the undergraduate program in Gerontology. Teaching the development, histology and physiology of the nervous, muscular and skeletal systems and the theories, biology and physiology of ageing. Autonomous University of Hidalgo State (UAEH) (Mexico). |

**COMUNICATION SKILLS**

| | |
|---|---|
| July/17 | Poster presentation at the Alzheimer's Association International Conference (AAIC) in London, England. |
| March/17 | Poster presentation at the 13th International Conference on Alzheimer's & Parkinson's Diseases (AD/PD) in Vienna, Austria. |

| | |
|---|---|
| June/15 | Oral presentation at the 10th Iberian Conference on Information Systems and Technologies (CISTI) in Agueda, Portugal |
| November/14 | Oral presentation at the GeT-In Program for Management in International Transfer in Berlin, Germany. |
| **LANGUAGE SKILLS** | Spanish (Native), English (fluent) and German (Basic A2). |
| **ADDITIONAL QUALIFICATIONS** | Laboratory Animal Science certificate of the FELASA (Category B) (04/2015). |

**PUBLICATIONS**

Rodríguez E.E*., Pliego-Pastrana P*., **Lopez-Noguerola J.S***. 2014 Cognitive Decline: An Analysis of the Elderly Population in Isolated Regions of Mexico. *The International Journal of Aging and Society* (3) 4: 11-22.

Bouter Y, **Lopez-Noguerola JS**, Tucholla P, Crespi GAN, Parker MW, Wiltfang J, Miles LA, Bayer TA. 2015. Abeta targets of the biosimilar antibodies of Bapineuzumab, Crenezumab, Solanezumab in comparision to an antibody against N-truncated Abeta in sporadic Alzheimer disease cases and mouse models. *Acta Neuropathol* 130:713-729

Martínez-Alcalá, C. I*., Pliego-Pastrana, P*., Rosales-Lagarde, A*., **Lopez-Noguerola, JS***., & Molina-Trinidad, E. M*. (2016). Information and Communication Technologies in the Care of the Elderly: Systematic Review of Applications Aimed at Patients With Dementia and Caregivers. JMIR Rehabilitation and Assistive Technologies, 3(1), e6. http://doi.org/10.2196/rehab.5226

**Lopez-Noguerola JS**, Giessen NME, Ueberück M, Meißner JN, Pelgrim CE, Adams J, Wirths O, Bouter Y, Bayer TA. (2016). Synergistic Effect on Neurodegeneration by N Truncated Aβ4-42 and Pyroglutamate Aβ3-42 in a Mouse Model of Alzheimer's Disease. *Front Aging Neurosci*. 2018 Mar 8;10:64. DOI: 10.3389/fnagi.2018.00064.

*equal contribution